Ferdowsi University of Mashhad

Iranian Food Science and Technology Research Journal

Iranian food science and technology Association

Vol.22 No.1

2026

ISSN:1735-4161

Contents

Iranian Food Science and Technology Research Journal

Vol. 22 No. 1 2026

Published by: Ferdowsi University of Mashhad, (College of Agriculture), Iran
Executive Manager: N. Shahnoushi, Department of Agricultural Economics, Ferdowsi University of Mashhad, Iran

Editor-in-Chief: M. Yavarmanesh, Department of Food Science and Technology, Ferdowsi University of Mashhad, Iran

Editorial Board:

Mortazavi, Seyed A.	Department of Food Science and Technology, Ferdowsi University of Mashhad, Iran
Shahidi, F.	Department of Food Science and Technology, Ferdowsi University of Mashhad, Mashhad, Iran
Habibi najafi, M.	Department of Food Science and Technology, Ferdowsi University of Mashhad, Mashhad, Iran
Razavi, Seyed M. A.	Department of Food Science and Technology, Ferdowsi University of Mashhad, Mashhad, Iran
Kashaninejad, M.	Department of Food Science and Technology, Agricultural Sciences & Natural Resources University of Gorgan, Gorgan, Iran
Khomeiri, M.	Department of Food Science and Technology, Agricultural Sciences & Natural Resources University of Gorgan, Gorgan, Iran
Farhoosh, R.	Department of Food Science and Technology, Ferdowsi University of Mashhad, Mashhad, Iran
Fazli Bazzaz, S.	Department of Pharmaceutical Chemistry, School of Pharmacy, Mashhad University of Medical Sciences, Mashhad, Iran
Koocheki, A.	Department of Food Science and Technology, Ferdowsi University of Mashhad, Mashhad, Iran
Mohebbi, M.	Department of Food Science and Technology, Ferdowsi University of Mashhad, Mashhad, Iran
Ghanbarzadeh, B.	Department of Food Science and Technology, Faculty of Agriculture, Tabriz University, Tabriz, Iran
Alemzadeh, I.	Department of Food Chemical Engineering, Faculty of Chemical and Petroleum Engineering, Sharif University of Technology, Tehran, Iran
Rajabzadeh, GH.	Department of Food Nanotechnology, Research Institute of Food Science and Technology, Mashhad, Iran
Heydarpour, M.	Brigham and Women's Hospital, Boston, Massachusetts. United States America
Ghoddusi, H. B.	School of Human Sciences, London Metropolitan University, England
Khosravidarani, K.	Department of Food Industry, School of Nutrition Sciences & Food Technology, Shahid Beheshti University of Medical Sciences, Tehran, Iran
Abbaszadegan, M.	Director Water & Environmental Technology Center, Arizona State University, United States of America
Mohammadifar, M. A.	Research Group for Food Production Engineering, Technical University of Denmark, Denmark
Vosoughi, M.	Department of Food Chemical Engineering, Faculty of Chemical and Petroleum Engineering, Sharif University of Technology, Tehran, Iran
Almasi, H.	Department of Food Science and Technology, Urmia University, Urmia, Iran
Fathi, M.	Department of Food Science and Technology, Isfahan University of Technology Isfahan, Iran
Abbasi, S.	Department of Food Science and Technology, Tarbiat Modares University, Tehran, Iran
Borges, N.	Faculty of Nutrition and Food Sciences, University of Porto; Portugal
Moazzami, Ali A.	Doctor of Philosophy, Department of Molecular Sciences, Swedish University, Sweden
Dr. Nkemnaso Obi C.	Department of Microbiology, Michael Okpara University of Agriculture, Umudike, Abia State, Nigeria
Dr, Olalekan Adeyeye S.A.	Department of Food Technology, Hindustan Institute of Technology and Science, Chennai, Tamil Nadu, India

Publisher Ferdowsi University of Mashhad
Address: College of Agriculture, Ferdowsi University of Mashhad, Iran
P.O.BOX: 91775- 1163
Fax: (98)051-38787430
E-Mail: ifstrj@um.ac.ir
Web Site: https://ifstrj.um.ac.ir

Contents

Iranian Food Science and Technology Research Journal
Homepage: https://ifstrj.um.ac.ir

Research Article
Vol. 22, No. 1, March- April, 2026, p. 1-16

Development and Characterization of Carboxymethylated Agar-based Film for Food Packaging Applications

F. Falahatgar[1], A. Babakhani[1], E. Zakipour Rahimabadi[1*], H. Rostamzad[1]

1- Fisheries Department, Faculty of Natural Resources, University of Guilan, Sowmeh Sara, Guilan, Iran
(*- Corresponding Author Email: e.zakipoor@guilan.ac.ir)

Received: 12.10.2025
Revised: 31.12.2025
Accepted: 31.01.2026
Available Online: 02.05.2026

How to cite this article:
Falahatgar, F., Babakhani, A., Zakipour Rahimabadi, E., & Rostamzad, H. (2026). Development and characterization of carboxymethylated agar-based film for food packaging applications. *Iranian Food Science and Technology Research Journal*, *22*(1), 1-16. https://doi.org/10.22067/ifstrj.2026.95783.1488

Abstract

The aim of this study was to develop and characterize carboxymethylated agar (CMA) based films crosslinked with citric acid, polyethylene glycol (PEG), and β-cyclodextrin for sustainable food packaging applications. The inherent brittleness, high hydrophilicity, and limited thermal stability of native agar films, which restrict their practical use in food packaging systems were considered as the aim of performing this study. Five distinct film formulations were prepared using different combinations of crosslinking agents, and their physicochemical, morphological, and thermal properties were systematically evaluated. The degree of substitution (DS) of carboxymethyl agar was determined to be 0.69, indicating successful chemical modification. Water contact angle analysis revealed that the CMA-P-β-A film exhibited the highest hydrophobicity, with a contact angle in the range of 80–89°, compared to approximately 67° for the control CMA film, demonstrating enhanced moisture resistance. Differential scanning calorimetry showed a significant increase in glass transition temperature (Tg), reaching 82.08 °C for the CMA-P-β-A formulation, compared to 52.54 °C for CMA, confirming the formation of a highly crosslinked polymer network. FTIR and XRD analyses confirmed successful carboxymethylation and crosslinking, accompanied by reduced crystallinity and improved structural flexibility. SEM micrographs revealed smooth and homogeneous surfaces with interconnected polymer networks. Overall, the integrative carboxymethylation crosslinking strategy effectively enhanced the hydrophobicity, thermal stability, and structural integrity of agar-based films, highlighting the CMA-P-β-A formulation as the most promising candidate for environmentally friendly food packaging applications. These findings provide valuable insights into the design of advanced biopolymer-based packaging materials.

Keywords: Algae, Carboxymethylated agar, Crosslinking, Packaging, Thermal properties

Authors retain the copyright. This is an open access article distributed under Creative Commons Attribution 4.0 International License (CC BY 4.0).

https://doi.org/10.22067/ifstrj.2026.95783.1488

Introduction

Agar is one of the earliest known natural polysaccharides extracted from red marine algae of the order Gracilariales. It is primarily composed of agarose and agaropectin, with agarose being the dominant fraction responsible for its gelling behavior. Agarose is a linear, electrically neutral polysaccharide consisting of repeating agarobiose units formed by alternating 3-O-linked β-D-galactopyranose and 4-O-linked 3,6-anhydro-α-L-galactopyranose residues (Villanueva, Sousa, Gonçalves, Nisson, & Hilliou, 2010). Owing to its biocompatibility, renewability, and film-forming ability, agar has been extensively used in food systems, pharmaceuticals, microbiological media, and biomedical applications (Surendran & Sherje, 2023). However, despite these advantages, native agar films suffer from several intrinsic limitations, including high brittleness, poor mechanical strength, excessive hydrophilicity, and limited thermal stability, which significantly restrict their application in practical food packaging systems (Zhang *et al.*, 2020). To overcome these drawbacks, chemical modifications of agar, such as carboxymethylation, have been explored. Carboxymethylation introduces carboxymethyl functional groups into the polymer backbone, improving the solubility, transparency, flexibility, and stability of polysaccharides, making them more suitable for film-forming applications. Additionally, carboxymethyl cellulose (CMC) is another derivative widely used in the food packaging industry. CMC improves water solubility and film-forming ability, providing excellent moisture resistance and mechanical properties, which are crucial for packaging materials. This study investigates the effects of carboxymethylation of agar and the incorporation of crosslinking agents, including citric acid, polyethylene glycol (PEG), and β-cyclodextrin, on the physicochemical, morphological, and thermal properties of polymer films for sustainable food packaging. The novelty of this work lies in the synergistic derivatization crosslinking strategy, which aims to mitigate the inherent limitations of agar and identify an optimized formulation suitable for environmentally friendly food packaging applications (Chakka & Zhou., 2020; Qi *et al*., 2022).

Materials and Methods

After carboxymethylation of agar, agar-based films were prepared using different crosslinking agents, and their physicochemical, structural, and thermal properties were evaluated to assess their potential application as food packaging materials, following approaches commonly reported for modified polysaccharide-based films (Roy, Kim, & Rhim, 2021; Abdollahi, Damirchi, Shafafi, Rezaei, & Ariaii, 2019).

Agar Extraction

Algae seedlings were collected from their natural habitat in Suru (Bandar Abbas, Iran) and transported to the laboratory for further processing. Agar was extracted from *Gracilaria* algae using an alkaline extraction method. Initially, the collected algae samples were thoroughly washed with distilled water to remove surface impurities, sand particles, and salts, and subsequently dried under ambient laboratory conditions. The dried algae were subjected to alkaline pretreatment using sodium hydroxide solution to facilitate the conversion of sulfate groups to 3,6-anhydrogalactose units and to improve agar gel strength and extraction yield. To remove residual alkali, the algae samples were then repeatedly washed with distilled water until neutral pH was achieved. Subsequently, the pretreated algae were soaked in distilled water and heated to initiate agar extraction. The resulting hot extract was filtered to remove insoluble residues and allowed to cool and form a gel at room temperature. The formed gels were dehydrated, washed with distilled water, and mechanically compressed to remove excess moisture. Finally, the extracted agar was dried in a hot air oven at 60 °C, ground into powder form, and stored in

airtight containers for subsequent analyses (Abraham *et al.*, 2018). The agar yield was calculated using the following equation:

Yield (%) = (Weight of extracted dry agar)/ (Weight of dried algae) × 100

Carboxymethylation of Agar

The preparation of carboxymethylated agar was performed following the method described by Qi *et al.* (2022), with minor modifications. Briefly, 2 g of agar powder extracted from *Gracilaria* algae was dispersed in 100 mL of 80% (v/v) isopropanol and stirred at room temperature (25 °C) for 30 min to ensure uniform swelling. Subsequently, 25 mL of sodium hydroxide solution (5 mol L^{-1}) was added gradually, and the mixture was continuously stirred for 1 h to achieve complete alkalization (Chakka & Zhou, 2020).

After alkalization, 7.5 g of monochloroacetic acid was gradually added, and the reaction mixture was maintained under continuous stirring for 5 h at 55 °C to promote the carboxymethylation reaction. Upon completion, the reaction was terminated by adding 85% methanol, followed by neutralization with 1 mol L^{-1} glacial acetic acid. The resulting product was filtered, washed thoroughly with 60% ethanol to remove residual salts and by-products, dried at 60 °C for 24 h, crushed, and sieved through an 80-mesh sieve to obtain carboxymethyl agar (Im, Lee, Rajabi Abhari, Youn, & Lee, 2018).

Preparation of Films

Agar-based films were prepared by dissolving 2 g of carboxymethyl agar powder in 50 mL of distilled water at 80 °C under continuous stirring until complete dissolution was achieved, following previously reported film-forming procedures for polysaccharide-based materials (Tammina & Rhim, 2023; Abdollahi *et al.*, 2019). Five formulations were prepared as follows: CMA, CMA-P, CMA-P-A, CMA-β-A, and CMA-P-β-A. After the addition of the respective crosslinking agents, the film-forming solutions were homogenized using a digital Ultra-Turrax homogenizer at 65 °C to ensure uniform dispersion and effective interaction among the components. The resulting homogeneous hydrogels were poured onto Petri dishes and dried in a hot air oven at 50 °C for 24 h, as commonly reported for crosslinked biopolymer films (Dharmalingam & Anandalakshmi, 2019).

Determination of Degree of Substitution (DS)

The degree of substitution (DS) of carboxymethyl agar was determined using a neutralization titration method. Carboxymethyl agar (0.1 g) was dissolved in 25 mL of distilled water, followed by the addition of 25 mL of standard NaOH solution (0.1 mol L^{-1}). The mixture was stirred for 10–15 min and subsequently titrated with standard HCl solution (0.1 mol L^{-1}) using phenolphthalein as an indicator until the endpoint was reached. The titration was performed in triplicate, and the average volume of HCl consumed was used for calculations.

The DS was calculated using Equations 1 and 2 (Chakka & Zhou, 2020).

$$DS = \frac{0.306X}{1-0.058X} \quad (1)$$

$$X = \frac{V_0 M_0 - V_1 M_1}{W} \quad (2)$$

Where, 0.306 is the molar mass of the disaccharide unit (g.mol^{-1}), 0.058 is the molar mass of the introduced carboxymethyl group (g.mol^{-1}), V_0 is the volume of NaOH added (mL), M_0 is the concentration of NaOH added (mol.L^{-1}), V_1 is the consumed volume of HCl (mL), M_1 is the concentration of HCl (mol.L^{-1}), and W is the sample weight (g).

Fourier Transform Infrared (FTIR) Spectroscopy

The FTIR spectra of unmodified agar and carboxymethylated agar were obtained using an FTIR spectrometer (EDX-GP, Shimadzu, Japan) equipped with KBr pellet accessories, following previously reported procedures for polysaccharide-based films (Siripatrawan & Harte, 2010; Lakshmi, Trivedi, & Reddy, 2017). Spectra were obtained in the range of 4000–400 cm^{-1} at a resolution of 4 cm^{-1} to

identify functional groups and confirm chemical modification.

Contact Angle Measurement

The wetting test was carried out using a contact angle measuring (CAM) device. The images were captured using a color industrial camera (Model PG-X, Switzerland). Ultra-high purity water was used as the probe liquid to measure the contact angle at room temperature. Prior to measurement, all film samples (3 cm × 7 cm) were fixed on a movable sample plate and leveled horizontally. A small droplet of pure water was gently deposited onto the surface of each film. For each film, surface hydrophobicity was determined from the initial contact angle values, calculated as the average of contact angles measured on both sides of the droplet almost immediately after deposition, to minimize spreading effects (Rbihi, Aboulouard, Laallam, & Jouaiti, 2020).

X-ray Diffraction (XRD) Analysis

X-ray diffraction (XRD) patterns of the samples were analyzed to determine crystallinity and investigate the internal atomic arrangement using an X-ray diffractometer (Philips, Netherlands) equipped with Ni-filtered Cu–Kα radiation, following the method described by Liu *et al*. (2020). The diffractometer was operated at 40 kV and 30 mA, and diffraction data were collected over a 2θ range of 5° to 60° at a scanning speed of 1° min^{-1}.

Scanning Electron Microscopy (SEM)

A scanning electron microscope (Evo25, Zeiss, Germany) was used to observe the surface and cross-sectional microstructures of the films. The microscope was operated at an accelerating voltage of 12 kV. Prior to analysis, film samples were coated with a thin layer of gold to enhance electrical conductivity. SEM images were recorded at magnifications of 300× and 500× to evaluate film homogeneity and microstructural features (Michler & Lebek, 2016).

Differential Scanning Calorimetry (DSC)

The glass transition temperature (Tg) of the films was determined using differential scanning calorimetry (Diamond DSC, PerkinElmer, USA). Film samples weighing approximately 10–15 mg were prepared using an analytical balance (± 0.002 mg) and sealed in aluminum hermetic pans, with an empty pan used as the reference. The samples were heated from 30 to 300 °C at a heating rate of 10 °C min^{-1} under an argon atmosphere. The Tg was identified as the midpoint of the baseline shift associated with changes in heat capacity during the glass transition (Arancibia, Alemán, López-Caballero, Gómez-Guillén, & Montero, 2015).

Statistical Analysis

Data were analyzed using analysis of variance (ANOVA) with SPSS software (version 23, IBM Corporation, Armonk, NY, USA). Differences among treatments were determined using Duncan's multiple range test at a significance level of 5% ($p < 0.05$). All results were expressed as mean ± standard deviation (SD).

Results and Discussion

Degree of Substitution (DS)

The degree of substitution (DS) is a critical parameter that directly influences the physicochemical properties of carboxymethylated polysaccharides, including solubility, viscosity, thermal behavior, and film-forming ability. In the present study, the DS of carboxymethyl agar was determined to be 0.69, confirming the successful introduction of carboxymethyl groups into the agar backbone. This DS value falls within the optimal range reported for commercially functional carboxymethylated polysaccharides and is suitable for film-based applications (Rahman *et al*., 2021; Zhao *et al*., 2025). The introduction of carboxymethyl groups enhances water solubility by increasing electrostatic repulsion between polymer chains and reducing intermolecular hydrogen bonding. Previous studies have shown that carboxymethyl agar exhibits improved solubility at room temperature when the DS exceeds

approximately 0.55 (Cao, Liu, Luan, & Zhang, 2014). The DS value obtained in this study is therefore expected to facilitate homogeneous film formation and improved compatibility with crosslinking agents. Comparable findings have been reported for carboxymethyl cellulose systems, where DS values in the range of 0.5–0.8 have been associated with favorable mechanical strength and reduced crystallinity (Casaburi, Rojo, Cerrutti, Vázquez, & Foresti, 2018). The DS value achieved in this work indicates a balanced modification level, sufficient to improve functional performance without compromising structural integrity.

Fourier Transform Infrared (FTIR) Spectroscopy

FTIR spectroscopy was employed to support the successful chemical modification of agar and the formation of intermolecular interactions within the film matrix. Fig. 1 presents the FTIR spectra of unmodified agar and carboxymethyl agar (CMA). The spectrum of native agar exhibited a broad absorption band in the range of 3300–3700 cm^{-1}, corresponding to O–H stretching vibrations of hydroxyl groups, which is characteristic of polysaccharide structures (Mostafa, Ali, El-Wassefy, Saad, & Hussein, 2024). Following carboxymethylation, a noticeable decrease in the intensity of the hydroxyl stretching band was observed, indicating partial substitution of hydroxyl groups by carboxymethyl functionalities. Additionally, new absorption bands appeared at approximately 1439 cm^{-1} and 1372 cm^{-1}, which are attributed to the asymmetric and symmetric stretching vibrations of carboxylate ($–COO^-$) groups and methylene ($–CH_2–$) scissoring vibrations, respectively (Wang *et al.*, 2012). The presence of absorption bands in the region of 1500–1700 cm^{-1} further confirms the successful introduction of carboxymethyl groups into the agar chains. These spectral changes are consistent with previous reports on carboxymethylated polysaccharides and verify the effectiveness of the chemical modification process (Rahman *et al.*, 2021; Bandyopadhyay, Sáha, Sanétrník, Saha, & Sáha, 2021).

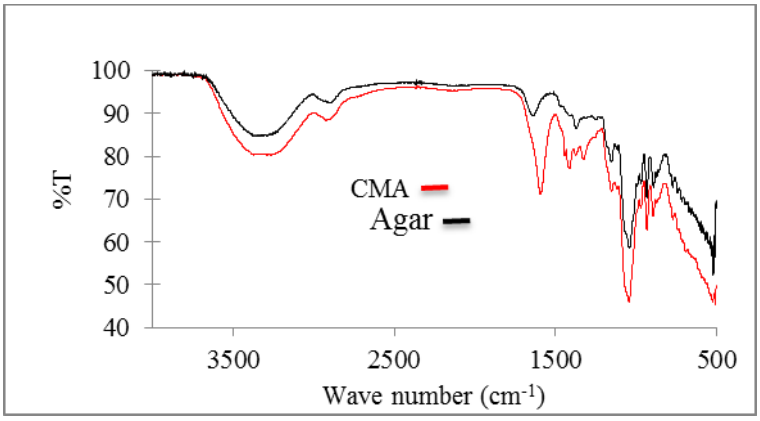

Fig. 1. The FTIR spectra of raw agar and CMA

FTIR Analysis of CMA-based Composite Films

FTIR spectroscopy was employed to investigate the intermolecular interactions and crosslinking behavior within CMA-based composite films containing polyethylene glycol (PEG), citric acid (CA), and β-cyclodextrin (β-CD). Fig. 2 presents the FTIR spectra of CMA film and its modified counterparts. The FTIR spectrum of pristine CMA film exhibited a broad absorption band in the range of 3200–3500 cm^{-1}, which is attributed to the stretching vibrations of hydroxyl (–OH) groups associated with the polysaccharide backbone and absorbed moisture. Upon incorporation of PEG (CMA+P), a noticeable reduction in the intensity of this band was observed, indicating enhanced hydrogen bonding interactions between CMA and PEG chains. Similar behavior has been reported for PEG-plasticized polysaccharide systems and is commonly

associated with improved chain mobility and intermolecular compatibility (Zhang *et al.*, 2020). The addition of citric acid resulted in more pronounced spectral changes. In the CMA+P+A and CMA+B+A films, the appearance and intensification of absorption bands in the region of 1700–1730 cm^{-1} were observed, corresponding to the C=O stretching vibrations of ester groups. This band is a key indicator of esterification reactions between the carboxyl groups of citric acid and the hydroxyl groups of CMA, PEG, and β-CD, confirming the formation of chemical crosslinks within the polymer network. Similar ester-related bands have been widely reported in citric-acid-crosslinked polysaccharide films, including carboxymethyl cellulose and starch-based systems (Smith, 2022; Rahman *et al.*, 2021). Additionally, the bands located at approximately 1400–1450 cm^{-1} and 1320–1380 cm^{-1}, attributed to asymmetric and symmetric stretching vibrations of carboxylate ($–COO^-$) groups and CH2 bending vibrations, exhibited increased intensity and slight shifts in the modified films. These changes further support the involvement of carboxyl groups in crosslinking reactions and enhanced intermolecular interactions, consistent with previous reports on carboxymethylated polysaccharide matrices (Qi *et al.*, 2022; Zhang *et al.*, 2019). In the fingerprint region (1000–1150 cm^{-1}), all composite films displayed intensified and broadened absorption bands corresponding to C–O and C–O–C stretching vibrations. The most significant changes were observed for the CMA+P-B+A film, indicating the formation of a more complex and interconnected network structure. The contribution of β-cyclodextrin to this region has been attributed to its cyclic oligosaccharide structure, which promotes additional hydrogen bonding and network stabilization, as reported in β-CD-based composite films (Velázquez-Contreras *et al.*, 2021). Overall, the progressive spectral evolution from CMA to CMA+P-B+A demonstrates a stepwise formation of hydrogen bonding interactions followed by ester crosslinking, resulting in a chemically integrated and stabilized film matrix. The observed FTIR features are in good agreement with previously reported citric-acid-crosslinked polysaccharide and cyclodextrin-containing film systems, confirming the successful design and optimization of the composite films.

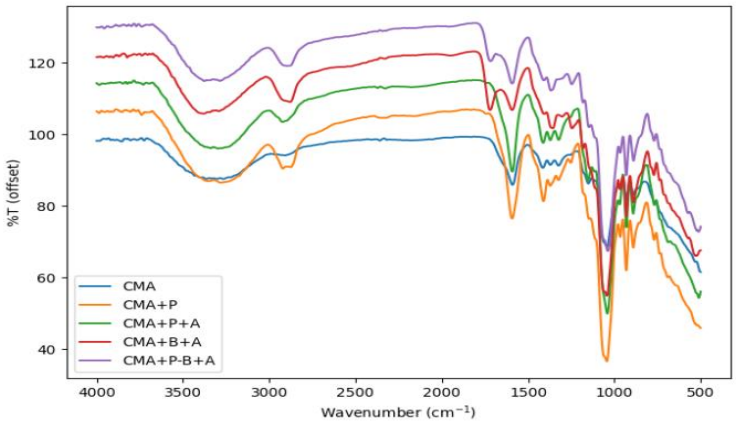

Fig. 2. The FTIR spectra of CMA-based composite films

Water Contact Angle (CA)

The surface wettability of the films was evaluated by water contact angle measurements, which provide insight into surface hydrophilicity and moisture resistance as two key parameters for food packaging materials. As shown in Fig. 3, the control CMA film exhibited a contact angle of approximately

67°, indicating a moderately hydrophilic surface. Among all formulations, only the CMA-P-β-A film exhibited a markedly higher contact angle in the range of 80–89°, demonstrating significantly enhanced surface hydrophobicity. This improvement can be attributed to the synergistic effect of polyethylene glycol, β-cyclodextrin, and citric acid, which promoted effective crosslinking and reduced the availability of hydrophilic functional groups on the film surface. Similar increases in contact angle have been reported for crosslinked polysaccharide films, where ester bond formation and network densification limit water–polymer interactions (Zhu *et al.*, 2022; Balçık Tamer, 2023). The enhanced hydrophobicity observed for the CMA-P-β-A formulation suggests improved resistance to moisture penetration, which is desirable for potentially extending the shelf life of packaged foods.

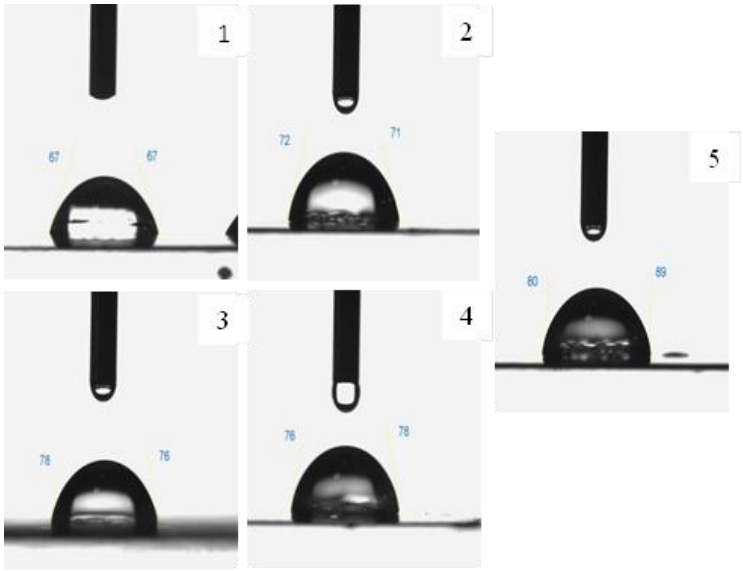

Fig. 3. Water contact angle: 1- Control (CMA), 2- CMA-P, 3- CMA-P-A, 4- CMA-β-A, and 5- CMA-P-β-A

X-ray Diffraction (XRD) Analysis

X-ray diffraction (XRD) analysis was performed to investigate the crystalline structure and structural ordering of carboxymethyl agar (CMA) films and their crosslinked formulations. Fig. 4 shows the XRD patterns of CMA, CMA-P, CMA-P-A, CMA-β-A, and CMA-P-β-A films. The CMA film exhibited a characteristic diffraction peak at approximately $2\theta = 20°$, along with a weaker peak near $2\theta = 12°$, which are typical of semi-crystalline agar-based materials (Casaburi *et al.*, 2018). Upon incorporation of polyethylene glycol, citric acid, and β-cyclodextrin, a noticeable reduction in peak intensity and peak broadening were observed, indicating a decrease in crystallinity and an increase in the amorphous phase of the polymer matrix. This behavior can be attributed to the substitution of hydroxyl groups by carboxymethyl groups and the formation of crosslinked networks that interfere with regular polymer chain packing (Zhu *et al.*, 2022). To ensure reliable interpretation of the diffraction patterns, background noise was minimized during data processing, and the overall trend of peak broadening rather than complete peak disappearance was considered. Similar reductions in crystallinity have been reported for crosslinked polysaccharide-based films, where esterification and hydrogen bonding interactions restrict molecular rearrangement and long-range order (Gieroba, Kalisz, Krysa, Khalavka, & Przekora, 2023; Wang, Xu, Qi, & Chen, 2024).

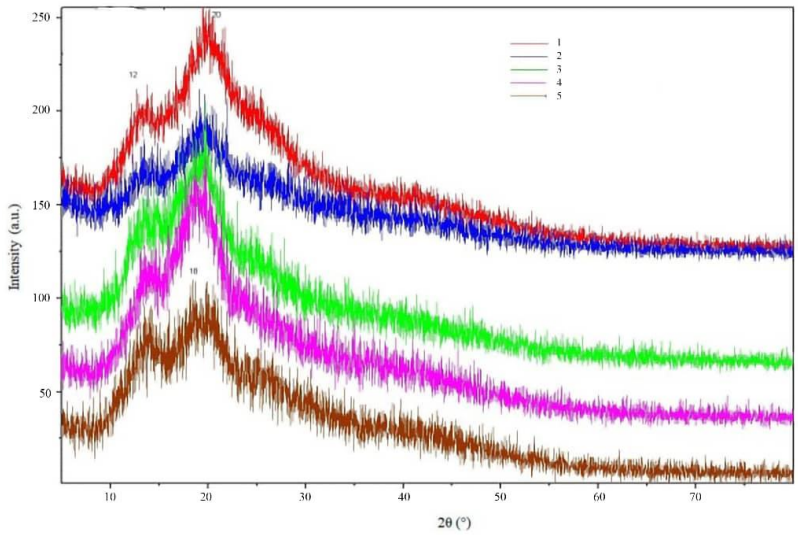

Fig. 4. XRD patterns of 1- Control (CMA), 2- CMA-P, 3- CMA-P-A, 4- CMA-β-A, and 5- CMA-P-β-A

Scanning Electron Microscopy (SEM)

Scanning electron microscopy (SEM) was used to examine the surface and cross-sectional morphologies of carboxymethyl agar (CMA) films with different formulations (Fig. 5). SEM analysis provides valuable information about film homogeneity, internal structure, and the effectiveness of crosslinking, which directly affect the mechanical, barrier, and thermal properties of biopolymer films (Roy *et al.*, 2021; Mirpoor *et al.*, 2025). The control CMA film exhibited a relatively rough and heterogeneous surface with visible micro-scale irregularities, which are commonly observed in unmodified or weakly modified polysaccharide-based films (Cazón, Velazquez, Ramírez, & Vázquez, 2017). These features can be attributed to limited intermolecular interactions and loosely packed polymer chains. In contrast, films containing polyethylene glycol, citric acid, and β-cyclodextrin (CMA-P, CMA-P-A, CMA-β-A, and CMA-P-β-A) showed smoother and more uniform surfaces, indicating improved compatibility among the film components and stronger intermolecular interactions. The incorporation of citric acid likely promoted ester bond formation between polymer chains, while β-cyclodextrin contributed to additional hydrogen bonding, resulting in a more cohesive polymer network (Zou *et al.*, 2021; Balçık Tamer, 2023). Cross-sectional SEM images further revealed clear structural differences among the formulations. The CMA film exhibited a porous and less compact internal structure, indicating a loosely packed polymer network. By comparison, the CMA-P-β-A film exhibited a dense, continuous, and homogeneous cross-section with significantly reduced porosity, confirming the formation of an interconnected and crosslinked polymer network. This compact structure restricts polymer chain mobility and enhances the overall structural integrity of the film (Rajawasam *et al.*, 2024; Keya, Li, Xu, & Xia, 2025). Similar morphological trends have been reported for citric acid-crosslinked and cyclodextrin-modified biopolymer films, where increased crosslink density leads to improved film uniformity and reduced void formation (Uyanga, Okpozo, Onyekwere, & Daoud, 2020; Escobar *et al.*, 2023). The observed SEM characteristics are consistent with the enhanced hydrophobicity and thermal stability of the CMA-P-β-A formulation, highlighting the strong relationship between microstructural organization and functional performance.

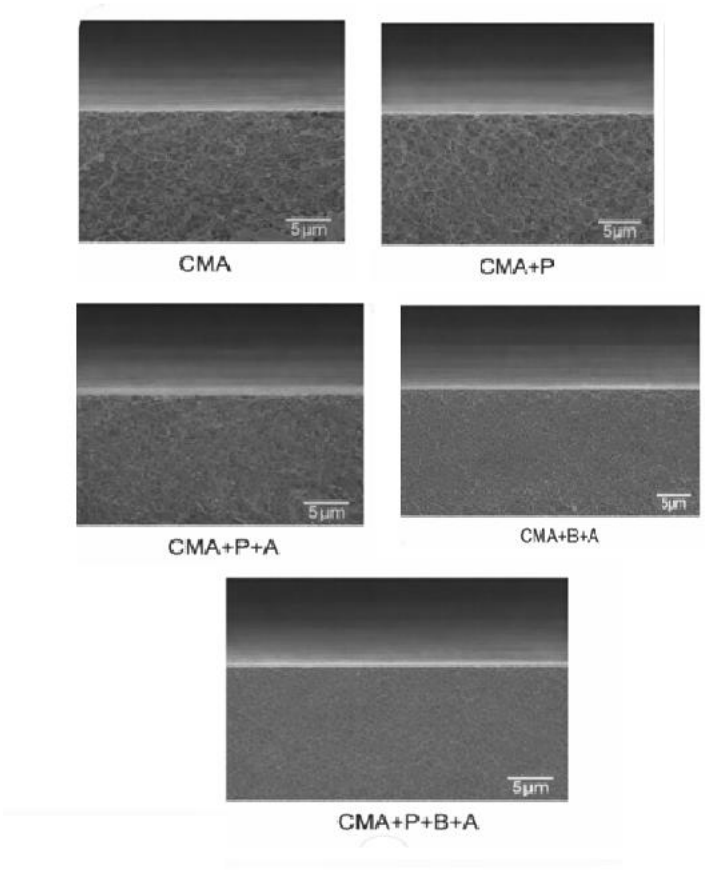

Fig. 5. SEM images of the films

Differential Scanning Calorimetry (DSC)

Differential scanning calorimetry (DSC) was used to evaluate the thermal behavior of CMA and crosslinked films, with particular emphasis on the glass transition temperature (Tg), which is a key parameter reflecting polymer chain mobility and thermal stability (Arancibia *et al.*, 2015; Jin & Torkelson, 2016). The DSC thermograms of the films are presented in Fig. 6. The control CMA film exhibited a Tg of 52.54 °C, which is characteristic of hydrophilic polysaccharide-based films containing a high density of hydroxyl groups (Rahman *et al.*, 2021). The relatively low Tg indicates greater molecular mobility and weaker intermolecular interactions within the polymer matrix, which may contribute to higher water sensitivity and lower thermal resistance. Upon incorporation of polyethylene glycol, citric acid, and β-cyclodextrin, a progressive increase in Tg was observed. The Tg values increased to 58.19 °C for CMA-P, 65.00 °C for CMA-P-A, 68.00 °C for CMA-β-A, and reached a maximum of 82.08 °C for the CMA-P-β-A formulation. This gradual increase in Tg reflects the increasing degree of crosslinking and intermolecular interactions within the polymer network (Uyanga *et al.*, 2020; Startsev, Vapirov, Lebedev, & Kychkin, 2020). The significant increase in Tg for crosslinked films can be attributed to restricted polymer chain mobility resulting from ester bond formation induced by citric acid and enhanced hydrogen bonding interactions associated with β-cyclodextrin. These interactions reduce the free volume within the polymer matrix and limit segmental motion, thereby improving thermal stability (Chen *et al.*, 2025). The absence of other thermal transitions, is related to no distinct melting or degradation peaks within the applied temperature range. This behavior is likely due

to the predominantly amorphous nature of carboxymethylated and crosslinked agar films, where Tg is the dominant thermal transition (Zhu *et al.*, 2022).

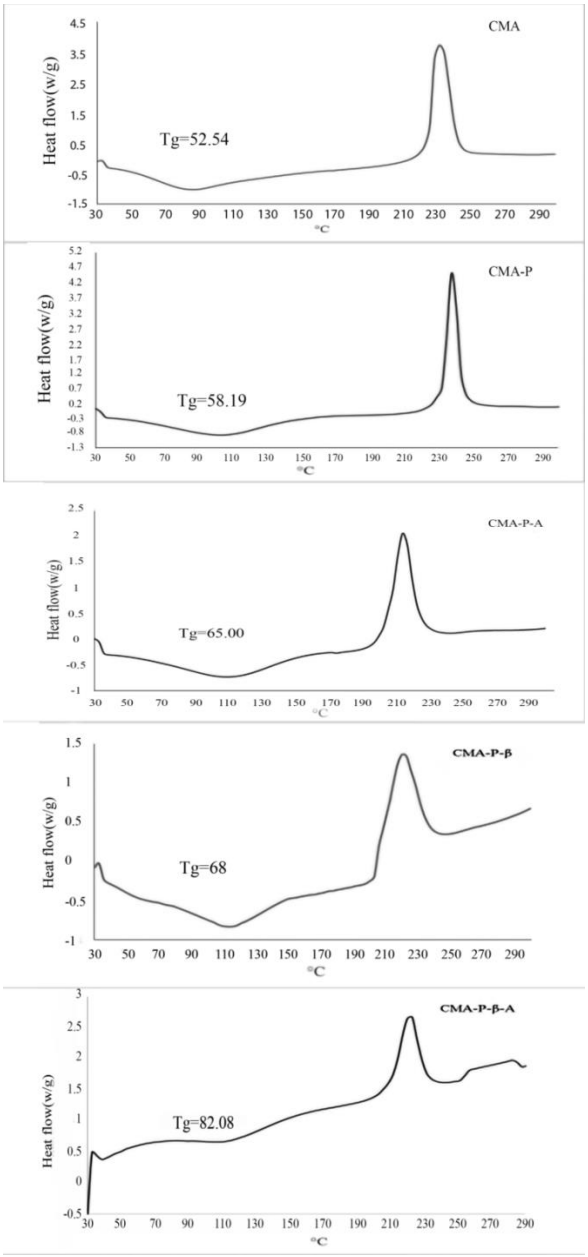

Fig. 6. DSC thermograms of the CMA and treated films

The highest Tg observed for the CMA-P-β-A formulation confirms the synergistic effect of polyethylene glycol, β-cyclodextrin, and citric acid on enhancing thermal stability, which is consistent with previous studies on citric acid-crosslinked and cyclodextrin modified biopolymer films (Han, Sathiyaseelan, Lu, Kim, & Wang, 2024; Torche *et al.*, 2025). Although the primary focus was on the glass transition temperature (Tg), other thermal transitions, such as melting and degradation points, were also considered. However, as mentioned earlier no distinct peaks for melting or degradation were clearly observed within the applied temperature range, likely due to the predominantly amorphous nature of the

carboxymethylated and crosslinked agar films. This behavior highlights the predominant role of Tg as the key thermal transition in the modified films.

Conclusion

This study demonstrated that chemical modification of agar through carboxymethylation, combined with a multi-agent crosslinking strategy, is an effective approach to overcome the inherent limitations of native agar films for food packaging applications. Carboxymethyl agar with a degree of substitution (DS) of 0.69 was successfully synthesized, providing improved solubility and compatibility with crosslinking agents. The incorporation of polyethylene glycol, citric acid, and β-cyclodextrin significantly influenced the structural, surface, and thermal properties of the films. Among all formulations, the CMA-P-β-A film exhibited the most favorable performance. This formulation showed a markedly higher water contact angle in the range of 80–89°, compared to approximately 67° for the control CMA film, indicating enhanced surface hydrophobicity and improved resistance to moisture penetration. SEM analysis confirmed the formation of a dense, homogeneous, and interconnected polymer network for this formulation, while XRD results revealed a pronounced reduction in crystallinity, suggesting increased amorphous character and improved flexibility. Thermal analysis further supported these findings, as the glass transition temperature (Tg) increased from 52.54 °C for CMA to 82.08 °C for the CMA-P-β-A film, reflecting restricted polymer chain mobility due to effective crosslinking. These results are consistent with previous reports on citric acid-crosslinked and cyclodextrin-modified biopolymer films, which have shown similar improvements in thermal stability and structural integrity (Balçık Tamer, 2023; Venkatesan, Vetcher, Al-Asbahi, & Kim, 2024). Overall, the synergistic effect of carboxymethylation and multi-component crosslinking resulted in films with enhanced hydrophobicity, reduced crystallinity, and superior thermal stability. Based on the combined physicochemical, morphological, and thermal evaluations, the CMA-P-β-A formulation was identified as the most promising candidate for environmentally friendly food packaging applications.

Scope of the Study and Limitations

The mechanical properties of the prepared films, including tensile strength and elongation at break, as well as barrier properties such as water vapor permeability and oxygen permeability, have been reported and discussed in our previously published studies. Therefore, to avoid redundancy and overlap with earlier publications, these properties were not included in the present manuscript. Accordingly, the scope of this study was intentionally limited to the structural, surface, and thermal characterization of carboxymethyl agar-based films. In addition, the thermal analysis primarily focused on the glass transition temperature (Tg), as other thermal transitions were not clearly distinguishable due to the predominantly amorphous nature of the modified films. Further investigations on film food interactions and biodegradation behavior under different environmental conditions remain important for comprehensive evaluation of practical packaging applications.

Author Contributions

F. Falahatgara: Conceptualization, Methodology, Data Curation, Writing–Original Draft. **A. Babakhania:** Methodology, Supervision, Data Curation, Visualization. **E. Zakipour Rahimabadi:** Conceptualization, Supervision, Project administration, Writing–review & editing. **H. Rostamzada:** Methodology, Data Curation.

Founding Source

This research did not receive any specific grant from funding agencies in the public, commercial, or not-for-profit sectors.

References

1. Abdollahi, M., Damirchi, S., Shafafi, M., Rezaei, M., & Ariaii, P. (2019). Carboxymethyl cellulose-agar biocomposite film activated with summer savory essential oil as an antimicrobial agent. *International Journal of Biological Macromolecules*, *126*, 561-568. https://doi.org/10.1016/j.ijbiomac.2018.12.115
2. Abraham, A., Afeweki, B., Tsegay, B., Ghebremedhin, H., Teklehaimanot, B., & Reddy, K.S. (2018). Extraction of agar and alginate from marine seaweeds in Red Sea region. *International Journal of Marine Biology and Research*, *3*, 1–8. https://doi.org/10.15226/24754706/3/2/00126
3. Arancibia, M.Y., Alemán, A., López-Caballero, M.E., Gómez-Guillén, M.C., & Montero, P. (2015). Development of active films of chitosan isolated by mild extraction with added protein concentrate from shrimp waste. *Food Hydrocolloids*, *43*, 91–99. https://doi.org/10.1016/j.foodhyd.2014.05.006
4. Balçık Tamer, Y. (2023). Development of citric acid crosslinked biodegradable chitosan/hydroxyethyl cellulose/organo-modified nanoclay composite films as sustainable food packaging materials. *Polymer-Plastics Technology and Materials*, *62*(9), 1138–1156. https://doi.org/10.1080/25740881.2023.2195908
5. Bandyopadhyay, S., Sáha, T., Sanétrník, D., Saha, N., & Sáha, P. (2021). Thermo compression of thermoplastic Agar-Xanthan gum-carboxymethyl cellulose blend. *Polymers (Basel)*, *13*(20), 3472. https://doi.org/10.3390/polym13203472
6. Cao, M., Liu, X., Luan, J., & Zhang, X. (2014). Characterization of physicochemical properties of carboxymethyl agar. *Carbohydrate Polymers*, *111*, 449–455. https://doi.org/10.1016/j.carbpol.2014.04.036
7. Casaburi, A., Rojo, Ú.M., Cerrutti, P., Vázquez, A., & Foresti, M.L. (2018). Carboxymethyl cellulose with tailored degree of substitution obtained from bacterial cellulose. *Food Hydrocolloids*, *75*, 147–156. https://doi.org/10.1016/j.foodhyd.2017.09.002
8. Cazón, P., Velazquez, G., Ramírez, J.A., & Vázquez, M. (2017). Polysaccharide-based films and coatings for food packaging: A review. *Food Hydrocolloids*, *68*(5), 1-10. https://doi.org/10.1016/j.foodhyd.2016.09.009
9. Chakka, V.P., & Zhou, T. (2020). Carboxymethylation of polysaccharides: Synthesis and bioactivities. *International Journal of Biological Macromolecules*, *165*, 2425–2431. https://doi.org/10.1016/j.ijbiomac.2020.10.178
10. Chen, J., Wu, J., Veldhuis, T., Picchioni, F., Raffa, P., & Koning, C.E. (2025). Mechanistic study on citric acid–based esterification: A versatile reaction for preparation of hydrophilic polymers. *ACS Sustainable Chemistry & Engineering*, *13*(1), 559-570. https://doi.org/10.1021/acssuschaemeng.4c07569
11. Dharmalingam, K., & Anandalakshmi, R. (2019). Fabrication, characterization and drug loading efficiency of citric acid crosslinked NaCMC-HPMC hydrogel films for wound healing drug delivery applications. *International Journal of Biological Macromolecules*, *134*, 815–829. https://doi.org/10.1016/j.ijbiomac.2019.05.027
12. Escobar, K., Garrido-Miranda, K.A., Pulido, R., Naveas, N., Manso-Silván, M., & Hernandez-Montelongo, J. (2023). Coatings of cyclodextrin/citric-acid biopolymer as drug delivery systems: A review. *Pharmaceutics*, *15*(1), 296, https://doi.org/10.3390/pharmaceutics15010296
13. Gieroba, B., Kalisz, G., Krysa, M., Khalavka, M., & Przekora, A. (2023). Application of vibrational spectroscopic techniques in the study of the natural polysaccharides and their cross-linking process. *International Journal of Molecular Sciences*, *24*(3), 2630. https://doi.org/10.3390/ijms24032630

14. Han, K., Sathiyaseelan, A., Lu, Y., Kim, K.M., & Wang, M.H. (2024). Agar/carboxymethyl cellulose composite film loaded with hydroxyapatite nanoparticles for bone regeneration. *Cellulose*, *31*(15), 9319-9334. https://doi.org/10.1007/s10570-024-06148-5
15. Im, W., Lee, S., Rajabi Abhari, A., Youn, H.J., & Lee, H.L. (2018). Optimization of carboxymethylation reaction as a pretreatment for production of cellulose nanofibrils. *Cellulose*, *25*, 3873-3883. https://doi.org/10.1007/s10570-018-1853-9
16. Jin, K., & Torkelson, J.M. (2016). Enhanced Tg-confinement effect in cross-linked polystyrene compared to its linear precursor: Roles of fragility and chain architecture. *Macromolecules*, *49*(14), 5092–5103. https://doi.org/10.1021/acs.macromol.6b01042
17. Keya, K.N., Li, Z., Xu, L., & Xia, W. (2025). Exploring cross-link density and additive effects on mechanical and morphological behaviors of cross-linked polymers. *Macromolecular Materials and Engineering*, *310*(5), 1-12. https://doi.org/10.1002/mame.202400383
18. Lakshmi, D.S., Trivedi, N., & Reddy, C.R.K. (2017). Synthesis and characterization of seaweed cellulose derived carboxymethyl cellulose. *Carbohydrate Polymers*, *157*, 1604-1610. https://doi.org/10.1016/j.carbpol.2016.11.042
19. Liu, S., Xiao, Y., Shen, M., Zhang, X., Wang, W., & Xie, J. (2020). Effect of sodium carbonate on the gelation, rheology, texture and structural properties of maize starch-mesona chinensis polysaccharide gel. *Food Hydrocolloids*, *87*, 943–951. https://doi.org/10.1016/j.foodhyd.2018.09.025
20. Michler, G.H., & Lebek, W. (2016). Electron microscopy of polymers. In: *Polymer Morphology: Principles, Characterization, and Processing*. Pp. 37-53. Guo, Q. Eds., John Wiley & Sons, inc. https://doi.org/10.1002/9781118892756.ch3
21. Mirpoor, S.F., Massironi, A., Winning, D., Lignou, S., Ghawi, S.K., Trotta, F., & Charalampopoulos, D. (2025). Agar/Carboxymethyl cellulose blended films with green-synthesised silver nanoparticles as a sustainable alternative for food packaging applications. *Polymers*, *17*(23), 3126. https://doi.org/10.3390/polym17233126
22. Mostafa, S.I., Ali, M.A., El-Wassefy, N.A., Saad, E.M., & Hussein, M.H. (2024). Adsorption and interaction studies of methylene blue dye onto agar-carboxymethylcellulose-silver nanocomposite in aqueous media. *Biomass Conversion and Biorefinery*, *14*(7), 1-10. https://doi.org/10.1007/s13399-022-02505-1
23. Qi, B., Yang, S., Zhao, Y., Wang, Y., Yang, X., Chen, S., Wu, Y., Pan, C., Hu, X., Li, C., & Wang, L. (2022). Comparison of the physicochemical properties of carboxymethyl agar synthesized by microwave-assisted and conventional methods. *Gels*, *8*(3), 162. https://doi.org/10.3390/gels8030162
24. Rahman, M.S., Hasan, M.S., Nitai, A.S., Nam, S., Karmakar, A.K., Ahsan, M.S., Shiddiky, M.J., & Ahmed, M.B. (2021). Recent developments of carboxymethyl cellulose. *Polymers*, *13*(8), 1345. https://doi.org/10.3390/polym13081345
25. Rajawasam, C.W., Dodo, O.J., Weerasinghe, M.S.N., Raji, I.O., Wanasinghe, S.V., Konkolewicz, D., & Watuthanthrige, N.D.A. (2024). Educational series: Characterizing crosslinked polymer networks. *Polymer Chemistry*, *15*(3), 1-47. https://doi.org/10.1039/d3py00914a
26. Rbihi, S., Aboulouard, A., Laallam, L., & Jouaiti, A. (2020). Contact angle measurements of cellulose based thin film composites: Wettability, surface free energy and surface hardness. *Surfaces and Interfaces*, *21*, 100708. https://doi/org/10.1016/j.surfin.2020.100708
27. Roy, S., Kim, H.J., & Rhim, J.W. (2021). Effect of blended colorants of anthocyanin and shikonin on carboxymethyl cellulose/agar-based smart packaging film. *International Journal of Biological Macromolecules*, *183*, 305-315. https://doi.org/10.1016/j.ijbiomac.2021.04.162

28. Siripatrawan, U., & Harte, B.R. (2010). Physical properties and antioxidant activity of an active film from chitosan incorporated with green tea extract. *Food Hydrocolloids*, *24*, 770–775. https://doi.org/10.1016/j.foodhyd.2010.04.003
29. Smith, B.C. (2022). Infrared spectroscopy of polymers, IX: Pendant ester polymers and polycarbonates. *Spectroscopy*, *37*(11), 16-19. https://doi.org/10.56530/spectroscopy.xn9369p8
30. Startsev, O.V., Vapirov, Y.M., Lebedev, M.P., & Kychkin, A.K. (2020). Comparison of glass-transition temperatures for epoxy polymers obtained by methods of thermal analysis. *Mechanics of Composite Materials*, *56*, 227-240. https://doi.org/10.1007/s11029-020-09875-5
31. Surendran, G., & Sherje, A.P. (2023). Biomedical applications of agar and its composites: A mini-review. *Natural Products Journal*, *13*(5), 23-30. https://doi.org/10.2174/2210315512666220615113320
32. Tammina, S.K., & Rhim, J.W. (2023). Carboxymethylcellulose/agar-based functional film incorporated with nitrogen-doped polyethylene glycol-derived carbon dots for active packaging applications. *Chemosphere*, *313*, 137627. https://doi.org/10.1016/j.chemosphere.2022.137627
33. Torche, A., Chouana, T., Akachat, B., Rekbi, F.M.L., Rahmani, Y., El Hadj, M.D.O., Uzun, Ş.A., Parlak, M.E., D'Elia, M., Rastrelli, L., & Sarıcaoğlu, F.T. (2025). Cassava starch films with green-synthesized ZnO nanoparticles from date palm pits for active packaging. *Food Chemistry*, *495*, 146392. https://doi.org/10.1016/j.foodchem.2025.146392
34. Uyanga, K.A., Okpozo, O.P., Onyekwere, O.S., & Daoud, W.A. (2020). Citric acid crosslinked natural bi-polymer-based composite hydrogels: Effect of polymer ratio and beta-cyclodextrin on hydrogel microstructure. *Reactive and Functional olymers*, *154*, 104682. https://doi.org/10.1016/j.reactfunctpolym.2020.104682
35. Velázquez-Contreras, F., Zamora-Ledezma, C., López-González, I., Meseguer-Olmo, L., Núñez-Delicado, E., & Gabaldón, J.A. (2021). Cyclodextrins in polymer-based active food packaging: A fresh look at nontoxic, biodegradable, and sustainable technology trends. *Polymers*, *14*(1), 104. https://doi.org/10.3390/polym14010104
36. Venkatesan, R., Vetcher, A.A., Al-Asbahi, B.A., & Kim, S.C. (2024). Chitosan-based films blended with tannic acid and *Moringa oleifera* for application in food packaging: The preservation of strawberries (*Fragaria ananassa*). *Polymers*, *16*(7), 937. https://doi.org/10.3390/polym16070937
37. Villanueva, R.D., Sousa, A.M.M., Gonçalves, M.P., Nisson, M., & Hilliou, L. (2010). Production and properties of agar from the invasive marine alga, *Gracilaria vermiculophylla* (Gracilariales, Rhodophyta). *Journal of Applied Phycology*, *22*(2), 211–220. https://doi.org/10.1007/s10811-009-9444-7
38. Wang, Y., Mo, Q., Li, Z., Lai, H., Lou, J., Liu, S., & Mao, J. (2012). Effects of degree of carboxymethylation on physicochemical and biological properties of pachyman. *International Journal of Biological Macromolecules*, *51*(5), 1052–1056. https://doi.org/10.1016/j.ijbiomac.2012.08.022
39. Wang, Z., Xu, C., Qi, L., & Chen, C. (2024). Chemical modification of polysaccharides for sustainable bioplastics. *Trends in Chemistry*, *6*(6), 314-331. https://doi.org/10.1016/j.trechm.2024.04.009
40. Zhang, C., An, D., Xiao, Q., Weng, H., Zhang, Y., Yang, Q., & Xiao, A. (2020). Preparation, characterization, and modification mechanism of agar treated with hydrogen peroxide at different temperatures. *Food Hydrocolloids*, *101*, 105527. https://doi.org/10.1016/j.foodhyd.2019.105527
41. Zhang, X., Chen, T., Lim, J., Gu, F., Fang, F., Cheng, L., Campanella, O.H., & Hamaker, B.R. (2019). Acid gelation of soluble laccase-crosslinked corn bran arabinoxylan and possible gel formation mechanism. *Food Hydrocolloids*, *92*, 1–9. https://doi.org/10.1016/j.foodhyd.2019.01.032

42. Zhao, C., Li, L., Xiao, H., Huang, Y., Zhao, Y., Ma, L., & Tian, Y. (2025). Physicochemical properties and structural characterization of crosslinking modifications of carboxymethyl cellulose with varying degrees of substitution. *Food Chemistry*, *496*(1), https://doi.org/10.1016/j.foodchem.2024.146617
43. Zhu, W., Zhang, D., Liu, X., Ma, T., He, J., Dong, Q., Din, Z.U., Zhou, J., Chen, L., Hu, Z., & Cai, J. (2022). Improving the hydrophobicity and mechanical properties of starch nanofibrous films by electrospinning and cross-linking for food packaging applications. *LWT- Food Science and Technology*, *169*, 114005. https://doi.org/10.1016/j.lwt.2022.114005
44. Zou, Y., Yuan, C., Cui, B., Sha, H., Liu, P., Lu, L., & Wu, Z. (2021). High-amylose corn starch/konjac glucomannan composite film: Reinforced by incorporating β-cyclodextrin. *Journal of Agricultural Food Chemistry*, *69*(8), 2493–2500. https://doi.org/10.1021/acs.jafc.0c06648

نشریه پژوهشهای علوم و صنایع غذایی ایران
https://ifstrj.um.ac.ir

مقاله پژوهشی
جلد ۲۲، شماره ۱، فروردین - اردیبهشت ۱۴۰۵، ص. ۱۶-۱

تولید و بررسی خصوصیات فیلم‌های بر پایه آگار کربوکسی متیله‌شده برای استفاده در بسته‌بندی محصولات غذایی

فریده فلاحتگر[۱]- آریا باباخانی[۱]- اسحق زکی‌پور رحیم‌آبادی[۱]*- هانیه رستم‌زاد[۱]

تاریخ دریافت: ۱۴۰۴/۰۷/۲۰
تاریخ پذیرش: ۱۴۰۴/۱۱/۱۱

چکیده

این مطالعه به‌منظور تعیین ویژگی‌های فیلم‌های کربوکسی متیل آگار با استفاده از عوامل اتصال عرضی شامل اسید سیتریک، بتا-سیکلودکسترین و پلی‌اتیلن گلیکول انجام شد. پنج نوع فیلم با عوامل اتصال دهنده عرضی مختلف تهیه گردید. در این تحقیق، ویژگی‌های مورفولوژیکی، زاویه تماس و خواص حرارتی فیلم‌ها برای استفاده در بسته‌بندی مواد غذایی مورد ارزیابی قرار گرفتند. نتایج زاویه تماس نشان داد که فیلم بهینه، متشکل از کربوکسی متیل آگار همراه با پلی‌اتیلن گلیکول، اسید سیتریک و بتا-سیکلودکسترین، زاویه تماس بالاتری نسبت به سایر فیلم‌ها نشان داد. آگارز با موفقیت کربوکسی کتیله شده و میزان کریستاله شدن آن کاهش یافته و این امر سبب افزایش انعطاف‌پذیری و بهبود خواص سدکنندگی فیلم‌ها گردید. دمای گذار شیشه‌ای به ۸۲/۰۲ درجه سانتی‌گراد رسید که نشان‌دهنده افزایش سختی ساختاری و کاهش جذب آب است که با آنالیز DSC تأیید گردید. این تحقیق نشان داد که فیلم بر پایه آگار کربوکسی متیله شده پتانسیل قابل توجه‌ای به‌عنوان جایگزین بسته‌بندی سازگار با محیط‌زیست دارد.

واژه‌های کلیدی: آگار کربوکسی متیله شده، اتصالات عرضی، جلبک، خصوصیات حرارتی

۱- گروه شیلات، دانشکده منابع طبیعی، دانشگاه گیلان، صومعه سرا، ایران
(*- نویسنده مسئول: Email: e.zakipoor@guilan.ac.ir)

https://doi.org/10.22067/ifstrj.2026.95783.1488

Iranian Food Science and Technology Research Journal
Homepage: https://ifstrj.um.ac.ir

Research Article
Vol. 22, No. 1, March- April, 2026, p. 17-34

Encapsulation of Vitamins E and C by Whey Protein Concentrate– Chitosan via Spray Drying: Optimization, Physicochemical Characterization, and Release Rate Analysis

P. Mojtahedi[1], M. Varidi[1*], A.M. Mortazavian[2]

1- Department of Food Science and Technology, Faculty of Agriculture, Ferdowsi University of Mashhad, Mashhad, Iran (*- Corresponding Author Email: m.varidi@um.ac.ir)
2- Department of Food Science and Technology, Faculty of Nutrition Sciences and Food Technology, National Nutrition and Food Technology Research Institute, Shahid Beheshti University of Medical Sciences, Tehran, Iran

Received: 22.10.2025
Revised: 09.01.2026
Accepted: 28.01.2026
Available Online: 02.05.2026

How to cite this article:
Mojtahedi, P., Varidi, M., & Mortazavian, A.M. (2026). Encapsulation of vitamins E and C by whey protein concentrate–chitosan via spray drying: Optimization, physicochemical characterization, and release rate analysis. *Iranian Food Science and Technology Research Journal*, *22*(1), 17-34.
https://doi.org/10.22067/ifstrj.2026.96109.1497

Abstract

Increasing concerns about human health have increased demand for functional bioactive compounds, such as vitamins E and C. However, their inherent instability and susceptibility to environmental conditions have restricted their direct application in food systems. Encapsulation strategies offer an effective approach to protect these vitamins from degradation and enable controlled release. This study aimed to develop a stable encapsulation system for vitamins E and C using a whey protein concentrate–chitosan (WPC–CS) complex through spray drying, enabling simultaneous delivery of hydrophilic and lipophilic vitamins. Response surface methodology (RSM) was applied to optimize the formulation with the objective of maximizing encapsulation efficiency while minimizing moisture content and hygroscopicity. The optimal microcapsule exhibited encapsulation efficiencies of 93.83% and 93.6% for vitamins E and C, respectively, with a low moisture content (3.17%) and controlled hygroscopicity (13.18%). Release studies demonstrated a phase-dependent behavior: vitamin C showed negligible release in simulated mouth fluid (0.07% after 10 min) but a substantial cumulative release in simulated gastric fluid (85.74% after 120 min). In contrast, vitamin E exhibited a slower and sustained release profile, with 31.45% released after 120 min in simulated gastric fluid and no detectable release under mouth conditions. Scanning electron microscopy (SEM) analysis revealed that the microcapsules had a predominantly spherical morphology with a wrinkled surface, characteristic of protein–polysaccharide matrices formed during rapid drying. Fourier transform infrared spectroscopy (FTIR) confirmed successful encapsulation of both vitamins through interactions between WPC and CS. These findings indicate that WPC–CS complexes produced via spray drying provide an effective co-encapsulation and controlled-release system, enhancing vitamin stability and offering promising applications in functional foods and pharmaceutical formulations.

Keywords: Controlled release, Microcapsules, Optimize, Spray drier

Introduction

Vitamins are indispensable micronutrients with potent antioxidant properties that play a fundamental role in maintaining cellular homeostasis and protecting biomolecules from oxidative stress. Among them, vitamin E (α-tocopherol) is a lipophilic antioxidant that prevents lipid peroxidation and contributes to

Authors retain the copyright. This is an open access article distributed under Creative Commons Attribution 4.0 International License (CC BY 4.0).

https://doi.org/10.22067/ifstrj.2026.96109.1497

the stabilization of biological membranes (Budinčić *et al*., 2021; Chen, Zhu, Zhao, Zhang, & Wang, 2022). In contrast, vitamin C (ascorbic acid, AA) is a hydrophilic antioxidant that exists in reduced (AA) and oxidized (dehydroascorbic acid, DHA) forms and is essential for scavenging free radicals in aqueous systems (Comunian *et al.*, 2013; Guldiken *et al.*, 2019). Together, these vitamins provide complementary protection against oxidative damage in both lipid and aqueous phases of biological systems. However, despite their recognized health-promoting effects, both vitamins exhibit inherent physicochemical limitations that restrict their practical applications. Vitamin E is poorly soluble in water and shows considerable instability when exposed to oxygen, heat, or light, which significantly limits its functionality in food and pharmaceutical formulations (Rabkin, Tirosh, & Kanner, 2022). Likewise, vitamin C undergoes rapid degradation due to its high sensitivity to oxidation, moisture, and environmental stressors such as temperature and light, leading to reduced stability and bioavailability (Katouzian & Jafari, 2016). These drawbacks highlight the urgent need for innovative approaches to preserve their activity and ensure efficient delivery. Microencapsulation has emerged as a promising solution to address these challenges. By entrapping bioactive molecules within protective wall materials, microencapsulation enhances stability, improves dispersibility, and provides controlled release at targeted sites. Moreover, this technique can be tailored to optimize the physicochemical and functional properties of encapsulated vitamins, thereby extending their shelf life and effectiveness. Various methods have been developed for microcapsule formation, including phase separation, extrusion, complex coacervation, polycondensation, and spray-drying. Among these, spray-drying has gained particular attention due to its scalability, cost-effectiveness, and ability to convert liquid formulations into stable powders with improved storage and release profiles (Chang & Nickerson, 2018; Lan, Ohm, Chen, & Rao, 2021; Li, Zhou, Huang, Li, & Xiao, 2022).

In this context, several studies have successfully applied spray-drying for vitamin encapsulation. For instance, vitamin C has been encapsulated using carriers such as gum Arabic/maltodextrin (Delaporte, Duchemin, Grisel, & Gore, 2024) and whey protein/maltodextrin (Agudelo-Chaparro, Ciro-Velásquez, Sepúlveda-Valencia, & Pérez-Monterroza, 2022) to reduce oxidative degradation. Similarly, vitamin E has been encapsulated with lipid-based or protein–polysaccharide matrices to improve its oxidative stability (Chen *et al.*, 2018; Yousefi, Rajaei, Nateghi, Nodeh, & Rashidi, 2023). Furthermore, co-encapsulation of vitamins C and E has been investigated to develop synergistic dual-phase antioxidant systems capable of functioning in both hydrophilic and lipophilic environments (Chang & Nickerson, 2018). Importantly, recent advances have focused on optimizing wall material composition, drying conditions, and encapsulation efficiency to maximize the stability and bioactivity of vitamins (Askari Vaselabadi *et al*., 2025).

WPC–CS spray-dried microcapsules offer distinct superiority over conventional carriers like liposomes or emulsions for co-encapsulating hydrophilic (e.g., vitamin C) and hydrophobic (e.g., vitamin E) compounds. Unlike liposomes, which suffer from inherent instability, leakage during storage/drying, poor scalability, and low entrapment efficiencies requiring complex stabilization, the protein–polysaccharide matrix yields robust, spherical powders with high efficiency, low moisture, and tailored pH-dependent release suitable for functional foods. This cost-effective, industrially scalable spray-drying process enhances environmental stability and controlled delivery, addressing key limitations of lipid-based systems.

Despite extensive investigations into individual encapsulating agents, the co-encapsulation of vitamins C and E using whey protein concentrate (WPC) and chitosan (CS) in

a controlled spray-drying process has been rarely addressed. Whey protein concentrate (WPC) was selected for its superior emulsifying and film-forming properties, enabling effective entrapment of lipophilic vitamin E. Chitosan (CS) complements WPC via electrostatic complexation, enhancing matrix strength and providing pH-responsive release in gastric conditions for hydrophilic vitamin C protection. The combined functionality of these wall materials in simultaneously protecting hydrophilic and lipophilic vitamins remains underexplored. Therefore, the present study aimed to design and optimize spray-dried microcapsules containing vitamins C and E by employing WPC and CS as wall materials. Specifically, the study investigated the influence of protein-to-polysaccharide ratios on encapsulation efficiency, moisture content, and release behavior under simulated oral and gastric conditions.

Materials and Method

Material

Vitamin E (α-tocopherol, 96% purity, w/w), vitamin C (L-ascorbic acid, 99% purity, w/w), pepsin (from porcine gastric mucosa), and medium molecular weight chitosan (CS, deacetylation degree ≈ 85%) were purchased from Sigma-Aldrich (St. Louis, MO, USA). Whey protein concentrate (WPC, 80% protein, w/w) was obtained from Fonterra (Auckland, New Zealand). Alpha-amylase and other analytical-grade reagents were purchased from Merck (Darmstadt, Germany)

Preparation of CS-WPC Complex Loaded with Vitamins C and E

Vitamin E/WPC Solution

Aqueous solutions of whey protein concentrate (WPC; 2, 3, and 4% w/w) were prepared by magnetic stirring at 1000 rpm for 2 h, followed by homogenization at 14,000 rpm for 3 min using a high-shear homogenizer (T25 digital ULTRA-TURRAX, IKA, Germany). An oil phase containing vitamin E (0.16% w/w), sunflower oil (4% w/w), and Tween 80 (1% w/w) was homogenized under identical conditions and subsequently incorporated into the WPC solution to obtain the vitamin E/WPC mixture (Luo, Zhang, Whent, Yu, & Wang, 2011; Wang *et al*., 2016).

Vitamin C/CS Solution

Chitosan (CS) solutions (0.25, 0.375, and 0.5% w/w) were prepared in 1% acetic acid, stirred at 1000 rpm for 10 min, and homogenized at 14,000 rpm for 3 min using the same homogenizer. Vitamin C (0.9 g/100 g) was then incorporated into the CS solution and homogenized under the same conditions (Desai & Park, 2006; Wang *et al.*, 2016). The CS–vitamin C solution was gradually added to the WPC–vitamin E solution while adjusting the pH to 4.3, followed by homogenization at 14,000 rpm for 2 min to ensure uniform dispersion.

Final Emulsion Characterization

Physicochemical properties (particle size, ζ-potential, viscosity, encapsulation efficiency) were measured according to established protocols and reported in our previous study (Mojtahedi, Mortazavian, & Varidi, 2023). The total solid content of the feed solution prior to spray drying was 3.5–5.5% (w/w), a critical parameter influencing drying efficiency, particle morphology, and microcapsule stability (Bazaria & Kumar, 2016; Fernandes, Borges, Botrel, & de Oliveira, 2014).

Spray Drying

Emulsions were spray-dried using a B-290 LabPlant spray dryer (Switzerland) under controlled conditions: feed rate 3 mL/min, compressed air flow 50 L/min, pump capacity 20%, aspirator speed 90%, inlet air temperature 165 °C, outlet temperature 99–100 °C. These operating conditions were optimized to balance encapsulation efficiency, particle morphology, and vitamin stability, ensuring reproducible production of stable microcapsules. These operating conditions were optimized to achieve a balance between encapsulation efficiency, particle morphology, and vitamin stability, thereby ensuring the production of stable microcapsules.

Encapsulation Efficiency

Encapsulation efficiency (EE) of vitamin C was determined using a modified method by (Desai & Park, 2006). A theoretical 90 mg of encapsulated vitamin C was dissolved in 10 mL of water, then was centrifuged at 4000×g for 30 min (Hettic, Universal 320, USA). The transparent part was passed through a 0.2 µm filter (Millipore, USA) and extracted by HCl (0.1 N) Its absorbance was then measured at 244 nm (ʎmax of vitamin C in HCL 0.1 N) after appropriate dilution using a UV spectrophotometer (Perkin Elmer Lambda-2 UV–Visible Spectrophotometer, Germany). The EE was calculated as:

$$EE(\%) = \frac{Total\ Vitamin\ C - free\ Vitamin\ C}{Total\ Vitamin\ C} \times 100 \quad (1)$$

Where Total Vitamin C indicate Theoretical vitamin C concentration in the emulsion and free vitamin C was obtained using a membrane separation method (Desai & Park, 2006).

For vitamin E, encapsulation efficiency was determined according to (Luo *et al.*, 2011). A theoretical 16 mg of vitamin E was dissolved in 10 mL of water, followed by centrifugation at 4000×g for 30 minutes (Hettic, Universal 320, USA). The transparent part was passed through a 0.2 µm filter and extracted by hexane. Then it was analyzed by measuring the absorbance at 290 nm with a UV/Vis spectrophotometer described in previous studies. Measurements were performed in triplicate for accuracy. EE was calculated using:

$$EE\ (\%) = \frac{Total\ Vitamin\ E - free\ Vitamin\ E}{Total\ Vitamin\ E} \times 100 \quad (2)$$

Moisture Content

The moisture content (MC) of the powdered sample was determined gravimetrically by drying in a forced-circulation oven (UFB 400, Memmert, Germany) at 105 °C until a constant weight was achieved, following the AOAC method (AOAC, 2005).

Moisture Absorption (Hygroscopicity)

The hygroscopicity of the produced powders was determined according to (Comunian *et al.*, 2013). Specifically, 0.2 g of sample was placed in a desiccator containing a saturated solution of Na_2SO_4 at 81% relative humidity. After a storage period of one week, hygroscopicity was expressed as the mass of water absorbed per 100 g of sample.

Cumulative Release

The release profile was examined under two simulated conditions: simulated mouth fluid (SMF) and simulated gastric fluid (SGF).

Release in Simulated Mouth Fluid (SMF) Condition

The *in vitro* release study was conducted in simulated mouth fluid (SMF), prepared with sodium bicarbonate, calcium chloride, potassium phosphates, and α-amylase, and adjusted to pH 6.8. The complex emulsion powder was dispersed in SMF and incubated at 37 °C with continuous stirring (100 rpm) for 10 min. Non-encapsulated vitamins were removed by centrifugation at 30,000×g, after which digestion was terminated by adjusting the pH to 7.5. Vitamin C and vitamin E were subsequently extracted using 0.1 M HCl and hexane, respectively. Their concentrations were quantified by UV–Vis spectrophotometry at 244 nm (vitamin C) and 290 nm (vitamin E) using calibration curves of free standards. Release profiles were obtained from measurements taken at 0, 5, and 10 min (Asprea, Leto, Bergonzi, & Bilia, 2017; Desai & Park, 2006; Luo *et al.*, 2011).

Vitamin Release in Simulated Gastric Fluid (SGF) Condition

Vitamin release was assessed in simulated gastric fluid (SGF; pH 2.0, containing 0.1 M HCl and 0.1% w/v pepsin) at 37 °C under continuous stirring for 2 h. The initial release kinetics were evaluated at 0, 60, and 120 min. Non-encapsulated vitamins were separated by centrifugation at 30,000×g, and digestion was terminated by adjusting the pH to 7.5. Vitamin C and vitamin E were subsequently extracted using 0.1 M HCl and hexane, respectively. Quantification was performed by UV–Vis spectrophotometry at 244 nm (vitamin C) and 290 nm (vitamin E), based on calibration curves of free standards (Desai & Park, 2006; Somchue, Sermsri, Shiowatana, & Siripinyanond, 2009).

Spectroscopic Characterization

The spectroscopic characterization of optimum sample, carriers, and vitamins was conducted using Fourier transform infrared (FTIR) spectroscopy, following the methodology described by (Desai & Park, 2005). Briefly, the powdered samples were compressed into KBr disks and analyzed with an FTIR spectrophotometer (Bruker Vector22, USA) within a wave number range of 4000–400 cm^{-1}.

Scanning Electron Microscopy

The microstructural characterization of the optimized powdered complex emulsion was performed using scanning electron microscopy (SEM, EVO 18 Special Edition, Zeiss, Germany), following a slightly modified method based on (Desai & Park, 2006). To examine the morphological properties, the powdered sample was fixed onto metallic adhesive tapes attached to metallic stubs, which were subsequently coated with a thin layer of gold using an evaporator. Imaging was conducted in secondary electron mode under an acceleration voltage of 15 kV.

Statistical Analysis

Response Surface Methodology (RSM) was applied using Design-Expert software (version 13.0, Stat-Ease Inc., Minneapolis, MN, USA) with a central composite design (CCD) to evaluate the effects of whey protein concentrate (2–4% w/w) and chitosan (0.25–0.5% w/w) on encapsulation efficiency (EE), moisture content (MC), and hygroscopicity. The optimization goals, specifying that the study aimed to maximize encapsulation efficiency while minimizing hygroscopicity and moisture content. Model adequacy was verified through analysis of variance (ANOVA), and coefficient of determination (R^2). Statistical comparisons were performed using Duncan's multiple range test in SPSS software (version 22.0), with significance defined at $p < 0.05$. Confirmatory experiments under the predicted optimal conditions showed close agreement between experimental and predicted values, confirming the reliability of the optimization model

Results and Discussion

Encapsulation Efficiency

The encapsulation efficiency (EE) of vitamins C and E was significantly influenced by the concentrations of whey protein concentrate (WPC) and chitosan (CS) via spray drying ($P \leq 0.05$). whereas the encapsulation efficiency of vitamin E was not significantly affected by these factors ($P > 0.05$). As shown in Table 1, the ANOVA results demonstrated that all examined factors had a significant effect on vitamin C encapsulation efficiency after drying ($p \leq 0.05$).

The model is statistically significant ($p < 0.05$), indicating that the fitted model for vitamin C encapsulation efficiency adequately describes the response within the experimental range. Among them, chitosan concentration had the greatest impact, based on the F-value. Increasing WPC or CS concentration reduced vitamin C encapsulation efficiency, ranging from 93.6% to 77.33% (Fig. 1-a), while vitamin E maintained consistently high efficiency (93.36%–93.83%) (Fig. 1-b) with minimal variation.

Table 1- ANOVA of the effect of chitosan and WPC concentration on the efficiency of vitamin C encapsulation

Source	Sum of Squares	df	Mean Square	F Value	p-value
Model	180.70	3	60.23	7.95	0.0238
WPC (g/100g)	55.05	1	55.05	7.27	0.0430
Chitosan (g/100g)	112.09	1	112.09	14.79	0.0120
WPC* Chitosan	13.57	1	13.57	1.79	0.2385
Residual	37.88	5	7.58		

This difference highlights the structural and physicochemical sensitivities of vitamin C compared to the superior stability of vitamin E under diverse formulation environments (Desai & Park, 2005; Hu *et al.*, 2020; Oliveira *et al.*, 2023). Equation 3 presents the regression model used to predict vitamin C encapsulation

efficiency (EE) based on the actual levels of the parameters (R^2 = 0.7904).

$$Vit\ C - EE(\%) = 96.2705 + 2.4961 * WPC\left(\frac{g}{100g}\right) + 9.6222 * Chitosan\left(\frac{g}{100g}\right) - 14.7333 * WPC\left(\frac{g}{100g}\right) * Chitosan(\frac{g}{100g}) \quad (3)$$

Increasing WPC concentration reduced EE due to protein aggregation, which created voids within the microcapsules and promoted surface deposition of the core compounds. This aggregation altered emulsion viscosity, diminished encapsulation uniformity, and reduced compound retention. The decline in EE may be related to larger particle sizes, which could lead to increased heterogeneity and reduced emulsion stability, ultimately compromising capsule integrity (De Queiroz *et al.*, 2018; Hinnenkamp, Reineccius, & Ismail, 2021; Mojtahedi *et al*., 2023).

Similarly, higher CS concentrations also reduced EE. As a polycation, CS interacts with WPC through electrostatic associations, steric crowding, and hydrogen bonding. When the WPC-to-CS ratio is imbalanced, excessive polymer entanglement decreases system stability and promotes leakage of hydrophilic compounds such as vitamin C.

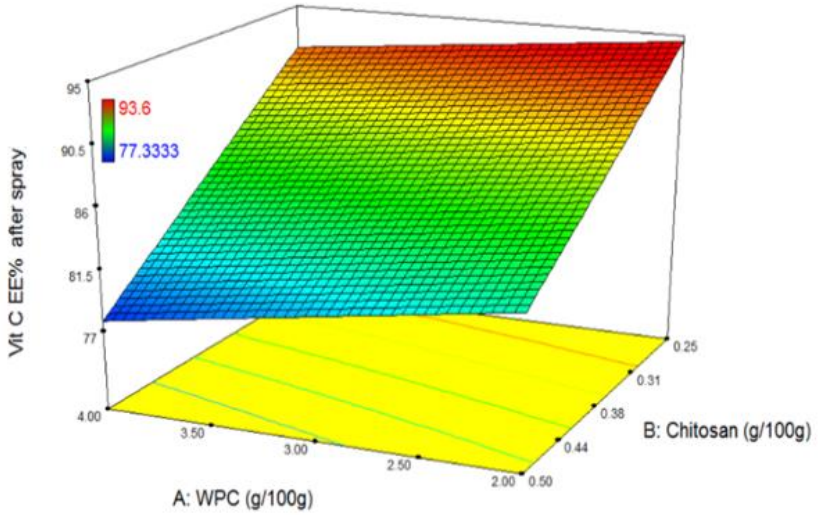

Fig. 1. a–Surface diagram of the effect of WPC and chitosan concentration on EE vitamin C

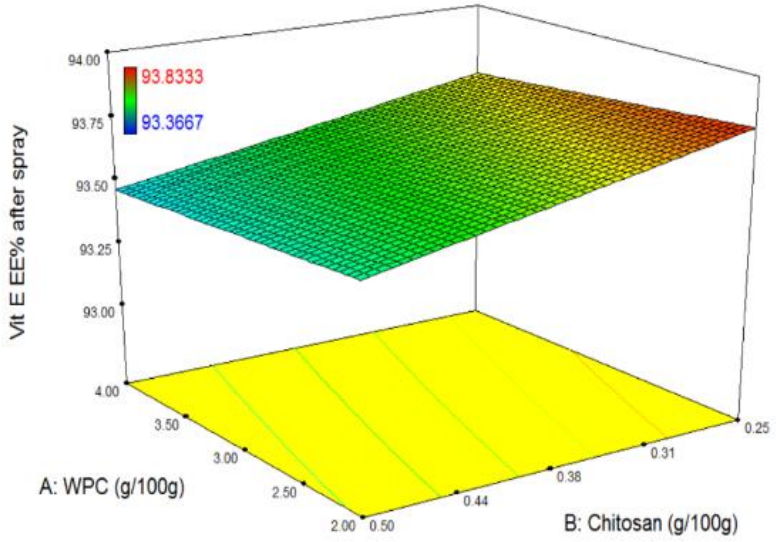

Fig. 1. b- Surface plot of the effect of WPC and chitosan concentration on EE vitamin E

This electrostatic-driven mechanism explains why balanced formulations maintained higher EE, whereas excessive wall material concentrations reduced efficiency (Liu, Jing, Han, Zhang, & Tian, 2019). In contrast, encapsulation efficiency for vitamin E remained relatively stable, owing to its lipophilic nature and lower sensitivity to variations in wall material concentration (Barbosa, Borsarelli, & Mercadante, 2005). This highlights the distinct physicochemical behavior of hydrophilic versus lipophilic compounds in encapsulation systems, where electrostatic interactions play a dominant role for hydrophilic molecules but less so for lipophilic ones. An increase in particle size combined with a decrease in zeta potential directly compromised colloidal stability and thereby reduced EE. Larger particles exhibited lower surface area-to-volume ratios and a higher tendency to aggregate, which led to void formation and heterogeneity in the capsule wall. At the same time, reduced zeta potential indicated weaker electrostatic repulsion between particles, facilitating aggregation and leakage of encapsulated compounds. This phenomenon was often accompanied by higher PDI values, confirming reduced uniformity and stability of the emulsion system.

These findings are consistent with previous studies, supporting and corroborating the results obtained in the present work. Mojtahedi *et al.* (2023) demonstrated that increased particle size and reduced zeta potential in protein-based complexes resulted in lower emulsion stability and decreased EE. Likewise, Hinnenkamp *et al*. (2021) and De Queiroz *et al*. (2018) showed that protein aggregation and diminished surface charge promoted particle heterogeneity and reduced encapsulation efficiency of hydrophilic compounds. Xu, Lv, Mu, Zhou, & Yang, (2021) reported an EE of 86.3% for α-tocopherol in WPC–CS complexes, while Agustinisari, Mulia, & Nasikin, (2020) demonstrated enhanced emulsion stability and improved EE for eugenol. Wang *et al. (2021)* highlighted superior efficiency (60.70%) in WPI nanocomplexes compared to ACNs, CS, and CMC formulations. De Queiroz *et al*. (2018) achieved remarkably high efficiencies (98.5%) for CS–WPC microcapsules, and Lekshmi *et al*. (2019) documented an EE of 75.40% for squalene encapsulated with WPC and CS. These studies reinforce the conclusion that balanced wall material systems are critical for achieving high encapsulation efficiency.

Moisture Content

The moisture content of microcapsules prepared with varying concentrations of WPC and CS was systematically analyzed. Results indicated a significant inverse relationship between wall material concentration and moisture content ($P < 0.05$), as illustrated in Table 2 and Fig. 2.

Table 2- ANOVA of the effect of chitosan and WPC concentration on the efficiency of moisture content

Source	Sum of Squares	df	Mean Square	F Value	p-value
Model	0.16	3	0.053	52.05	0.0003
WPC (g/100g)	0.15	1	0.15	148.9	0.0001
Chitosan (g/100g)	0.00735	1	0.00735	7.18	0.0439
WPC* Chitosan	0.00007	1	0.00007	0.068	0.8050
Residual	0.00512	5	0.00104		

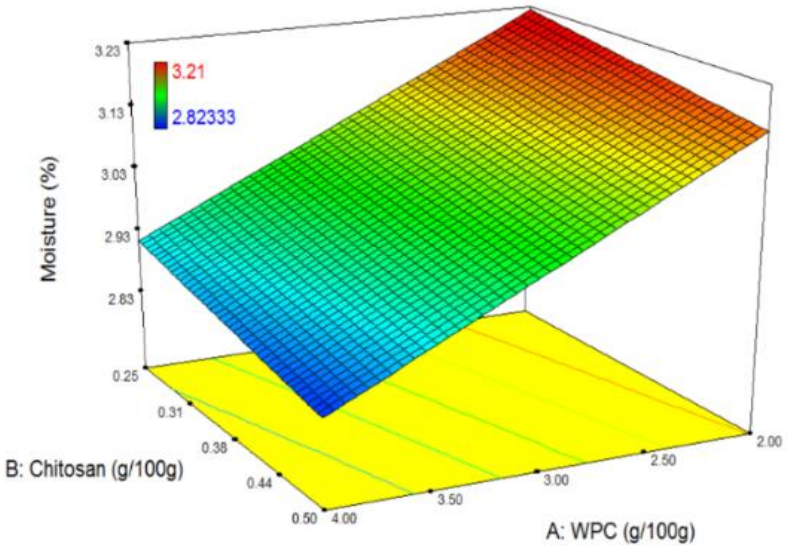

Fig. 2. Surface plot of the effect of WPC and chitosan concentration on moisture content

The model was found to be statistically significant ($p < 0.05$), suggesting that it provides an adequate representation of the response across the experimental range. Higher concentrations of WPC and CS reduced moisture content (2.82% at 4% WPC, 0.5% CS), whereas lower concentrations resulted in greater retention (3.21%). This reduction highlights the role of wall materials in regulating water evaporation and underscores final moisture content as a key quality control parameter affecting stability and product quality (Díaz-Montes, 2023). Equation 4 presents the regression model used to predict the moisture content of microcapsules based on the actual levels of the parameters (R^2 = 0.9690).

$$Moisture(\%) = 3.5795 - 0.1469 * WPC\left(\frac{g}{100g}\right) - 0.18 * Chitosan\left(\frac{g}{100g}\right) - 0.0333 * WPC\left(\frac{g}{100g}\right) * Chitosan\left(\frac{g}{100g}\right) \quad (4)$$

The functional groups in WPC (–NH_2, –COOH, –OH) and CS (–OH, –NH_2) facilitate stronger interactions with water molecules, promoting faster evaporation and thereby reducing residual moisture in the final powder. At higher concentrations, these groups facilitate more efficient water binding during atomization and promote faster evaporation during spray-drying, thereby reducing residual moisture. This functional group-driven mechanism explains the observed decrease in moisture content with increasing wall material concentration, consistent with previous studies (Chen *et al.*, 2018; Pinto *et al.*, 2021).

Similar findings have been reported for other wall materials such as gum Arabic (Frascareli, Silva, Tonon, & Hubinger, 2012) and UDP-coated WPC (Choi & Chang, 2018), where functional groups enhanced water interactions and reduced moisture retention. Maintaining moisture levels within the range of 3–10% has been shown to improve oxidative stability of microencapsulated oils (Klaypradit & Huang, 2008), while a final moisture content of ~5% is considered optimal for structural stability and retention of bioactive compounds (Stabrauskiene, Pudziuvelyte, & Bernatoniene, 2024).

Moisture Absorption (Hygroscopicity)

The encapsulation system's hygroscopicity was significantly influenced by WPC concentration ($P \leq 0.05$), while its interaction with CS was not significant ($P > 0.05$). As shown in Table 3, the ANOVA results demonstrated that all factors had a significant effect on hygroscopicity ($p \leq 0.05$).

Table 3- ANOVA of the effect of chitosan and WPC concentration on the efficiency of moisture absorption

Source	Sum of Squares	df	Mean Square	F Value	p-value
Model	8.97	3	2.99	82.01	0.0001
WPC (g/100g)	8.09	1	8.09	221.84	0.0001
Chitosan (g/100g)	0.88	1	0.88	24.18	0.0044
WPC* Chitosan	0.00027	1	0.00027	0.0076	0.9338
Residual	0.18	5	0.036		

The model is statistically significant ($p < 0.05$), indicating that the fitted model adequately describes the response within the experimental range. Equation 5 presents the regression model used to predict the moisture absorption of microcapsules based on the actual levels of the parameters ($R^2 = 0.9801$).

$$Moisture(\%) = 9.775 + 1.1361 * WPC\left(\frac{g}{100g}\right) + 2.8666 * Chitosan\left(\frac{g}{100g}\right) + 0.0666 * WPC\left(\frac{g}{100g}\right) * Chitosan\left(\frac{g}{100g}\right) \quad (5)$$

Increasing WPC and CS levels raised hygroscopicity up to 15.8%, indicating their role in water retention and microcapsule stability (Fig. 3). The hydrophilic functional groups of chitosan (–OH, $–NH_2$) and WPC promote moisture uptake (Carvalho-Silva, 2013), which contributes to controlled swelling and the formation of a gel-like matrix. This matrix acts as a physical barrier, limiting oxygen and light penetration and thereby enhancing the stability of encapsulated bioactive compounds (Chen, Mao, Hou, Yuan, & Gao, 2020). Moisture absorption also improves the physical integrity of spray-dried microcapsules by softening the wall structure and reducing cracking or rupture (Li *et al.*, 2022). When the dried powders are exposed to ambient humidity, the hydrophilic functional groups act as active sites for water sorption. Their abundance in CS and WPC increases the powder's affinity for atmospheric moisture, leading to higher hygroscopicity. From a biological perspective, enhanced hydration increases biocompatibility and supports controlled release in gastrointestinal environments (Pateiro *et al.*, 2021).

However, excessive moisture absorption may compromise wall integrity, accelerate compound release, and promote microbial growth, underscoring the need for optimized wall composition and humidity control. Comparisons with previous studies confirm the hygroscopic nature of WPC-based formulations. Beetroot spray-dried microparticles retained 11.13–15.59% moisture (Bazaria & Kumar, 2016), while WPC–inulin blends encapsulating rosemary essential oil absorbed 15.7–17.1% moisture (Fernandes *et al.*, 2014). These findings highlight the importance of balancing WPC and CS concentrations to achieve structural stability while minimizing adverse effects of excessive hydration.

Release of Encapsulated Vitamins C and E under Simulated Mouth Fluids

The release behaviors of vitamins C and E under SMF conditions at 0, 5, and 10 minutes are shown in Table 4, Statistical analysis confirmed that neither chitosan nor WPC concentration had a significant effect on the release of vitamins E and C under simulated mouth conditions ($p > 0.05$). Vitamin E showed no measurable release throughout the 10-minute testing period, indicating strong retention within the encapsulation matrix under neutral pH conditions. In contrast, vitamin C exhibited only a minimal release (~0.1%), likely due to electrostatic interactions between WPC and CS at neutral pH, which restrict diffusion and solubility. Such interactions play a key role in controlling release behavior.

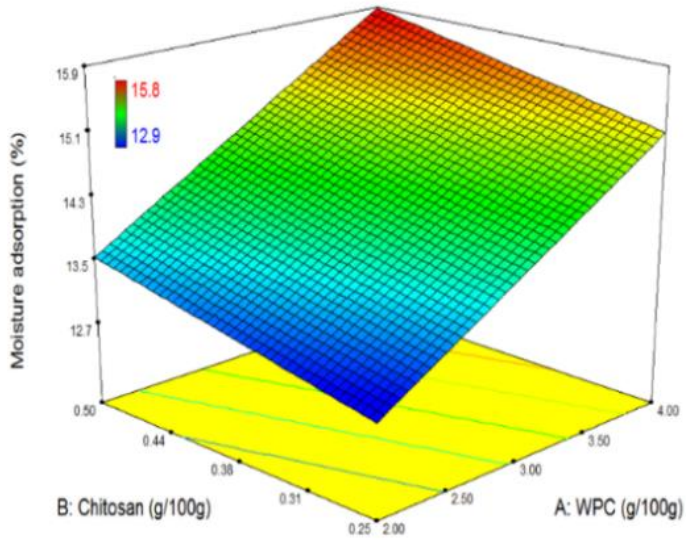

Fig. 3. Surface plot of the effect of WPC and chitosan concentration on moisture absorption

Table 4- Comparison of average results of vitamin E and C release studies in simulated mouth fluid

Row	WPC (%)	Chitosan (%)	Time (Min)	Vitamin C release (%)	Vitamin E release (%)
1	2	0.25	0	0.06[a]	0[a]
2	2	0.25	5	0.07[a]	0[a]
3	2	0.25	10	0.07[a]	0[a]

Different letters in each column indicate significant differences (P<0.05).

The remarkably low release observed under SMF conditions has important practical implications. By preventing premature diffusion of bioactive compounds in the oral cavity, the encapsulation system effectively avoids undesirable taste perception and enhances consumer acceptability. This functional control ensures that sensitive compounds remain protected until reaching the stomach, where targeted release and absorption can occur.

Encapsulation plays a pivotal role in controlling the release of bioactive compounds within target environments. The strong retention of vitamins in neutral conditions (e.g., SMF) ensures that premature release is minimized. This functional control must be maintained across different stages of digestion to guarantee that bioactive compounds are only released in the intended site, such as the stomach, where absorption can occur effectively. The controlled release of vitamins provides an advantage by reducing nitrite accessibility through enhanced interaction with encapsulated antioxidants. This targeted release not only improves product stability but also strengthens food safety by limiting nitrosamine formation (Rot, Kovačević, Habschied, & Mastanjević, 2025).

Previous studies have highlighted similar applications of encapsulation systems. For instance, Mohammadi, Ehsani, & Bakhoda, (2018) demonstrated that alginate-based microcapsules modulated caffeine release, while De Queiroz *et al*. (2018), reported high retention efficiencies in CS–WPC complexes. Similar findings have been reported in probiotic encapsulation studies, where controlled release ensured survival through the oral phase and targeted delivery in the intestine (Anal & Singh, 2007).

Release of Encapsulated Vitamins C and E under Simulated Gastric Fluid

Table 5 provides a comparative overview of the release patterns of vitamins C and E under simulated gastric fluid (SGF) conditions at 0, 60, and 120 minutes, using optimized samples obtained through response surface

methodology (RSM). Both vitamins C and E exhibited a clear time-dependent increase in release under simulated gastric conditions. Statistical analysis confirmed significant differences among the three sampling times ($p < 0.05$).

Table 5- Comparison of average results of vitamin E and C release studies in simulated gastric floid

Row	WPC (%)	Chitosan (%)	Time (Min)	Vitamin C Release (%)	Vitamin E Release (%)
1	2	0.25	0	56.85[a]	0.93[a]
2	2	0.25	60	69.44[b]	9.58[b]
3	2	0.25	120	85.74[c]	31.45[c]

Different letters in each column indicate significant differences (P<0.05).

Vitamin E exhibited minimal release at the beginning (0.93%), which gradually increased to 31.45% after 120 minutes. In contrast, vitamin C showed a markedly higher release, with 56.85% released initially and a cumulative release of 85.74% after 120 minutes. This behavior can be explained by several mechanistic factors. First, under SGF conditions, the release mechanism is strongly influenced by gastric acidity and enzymatic activity. The acidic pH (pH ≈ 1.2) leads to protonation of CS, which reduces its electrostatic binding capacity and accelerates vitamin C diffusion. Simultaneously, pepsin-induced denaturation of whey protein disrupts the protein matrix, further enhancing release. In contrast, vitamin E release remains limited because of its hydrophobic nature and stronger entrapment within the polymeric wall, which resists enzymatic degradation and proton-mediated diffusion (Tan *et al.*, 2020; Xu, Tang, Yang, Wang, & Zhou, 2020). Consistent with these observations, Hu *et al.* (2020) reported curcumin release values between 20.3% and 24.8% from whey protein–CS microcapsules after two hours in SGF, reinforcing the influence of wall material composition, electrostatic interactions, and gastric acidity on controlled release. Similarly, Pudjiastuti *et al.* (2020) emphasized that release is governed not only by solubility but also by polymer structure and capsule integrity. Xu *et al.* (2021) reported accelerated release of hydrophilic bioactive in acidic environments due to protonation-induced matrix loosening, while Barbosa *et al.* (2005), emphasized the stability of lipophilic compounds in protein–polysaccharide complexes. These findings emphasize that nutrient release is not solely dependent on solubility but is governed by a complex interplay of polymer structure, electrostatic binding, enzymatic degradation, and matrix hydrophobicity, all of which must be considered in designing targeted encapsulation strategies for enhanced bioavailability.

Scanning Electron Microscopy

Scanning electron microscopy (SEM) images revealed notable variations in particle size and surface morphology among the encapsulated vitamins C and E, indicating a polydisperse nature of the microcapsules (Fig. 4). This observation is consistent with the inherent characteristics of spray-drying processes, where atomization typically generates particles with non-uniform sizes due to rapid droplet formation and drying kinetics (Lekshmi *et al.*, 2019). Such polydispersity is a well-documented phenomenon in spray-dried systems and is often influenced by nozzle type, feed composition, and drying temperature (Schmitt, Baumann, & Morgen, 2022).

The wrinkled surface morphology observed in the SEM micrographs is likely a result of premature solidification of the wall material prior to complete internal vapor expansion. This leads to surface collapse and structural deformation, as previously reported in systems encapsulating linoleic acid with maltodextrin and WPC (Choi, Ryu, Kwak, & Ko, 2010). Similar morphological features have been described in recent studies, where wall material composition and drying conditions were shown to significantly affect particle shape and integrity (Díaz-Montes, 2023; Wang & Mutukumira, 2022).

Moreover, the sample containing 2% WPC and 0.25% chitosan exhibited smaller particle size and higher dispersion, suggesting improved emulsification and stabilization during atomization. This aligns with findings by (Suwannasang *et al.*, 2022), who demonstrated that optimized protein–polysaccharide combinations enhance colloidal stability and reduce particle aggregation in spray-dried formulations. Overall, the observed polydispersity and morphological variations underscore the importance of wall material selection and process optimization in achieving consistent particle characteristics.

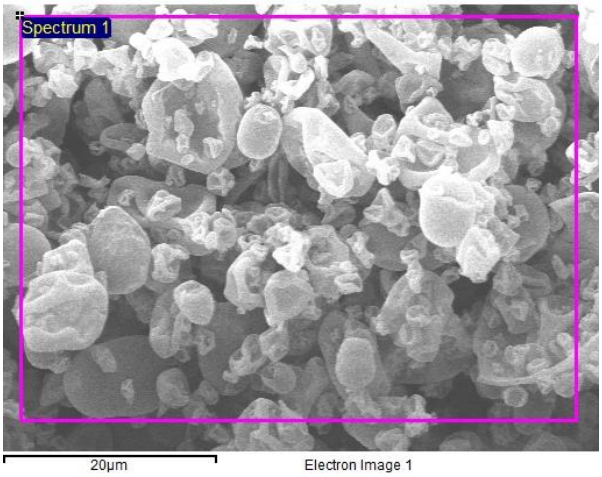

Fig. 4. Scanning electron microscope images of sample9

FT-IR Analysis

The FT-IR analysis can be applied to the intermolecular and structural characterization of complex materials. The FTIR spectrums of encapsulated vitamin C and vitamin E in samples (9) are shown in Fig. 5. Vitamin C shows property bands in the number of waves that vary from 2924–3989 cm^{-1} owing to CH3 stretching. Vitamin E exhibits symmetric bending and methyl asymmetric peaks emerge at 1403 cm^{-1} and 1442 cm^{-1}, respectively. The ether group emerges at 1075 cm^{-1}. The phenol C–O stretching emerges at 1245 cm^{-1} while the C–H stretching absorption peak appears at 2924 cm^{-1} and 2966 cm^{-1}.

FTIR analysis revealed characteristic peaks for vitamin C (2911–3024 cm^{-1}) and vitamin E (1378 and 1466 cm^{-1}), along with functional groups such as ether (1093 cm^{-1}), phenol (1260 cm^{-1}), and C-H stretching (2847 and 2918 cm^{-1}), that are consistent with Pang *et al.* (2017). WPC showed distinctive bands between 1651 and 1547 cm^{-1} corresponding to amide I and II, in line with Dickinson, Radford, & Golding, (2003), who reported peaks in this range. An amide III band at 1245 cm^{-1}, attributed to N-H deformation and C=N stretching, was also observed. Chitosan exhibited peaks at 1075 cm^{-1} (C-O-C), 3289 cm^{-1} (-OH and NH2 stretching), 1651 cm^{-1} (amide I), and 2966 cm^{-1} (CH stretching), as reported by Lekshmi *et al.* (2019). All characteristic peaks of the wall materials and vitamins appeared similarly in the spectra of encapsulated samples, indicating no structural interaction between core and wall materials. Muley & Singhal (2020) confirmed conjugation between chitosan and WPI through bands at 1546.09 and 1639.58 cm^{-1}. Finally, in our study, the conjugation confirmation between CS and WPC was seen from bands at 1547 and 1651 cm^{-1} that showed the Schiff base formation. It was formed between the groups of amino (CS and WPC) and the groups of carboxylic and/or hydroxyl of acetic acid. The observed alterations in the structural fractions might result from the conjugation of WPC with CS.

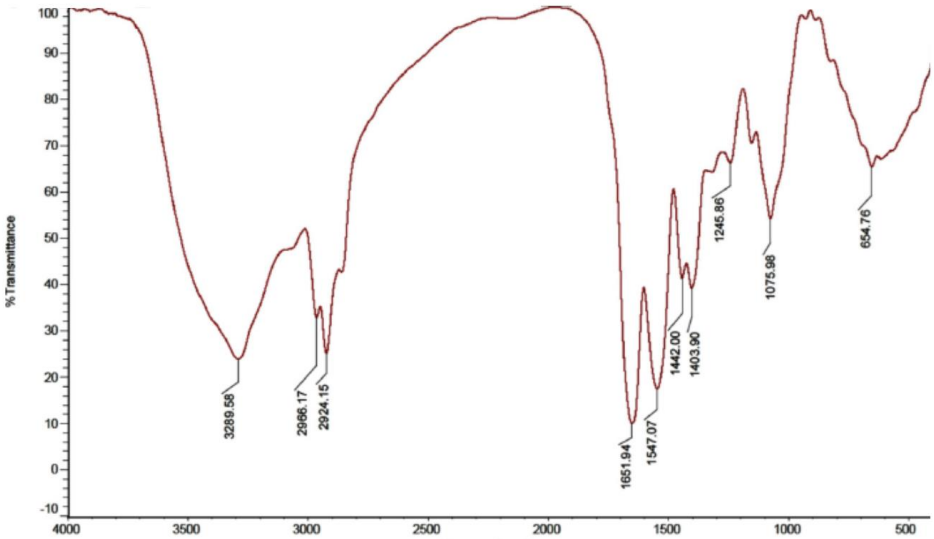

Fig. 5. FTIR spectra of sample 9

Conclusion

A new set of wall materials was used to prepare microcapsules. CS-WPC was confirmed as an effective delivery system for vitamins C and E, showing high encapsulation efficiency and optimal moisture content and water absorption capacity. The optimal formulation, with WPC at 2.0%, CS at 0.25%, was selected. The microcapsules were mostly spherical with rugged surfaces. SEM images revealed that the particle size was fine and well-scattered. Schiff base formation between CS and WPC was confirmed by bands at 1547 and 1651 cm^{-1}, indicating a reaction between acetic acid's carboxyl groups and amino groups in both polymers. These structural changes are likely due to the conjugation process. The results showed that the encapsulated vitamins remained stable in SMF but were released in SGF. Overall, encapsulating vitamins C and E in CS-WPC via spray drying appears to be a promising approach for developing stable encapsulates for functional foods.

Author Contribution

Pooneh Mojtahedi: Conceptualization, Data curation, Formal analysis, Investigation, Methodology, Software, Validation, Visualization, Writing – original draft. **Mehdi Varidi:** Supervision, Project administration, Resources, Funding acquisition, Validation, Writing– review and editing. **Amir M. Mortazavian:** Supervision, Project administration, Resources, Funding acquisition, Validation, Writing – review and editing.

Founding Source

The authors declare that they have no competing interests and no funding source.

References

1. Agudelo-Chaparro, J., Ciro-Velásquez, H.J., Sepúlveda-Valencia, J.U., & Pérez-Monterroza, E.J. (2022). Microencapsulation of *Lactobacillus rhamnosus* ATCC 7469 by spray drying using maltodextrin, whey protein concentrate and trehalose. *Food Science and Technology International*, *28*(6), 476-488. https://doi.org/10.1177/10820132211020621
2. Agustinisari, I., Mulia, K., & Nasikin, M. (2020). Physical and chemical properties of encapsulated eugenol using whey protein-maltodextrin mixed solution and chitosan as

emulsifier and wall materials. *AIP Conference Proceedings, 2255*(1), 1-7. https://doi.org/10.1063/5.0013758

3. Anal, A.K., & Singh, H. (2007). Recent advances in microencapsulation of probiotics for industrial applications and targeted delivery. *Trends in Food Science & Technology*, *18*(5), 240-251. https://doi.org/10.1016/j.tifs.2007.01.004
4. AOAC. (2005). Determination of moisture, ash ,protein and fat. Official method of analysis of the association of analytical chemists. In: AOAC Washington DC.
5. Askari Vaselabadi, S., Gharibzahedi, S.M.T., Greiner, R., Vale, J.M., Ovenseri, A.C., Rashidinejad, A., & Roohinejad, S. (2025). Advancements in spray-drying for the microencapsulation of fat-soluble vitamins: Stability, bioavailability, and applications. *Journal of Food Biochemistry*, *2025*(1), 9974476. https://doi.org/10.1155/jfbc/9974476
6. Asprea, M., Leto, I., Bergonzi, M.C., & Bilia, A.R. (2017). Thyme essential oil loaded in nanocochleates: Encapsulation efficiency, in vitro release study and antioxidant activity. *LWT*, *77*, 497-502. https://doi.org/10.1016/j.lwt.2016.12.006
7. Barbosa, M., Borsarelli, C., & Mercadante, A. (2005). Light stability of spray-dried bixin encapsulated with different edible polysaccharide preparations. *Food Research International*, *38*(8-9), 989-994. https://doi.org/10.1016/j.foodres.2005.02.018
8. Bazaria, B., & Kumar, P. (2016). Effect of whey protein concentrate as drying aid and drying parameters on physicochemical and functional properties of spray dried beetroot juice concentrate. *Food Bioscience*, *14*, 21-27. https://doi.org/10.1016/j.fbio.2015.11.002
9. Budinčić, J.M., Petrović, L., Đekić, L., Fraj, J., Bučko, S., Katona, J., & Spasojević, L. (2021). Study of vitamin E microencapsulation and controlled release from chitosan/sodium lauryl ether sulfate microcapsules. *Carbohydrate polymers*, *251*, 116988. https://doi.org/10.1016/J.CARBPOL.2020.116988
10. Carvalho-Silva, L.B.D. (2013). Physico-chemical properties of milk whey protein agglomerates for use in oral nutritional therapy *Food and Nutrition Sciences*, *4*(9), 69-78. https://doi.org/10.4236/fns.2013.49a210
11. Chang, C., & Nickerson, M.T. (2018). Encapsulation of omega 3-6-9 fatty acids-rich oils using protein-based emulsions with spray drying. *Journal of Food Science and Technology*, *55*(8), 2850-2861. https://doi.org/10.1007/s13197-018-3257-0
12. Chen, H., Mao, L., Hou, Z., Yuan, F., & Gao, Y. (2020). Roles of additional emulsifiers in the structures of emulsion gels and stability of vitamin E. *Food Hydrocolloids*, *99*, 105372. https://doi.org/10.1016/j.foodhyd.2019.105372
13. Chen, X., McClements, D.J., Wang, J., Zou, L., Deng, S., Liu, W., Yan, C., Zhu, Y., Cheng, C., & Liu, C. (2018). Coencapsulation of (−)-Epigallocatechin-3-gallate and quercetin in particle-stabilized W/O/W emulsion gels: Controlled release and bioaccessibility. *Journal of Agricultural and Food Chemistry*, *66*(14), 3691-3699. https://doi.org/10.1021/ACS.JAFC.7B05161
14. Chen, Y., Zhu, C., Zhao, Y., Zhang, S., & Wang, W. (2022). Transcriptomics integrated with changes in cell wall material of chestnut (*Castanea mollissima* Blume) during storage provides a new insight into the "calcification" process. *Foods*, *11*(8), 1136. https://doi.org/10.3390/foods11081136
15. Choi, K.-O., Ryu, J., Kwak, H.-S., & Ko, S. (2010). Spray-dried conjugated linoleic acid encapsulated with Maillard reaction products of whey proteins and maltodextrin. *Food Science and Biotechnology*, *19*(4), 957-965. https://doi.org/10.1007/S10068-010-0134-7
16. Choi, Y.-R., & Chang, Y.H. (2018). Microencapsulation of gallic acid through the complex of whey protein concentrate-pectic polysaccharide extracted from *Ulmus davidiana*. *Food Hydrocolloids*, *85*, 222-228. https://doi.org/10.1016/j.foodhyd.2018.07.022.

17. Comunian, T.A., Thomazini, M., Alves, A.J.G., de Matos Junior, F.E., de Carvalho Balieiro, J.C., & Favaro-Trindade, C.S. (2013). Microencapsulation of ascorbic acid by complex coacervation: Protection and controlled release. *Food Research International*, *52*(1), 373-379. https://doi.org/10.1016/j.foodres.2013.03.028
18. De Queiroz, J.L.C., Costa, R.O.D.A., Matias, L.L.R., De Medeiros, A.F., Gomes, A.F.T., Pais, T.D.S., Passos, T.S., Maciel, B.L.L., Dos Santos, E.A., & Morais, A.H.D.A. (2018). Chitosan-whey protein nanoparticles improve encapsulation efficiency and stability of a trypsin inhibitor isolated from *Tamarindus indica* L. *Food Hydrocolloids*, *84*, 247-256. https://doi.org/10.1016/j.foodhyd.2018.06.010
19. Delaporte, A., Duchemin, B., Grisel, M., & Gore, E. (2024). Impact of wall material-to-active ratio in the stability of spray-dried ascorbic acid using maltodextrin and gum arabic. *Molecules*, *29*(15), 3587. https://doi.org/10.3390/molecules29153587
20. Desai, K., & Park, H. (2005). Encapsulation of vitamin C in tripolyphosphate cross-linked chitosan microspheres by spray drying. *Journal of Microencapsulation*, *22*(2), 179-192. https://doi.org/10.1080/02652040400026533
21. Desai, K., & Park, H.J. (2006). Effect of manufacturing parameters on the characteristics of vitamin C encapsulated tripolyphosphate-chitosan microspheres prepared by spray-drying. *Journal of Microencapsulation*, *23*(1), 91-103. https://doi.org/10.1080/02652040500435436
22. Díaz-Montes, E. (2023). Wall materials for encapsulating bioactive compounds via spray-drying: A review. *Polymers*, *15*(12), 2659. https://doi.org/10.3390/polym15122659
23. Dickinson, E., Radford, S.J., & Golding, M. (2003). Stability and rheology of emulsions containing sodium caseinate: combined effects of ionic calcium and non-ionic surfactant. *Food Hydrocolloids*, *17*(2), 211-220. https://doi.org/10.1016/S0268-005X(02)00055-3
24. Fernandes, R.V.D.B., Borges, S.V., Botrel, D.A., & de Oliveira, C.R. (2014). Physical and chemical properties of encapsulated rosemary essential oil by spray drying using whey protein–inulin blends as carriers. *International Journal of Food Science and Technology*, *49*(6), 1522-1529. https://doi.org/10.1111/ijfs.12449
25. Frascareli, E., Silva, V., Tonon, R., & Hubinger, M. (2012). Effect of process conditions on the microencapsulation of coffee oil by spray drying. *Food and Bioproducts Processing*, *90*(3), 413-424. https://doi.org/10.1016/j.fbp.2011.12.002
26. Guldiken, B., Linke, A., Capanoglu, E., Boyacioglu, D., Kohlus, R., Weiss, J., & Gibis, M. (2019). Formation and characterization of spray dried coated and uncoated liposomes with encapsulated black carrot extract. *Journal of Food Engineering*, *246*, 42-50. https://doi.org/10.1016/j.jfoodeng.2018.10.025
27. Hinnenkamp, C., Reineccius, G., & Ismail, B.P. (2021). Efficient encapsulation of fish oil: Capitalizing on the unique inherent characteristics of whey cream and hydrolyzed whey protein. *Journal of Dairy Science*, *104*(6), 6472-6486. https://doi.org/10.3168/jds.2020-19880
28. Hu, Y., He, C., Jiang, C., Liao, Y., Xiong, H., & Zhao, Q. (2020). Complexation with whey protein fibrils and chitosan: A potential vehicle for curcumin with improved aqueous dispersion stability and enhanced antioxidant activity. *Food Hydrocolloids*, *104*, 105729. https://doi.org/10.1016/j.foodhyd.2020.105729
29. Katouzian, I., & Jafari, S.M. (2016). Nano-encapsulation as a promising approach for targeted delivery and controlled release of vitamins. *Trends in Food Science & Technology*, *53*, 34-48. https://doi.org/10.1016/j.tifs.2016.05.002
30. Klaypradit, W., & Huang, Y.-W. (2008). Fish oil encapsulation with chitosan using ultrasonic atomizer. *LWT-Food Science and Technology*, *41*(6), 1133-1139. https://doi.org/10.1016/j.lwt.2007.06.014
31. Lan, Y., Ohm, J.-B., Chen, B., & Rao, J. (2021). Microencapsulation of hemp seed oil by pea protein isolate −sugar beet pectin complex coacervation: Influence of coacervation pH and

wall/core ratio. *Food Hydrocolloids*, *113*, 106423. https://doi.org/10.1016/j.foodhyd.2020.106423

32. Lekshmi, R.K., Rahima, M., Chatterjee, N., Tejpal, C., Anas, K., Vishnu, K., Sarika, K., Asha, K., Anandan, R., & Suseela, M. (2019). Chitosan–Whey protein as efficient delivery system for squalene: Characterization and functional food application. *International Journal of Biological Macromolecules*, *135*, 855-863. https://doi.org/10.1016/j.ijbiomac.2019.05.153
33. Li, K.-Y., Zhou, Y., Huang, G.-Q., Li, X.-D., & Xiao, J.-X .(2022). Preparation of powdered oil by spray drying the Pickering emulsion stabilized by ovalbumin–gum Arabic polyelectrolyte complex. *Food Chemistry*, *391*, 133223. https://doi.org/10.1016/J.FOODCHEM.2022.133223
34. Liu, Q., Jing, Y., Han, C., Zhang, H., & Tian, Y. (2019). Encapsulation of curcumin in zein/caseinate/sodium alginate nanoparticles with improved physicochemical and controlled release properties. *Food Hydrocolloids*, *93*, 432-442. https://doi.org/10.1016/j.foodhyd.2019.02.003
35. Luo, Y., Zhang, B., Whent, M., Yu, L.L., & Wang, Q. (2011). Preparation and characterization of zein/chitosan complex for encapsulation of α-tocopherol, and its in vitro controlled release study. *Colloids and Surfaces B: Biointerfaces*, *85*(2), 145-152. https://doi.org/10.1016/J.COLSURFB.2011.02.020
36. Mohammadi, N., Ehsani, M.R., & Bakhoda, H. (2018). Design and evaluation of the release characteristics of caffeine-loaded microcapsules in a medicated chewing gum formulation. *Food Biophysics*, *13*(3), 240-249. https://doi.org/10.1007/s11483-018-9530-y
37. Mojtahedi, P., Mortazavian, S.A.M., & Varidi, M. (2023). Encapsulation of vitamins E and C in whey protein concentrate-chitosan emulation: Physicochemical properties. *Management Strategies and Engineering Sciences*, *5*(4), 136-146. https://msesj.com/index.php/mses/article/view/183
38. Muley, A.B., & Singhal, R.S. (2020). Extension of postharvest shelf life of strawberries (*Fragaria ananassa*) using a coating of chitosan-whey protein isolate conjugate. *Food Chemistry*, *329*, 12-72. https://doi.org/10.1016/j.foodchem.2020.127213
39. Oliveira, N.L., Espinal-Ruiz, M., Neves, I.C.O., Silva, S.H., de Resende, J.V., & Rogers, M.A. (2023). Evaluation of α-tocopherol microencapsulation stability with either coconut oil or canola oil cores in Greek yogurt and butter. *Food Chemistry Advances*, *2*, 100277. https://doi.org/10.1016/j.focha.2023.100277
40. Pang, Y., Qin, A., Lin, X., Yang, L., Wang, Q., Wang, Z., Shan, Z., Li, S., Wang, J., & Fan, S. (2017). Biodegradable and biocompatible high elastic chitosan scaffold is cell-friendly both in vitro and in vivo. *Oncotarget*, *8*(22), 35583. https://doi:10.18632/oncotarget.14709
41. Pateiro, M., Gómez, B., Munekata, P.E., Barba, F.J., Putnik, P., Kovačević, D.B., & Lorenzo, J.M. (2021). Nanoencapsulation of promising bioactive compounds to improve their absorption, stability, functionality and the appearance of the final food products. *Molecules*, *26*(6), 1547. https://doi.org/10.3390/molecules26061547
42. Pinto, J.T., Faulhammer, E., Dieplinger, J., Dekner, M., Makert, C., Nieder, M., & Paudel, A. (2021). Progress in spray-drying of protein pharmaceuticals: Literature analysis of trends in formulation and process attributes. *Drying Technology*, *39*(11), 1415-1446. https://doi.org/10.1080/07373937.2021.1903032
43. Pudjiastuti, P., Wafiroh, S., Hendradi, E., Darmokoesoemo, H., Harsini, M., Fauzi, M.A.R.D., Nahar, L., & Sarker, S.D. (2020). Disintegration, in vitro dissolution, and drug release kinetics profiles of k-carrageenan-based nutraceutical hard-shell capsules containing salicylamide. *Open Chemistry*, *18*(1), 226-231. https://doi.org/10.1515/chem-2020-0028
44. Rabkin, B., Tirosh, O., & Kanner, J. (2022). Reactivity of vitamin E as an antioxidant in red meat and the stomach medium. *Journal of Agricultural and Food Chemistry*, *70*(38), 12172-12179. https://doi.org/10.1021/ACS.JAFC.2C03674

45. Rot, T., Kovačević, D., Habschied, K., & Mastanjević, K. (2025). N-nitrosamines in meat products: formation, detection and regulatory challenges. *Processes*, *13*(5), 1555. https://doi.org/10.3390/pr13051555
46. Schmitt, J.M., Baumann, J.M., & Morgen, M.M. (2022). Predicting spray dried dispersion particle size via machine learning regression methods: Schmitt, Baumann and Morgen. *Pharmaceutical Research*, *39*(12), 3223-3239. https://doi.org/10.1007/s11095-022-03370-3
47. Somchue, W., Sermsri, W., Shiowatana, J., & Siripinyanond, A. (2009). Encapsulation of α-tocopherol in protein-based delivery particles. *Food Research International*, *42*(8), 909-914. https://doi.org/10.1016/J.FOODRES.2009.04.021
48. Stabrauskiene, J., Pudziuvelyte, L., & Bernatoniene, J. (2024). Optimizing encapsulation: Comparative analysis of spray-drying and freeze–drying for sustainable recovery of bioactive compounds from *Citrus x paradisi* L. peels. *Pharmaceuticals*, *17*(5), 596. https://doi.org/10.3390/ph17050596
49. Suwannasang, S., Zhong, Q., Thumthanaruk, B., Uttapap, D., Puttanlek, C., Vatanyoopaisarn, S., & Rungsardthong, V. (2022). Optimization of wall material composition for production of spray-dried Sacha inchi oil microcapsules with desirable physicochemical properties. *Food and Bioprocess Technology*, *15*(11), 2499-2514. https://doi.org/10.1007/s11947-022-02893-2
50. Tan, Y., Li, R., Liu, C., Mundo, J.M., Zhou, H., Liu, J., & McClements, D.J. (2020). Chitosan reduces vitamin D bioaccessibility in food emulsions by binding to mixed micelles. *Food & Function*, *11*(1), 187-199. https://doi.org/10.1039/C9FO02164G
51. Wang, F., & Mutukumira, A.N. (2022). Microencapsulation of *Limosilactobacillus reuteri* DPC16 by spray drying using different encapsulation wall materials. *Journal of Food Processing and Preservation*, *46*(10), e16880. https://doi.org/10.1111/jfpp.16880
52. Wang, L., Gao, Y., Li, J., Subirade, M., Song, Y., & Liang, L. (2016). Effect of resveratrol or ascorbic acid on the stability of α-tocopherol in O/W emulsions stabilized by whey protein isolate: Simultaneous encapsulation of the vitamin and the protective antioxidant. *Food Chemistry*, *196*, 466-474. https://doi.org/10.1016/j.foodchem.2015.09.071
53. Wang, S., Ye, X., Sun, Y., Liang, J., Yue, P., & Gao, X. (2021). Nanocomplexes derived from chitosan and whey protein isolate enhance the thermal stability and slow the release of anthocyanins in simulated digestion and prepared instant coffee. *Food Chemistry*, *336*, 127707. https://doi.org/10.1016/j.foodchem.2020.127707
54. Xu, W., Lv, K., Mu, W., Zhou, S., & Yang, Y. (2021). Encapsulation of α-tocopherol in whey protein isolate/chitosan particles using oil-in-water emulsion with optimal stability and bioaccessibility. *LWT*, *148*, 111724. https://doi.org/10.1016/j.lwt.2021.111724
55. Xu, W., Tang, Y., Yang, Y., Wang, G., & Zhou, S. (2020). Establishment of a stable complex formed from whey protein isolate and chitosan and its stability under environmental stresses. *International Journal of Biological Macromolecules*, *165*, 2823-2833. https://doi.org/10.1016/j.ijbiomac.2020.10.130
56. Yousefi, S., Rajaei, P., Nateghi, L., Nodeh, H.R., & Rashidi, L. (2023). Encapsulation of sesamol and retinol using alginate and chitosan-coated W/O/W multiple emulsions containing Tween 80 and Span 80. *International Journal of Biological Macromolecules*, *242*, 124766. https://doi.org/10.1016/j.ijbiomac.2023.124766

نشریه پژوهشهای علوم و صنایع غذایی ایران
https://ifstrj.um.ac.ir

مقاله پژوهشی

جلد ۲۲، شماره ۱، فروردین- اردیبهشت ۱۴۰۵، ص. ۳۴-۱۷

کپسوله‌سازی ویتامین‌های E و C با استفاده از کنسانتره پروتئین آب‌پنیر-کیتوزان از طریق خشک‌کردن پاششی: بهینه‌سازی، ویژگی‌های فیزیکوشیمیایی و تحلیل نرخ رهایش

پونه مجتهدی[۱]- مهدی وریدی[۱*]- امیرمحمد مرتضویان[۲]

تاریخ دریافت: ۱۴۰۴/۰۷/۳۰
تاریخ پذیرش: ۱۴۰۴/۱۱/۰۸

چکیده

نگرانی‌های فزاینده در مورد سلامت انسان، تقاضا برای ترکیبات زیست‌فعال عملکردی مانند ویتامین‌های E و C را افزایش داده است. با این حال، ناپایداری ذاتی و حساسیت آنها به شرایط محیطی، کاربرد مستقیم آنها را در سیستم‌های غذایی محدود کرده است. استراتژی‌های کپسوله‌سازی، رویکردی مؤثر برای محافظت از این ویتامین‌ها در برابر تخریب و آزادسازی کنترل‌شده ارائه می‌دهند. این مطالعه با هدف توسعه یک سیستم کپسوله‌سازی پایدار برای ویتامین‌های E و C با استفاده از کمپلکس کنسانتره پروتئین آب پنیر-کیتوزان (WPC-CS) از طریق خشک کردن پاششی انجام شد که امکان تحویل همزمان ویتامین‌های آب‌دوست و لیپوفیل را فراهم می‌کند. روش‌شناسی سطح پاسخ (RSM) برای بهینه‌سازی فرمولاسیون با هدف به حداکثر رساندن راندمان کپسوله‌سازی و در عین حال به حداقل رساندن میزان رطوبت و رطوبت‌پذیری به کار گرفته شد. میکروکپسول بهینه، راندمان کپسوله‌سازی ۹۳.۸۳٪ و ۹۳.۶٪ را برای ویتامین‌های E و C به‌ترتیب با رطوبت کم (۳.۱۷٪) و رطوبت‌پذیری کنترل‌شده (۱۳.۱۸٪) نشان داد. مطالعات آزادسازی، رفتار وابسته به فاز را نشان دادند: ویتامین C آزادسازی ناچیزی در مایع شبیه‌سازی شده دهان (۰.۰۷٪ پس از ۱۰ دقیقه) نشان داد، اما آزادسازی تجمعی قابل توجهی در مایع شبیه‌سازی شده معده (۸۵.۷۴٪ پس از ۱۲۰ دقیقه) داشت. در مقابل، ویتامین E پروفایل آزادسازی آهسته‌تر و پایدارتری را نشان داد، به‌طوری‌که ۳۱.۴۵٪ پس از ۱۲۰ دقیقه در مایع شبیه‌سازی شده معده آزاد شد و هیچ آزادسازی قابل تشخیصی در شرایط دهان مشاهده نشد. آنالیز میکروسکوپ الکترونی روبشی (SEM) نشان داد که میکروکپسول‌ها دارای مورفولوژی عمدتاً کروی با سطح چروکیده هستند که مشخصه ماتریس‌های پروتئین-پلی‌ساکارید تشکیل شده در طول خشک کردن سریع است. طیف‌سنجی مادون قرمز تبدیل فوریه (FTIR) کپسوله کردن موفقیت‌آمیز هر دو ویتامین را از طریق برهمکنش‌های بین WPC و CS تأیید کرد. این یافته‌ها نشان می‌دهد که کمپلکس‌های WPC-CS تولید شده از طریق خشک کردن پاششی، یک سیستم کپسوله کردن همزمان و آزادسازی کنترل‌شده مؤثر را فراهم می‌کنند که پایداری ویتامین را افزایش داده و کاربردهای امیدوارکننده‌ای را در غذاهای کاربردی و فرمولاسیون‌های دارویی ارائه می‌دهند.

واژه‌های کلیدی: بهینه‌سازی، خشک‌کن پاششی، رهایش کنترل‌شده، میکروکپسول

۱- گروه علوم و صنایع غذایی، دانشکده کشاورزی، دانشگاه فردوسی مشهد، مشهد، ایران
(*- نویسنده مسئول: Email: m.varidi@um.ac.ir)
۲- گروه علوم و صنایع غذایی، دانشکده علوم تغذیه و صنایع غذایی، انستیتو تحقیقات تغذیه‌ای و صنایع غذایی کشور، دانشگاه علوم پزشکی شهید بهشتی، تهران، ایران
https://doi.org/10.22067/ifstrj.2026.96109.1497

Iranian Food Science and Technology Research Journal
Homepage: https://ifstrj.um.ac.ir

Research Article
Vol. 22, No. 1, March- April, 2026, p. 35-49

Effect of Extraction Conditions on Total Anthocyanin Content from *Perilla frutescens* (L.) Britton and Its Application in Coloring Butter Biscuit

P.T.M. Tram[1*], N.N.T. Phuong[1]

1- Institute of Green and Sustainable Technology, Thu Dau Mot University, Ho Chi Minh City, Vietnam
(*- Corresponding Author Email: tramptm@tdmu.edu.vn)

Received: 10.11.2025
Revised: 21.12.2025
Accepted: 07.01.2026
Available Online:02.05.2026

How to cite this article:
Tram, P.T.M., & Phuong, N.N.T. (2026). Effect of extraction conditions on total anthocyanin content from *Perilla frutescens* (L.) britton and its application in coloring butter biscuit. *Iranian Food Science and Technology Research Journal, 22*(1), 35-49. https://doi.org/10.22067/ifstrj.2026.96395.1506

Abstract

The consumer trend toward safe and healthy food has spurred research and application of natural colors in traditional biscuit products to improve quality and sensory value. *Perilla frutescens* (L.) Britton is a member of the Lamiaceae family and is widely found in East Asian regions, where it is used as both a spice in cooking and in traditional medicine. It is rich in anthocyanins, a class of polyphenolic compounds that act as natural colorants and possess strong antioxidant properties. This study aimed to evaluate the extraction process of perilla leaf for enriching the total anthocyanin content, which is applied in coloring butter biscuits. The investigated factors included the sample-to-water ratio for extraction (1:10, 1:15, 1:20, and 1:25 g:mL), extraction temperatures (60°C, 70°C, 80°C, and 90°C), and extraction times (20, 25, 30, and 35 minutes). The obtained extract was analyzed for anthocyanin content using the pH differential method. The findings suggested that a sample-to-water ratio of 1:20 g:mL, an extraction temperature of 90°C, and an extraction duration of 30 minutes were the most suitable extraction conditions to achieve a high total anthocyanin content (1.70 $mg.g^{-1}$ DW). The addition of perilla leaf extract (PLE) significantly affected the physical properties of the biscuits (diameter, yield, brightness, and hardness of the biscuits); the higher the amount of PLE added, the darker and crispier the biscuits became. Sensory analysis showed that biscuits supplemented with PLE were rated higher than the control in terms of texture, color, and flavor. The results showed that the biscuits that received the highest scores across all parameters were supplemented with PLE at a rate of 7.5%. Overall, the analysis suggests that it is possible to produce butter biscuits with a characteristic color and improved nutritional profile by adding PLE.

Keywords: Anthocyanin, Butter biscuit, Extraction, Lamiaceae, *Perilla frutescens*

Introduction

Customers find food more attractive and appealing when it is presented in a visually appealing color. Due to their low cost, color stability during storage, synthetic colorants are commonly used in food. Aromatic rings and azo functional groups are included in the majority of synthetic colorants, which can lead to cancer, allergic responses, hyperactivity, or asthma episodes (Singh, Pandey, Dash, Zanwar, & Singh, 2023). Finding natural and safe colorants with biological activity is the current focus of research (Vega, Ciudad-Mulero, Fernández-Ruiz, Barros, & Morales, 2023). The environment contains the most representative substances with the ability to produce color, including anthocyanins (red, blue, and purple), carotenoids (orange and yellow), or chlorophyll (green) (Singh *et al.*, 2023).

Authors retain the copyright. This is an open access article distributed under Creative Commons Attribution 4.0 International License (CC BY 4.0).
https://doi.org/10.22067/ifstrj.2026.96395.1506

Anthocyanins are polyphenolic compounds responsible for the shades of pink, red, purple, and blue found in flowers, vegetables, and fruits. Plant security systems, physiology, and propagation largely rely on anthocyanins (Alappat & Alappat, 2020). Anthocyanins are essential for food coloring, drugs, functional foods, flavoring, and preservation in human life (Alappat & Alappat, 2020; Patra, Makhal, Jaryal, More, & Kaki, 2022). The anthocyanin content of perilla leaves is quite high. According to Meng, Lozano, Bombarda, Gaydou, & Li, (2009), the total anthocyanin content of two *Perilla* varieties (*frutescens* var. *frutescens*) from different regions of China was recorded as 1.6 $mg.g^{-1}$ (dry matter) and 1.8 $mg.g^{-1}$ (dry matter), respectively, while the total anthocyanin content of two varieties (*frutescens* var. *crispa*) from China and Japan was 0.7 $mg.g^{-1}$ (dry matter) and 1.6 $mg.g^{-1}$ (dry matter), respectively.

A genus of the Lamiaceae family, *Perilla frutescens* (L.) Britton, commonly known as perilla, is found through East Asian regions including China, Japan, South Korea, Vietnam, and India. It is grown as a vegetable and has been used in traditional medicine since antiquity (Ahmed, 2019; Hou *et al*., 2022). Currently, perilla has attracted more attention from several scientists due to its therapeutic properties and phytochemicals, including essential oils, triterpenoids, polyphenols, anthocyanins, omega-3 fatty acids, vitamins, and minerals (Adam *et al*., 2023; Hoang, Nguyen, Nguyen, Tran, & Le, 2024). Numerous studies have demonstrated that perilla leaves contain a range of polyphenolic compounds with potent antioxidant properties. Tea made from perilla leaves is very popular in East Asian countries due to its high antioxidant capacity, and has been used to treat crab and fish poisoning in these nations (Hou *et al*., 2022). Perilla is easy to grow and suitable for Vietnam's climate; developing this application will create additional income for farmers (Cuong, Tung, Duc, & Quynh, 2021).

Although anthocyanins have been extensively studied, research on extracting them from perilla leaves and utilizing them as a natural coloring in baked products remains limited. Therefore, " Study on optimal conditions for extracting anthocyanins from perilla leaves (*P. frutescens* (L.) Britton) and its application in coloring butter biscuit" was conducted to obtain anthocyanin-rich extracts and evaluate their application in biscuits. This study aims to introduce more types of naturally colored biscuits with enhanced nutritional value and antioxidant properties, contributing to the trend of using natural and functional foods in food science.

Materials and Methods

Materials, Chemicals, and Instruments

Perilla (*P. frutescens* (L.) Britton) leaves (Fig. 1 A) bought in Binh Diem market, Phu Loi town, Ho Chi Minh city, were transported to Thu Dau Mot University laboratory, washed thoroughly with water to remove dust. The fresh leaves were separated and dried in the sunlight until they reached a consistent weight. After that, they were ground and sieved through a 1 mm mesh and stored in sealed glass jars at room temperature before being used in experiments (Fig. 1 B).

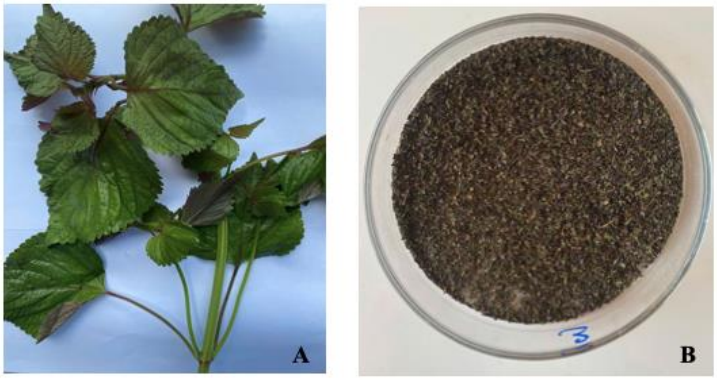

Fig. 1. *P. frutescens* (L.) Britton. A. whole plant, B. perilla leaf powder

The ingredients for the butter biscuits include flour, unsalted butter, sugar, eggs, salt, baking soda, and vanilla, which were purchased from Co-opmart Binh Duong supermarket in Thu Dau Mot Ward, Ho Chi Minh City, Vietnam.

Phytochemical Screening for Flavonoids and Polyphenols in Perilla Leaf Extract

Flavonoids and polyphenols in perilla leaf extract were qualitatively analyzed according to the method described by Apoorva, Pooja, & Vidyasagar, (2021).

Briefly, perilla leaf powder (1 g) was added to 20 mL of water in a 100 mL Erlenmeyer flask, then heated in a reciprocal shaker bath (Firstek B601D, Taiwan) at 70°C for 30 minutes. The mixture was filtered through NewStar filter paper (Ø11 cm) and used for qualitative analysis. The tests were conducted as shown in Table 1. The flavonoid test produced a yellow precipitate, whereas the polyphenol test yielded a bluish-green coloration. These observations confirm the presence of both flavonoids and polyphenols in the extract.

Table 1- Phytochemical screening for flavonoids and polyphenols in perilla leaf extract (Apoorva *et al.*, 2021)

Bioactive compounds	Qualitative chemical reaction	Signs of recognition
Flavonoids	0.5 mL extract + 0.5 mL $Pb(CH_3COO)_2$ 10%	Yellow precipitate
Polyphenols	0.5 mL extract + 3-4 drops $FeCl_3$ 5%	Bluish-green appearance

Anthocyanin Extraction

Effect of sample-to-water ratio on total anthocyanin content in perilla leaf

The perilla leaves powder (1 g) was extracted with water at 70 C for 30 minutes in a reciprocal shaker bath. The varying sample-to-water ratios were studied at the following concentrations: 1:10, 1:15, 1:20, and 1:25 (g:mL), which were selected based on previous reports demonstrating their effectiveness for anthocyanin extraction (Dam & Lam, 2013; Nhon, Tran, Phuc, Linh, & Anh, 2025). After extracting, the mixtures were passed through filter paper and used directly to analyze total anthocyanin concent (TAC).

Effect of Extraction Temperature on Total Anthocyanin Content in Perilla Leaf

In order to determine the optimum temperature , the extract temperatures were adjusted at 60°C, 70°C, 80°C, and 90°C. After 30 minutes, the extracts were filtered to analyze TAC.

Effect of Extraction Time on Total Anthocyanin Content in Perilla Leaf

The perilla leaf powder was extracted with water at an appropriate ratio in a reciprocal shaker bath at a proper extract temperature (determined in the previous experiment). The extraction times were set for 20, 25, 30, and 35 minutes. Then, the mixtures were filtered to determine TAC.

Anthocyanin Quantification Method

Total anthocyanin content (TAC) is determined based on the principle that monomeric anthocyanin pigments change color reversibly when pH changes (Lee, 2005; Hoang *et al*., 2024).

The perilla extract was diluted with buffer solution (KCl 0.025M, pH 1.0) and (CH_3COONa 0.4M, pH 4.5), let stands for 30 minutesThe absorbance was then measured using a spectrophotometer (Biochrom WPA Biowave II, UK) at 520 and 700 nm. The diluted test samples were compared to the control tube containing distilled water. TAC in the extract was calculated as follows:

$$TAC\ (mg.g^{-1}) = \left[\frac{A.M.K.V.10^3}{\varepsilon.L.m}\right] \quad (1)$$

In which:

A: absorption of anthocyanin with A = (A_{520} - A_{700}) pH=1) - (A_{520} - A_{700}) pH= 4.5)

M: molecular weight of cyanidin 3-glucoside (449.2 $g.mol^{-1}$)

L: length of cuvette (1 cm)

K: dilution factor

ε: molar absorption coefficient (26900 $L.mol^{-1}.cm^{-1}$)

V: volume of diluted samples (L)

m: weight of the sample (g)

Application of Perilla Leaf Extract in Coloring Butter Biscuits

Biscuits Preparation

The butter biscuits were prepared based on the formulation described by Phuc, Ngoc, & Thu, (2022) with minor adjustments (Fig. 2). The initial step of making butter biscuits was to mix wheat flour with other ingredients (sugar (56%), butter (60%), eggs yolk (17%), baking soda (1%), vanilla (1%), and salt (0.5%)), based on the weight of the wheat flour. Perilla leaf extract (PLE) was added to the butter biscuits according to Moczkowska‐Wyrwisz, Jastrzębska, & Wyrwisz, (2022) at different quantities of 5%, 7%, and 9% with 0.1% citric acid relative to the total mass of the dough after the ingredients had been well blended. After resting for twenty minutes, the dough was divided into small parts (10 g), shaped into the round shapes, and baked for 25 -30 minutes at 150°C in a preheated oven. The butter biscuits were cooled for 5 minutes at room temperature before being wrapped in a bag, sealed for further analysis.

Physical Analysis

Dimensions of the Biscuits after Baking

The biscuit's diameter and weight after baking were measured using a caliper and an analytical balance, respectively. The average values were calculated from 10 samples. The biscuit yield was determined according to Moczkowska‐Wyrwisz *et al*. (2022) and calculated as follows:

$$BY = \left[\frac{W_b}{W_a}\right] \times \mathbf{100} \quad (2)$$

In which:

BY: cooking yield (%)

Wb: weight of sample before baking (g)

Wa: weight of sample after baking and cooling (g)

Color Analysis

The color of PLE biscuit samples was determined using a colorimeter (CR-410, Konica Minolta, Japan) based on the L^*, a^*, b^* color system, where L^* represents lightness (0 = black, 100= white), a^* indicates the green–red component, and b^* represents the blue–yellow component (Azuan, Mohd Zin, Hasmadi, Rusli, & Zainol, 2020). The hue angle (h◦) was calculated according to formula: $h^\circ = \tan^{-1}(b^*/a^*)$ (3) (Biswas *et al*., 2025). Three biscuits were analyzed for each formulation.

Texture Analysis

The hardness of the biscuit samples was determined using a texture analyzer (BROOKFIELD CT3, USA). The pre-test and test speeds were 2 and 1 $mm.s^{-1}$, respectively. Hardness, defined as the maximum peak force, was measured in triplicate and expressed in kilograms (Najjar, Alkaabi, Alketbi, Stathopoulos, & Ranasinghe, 2022).

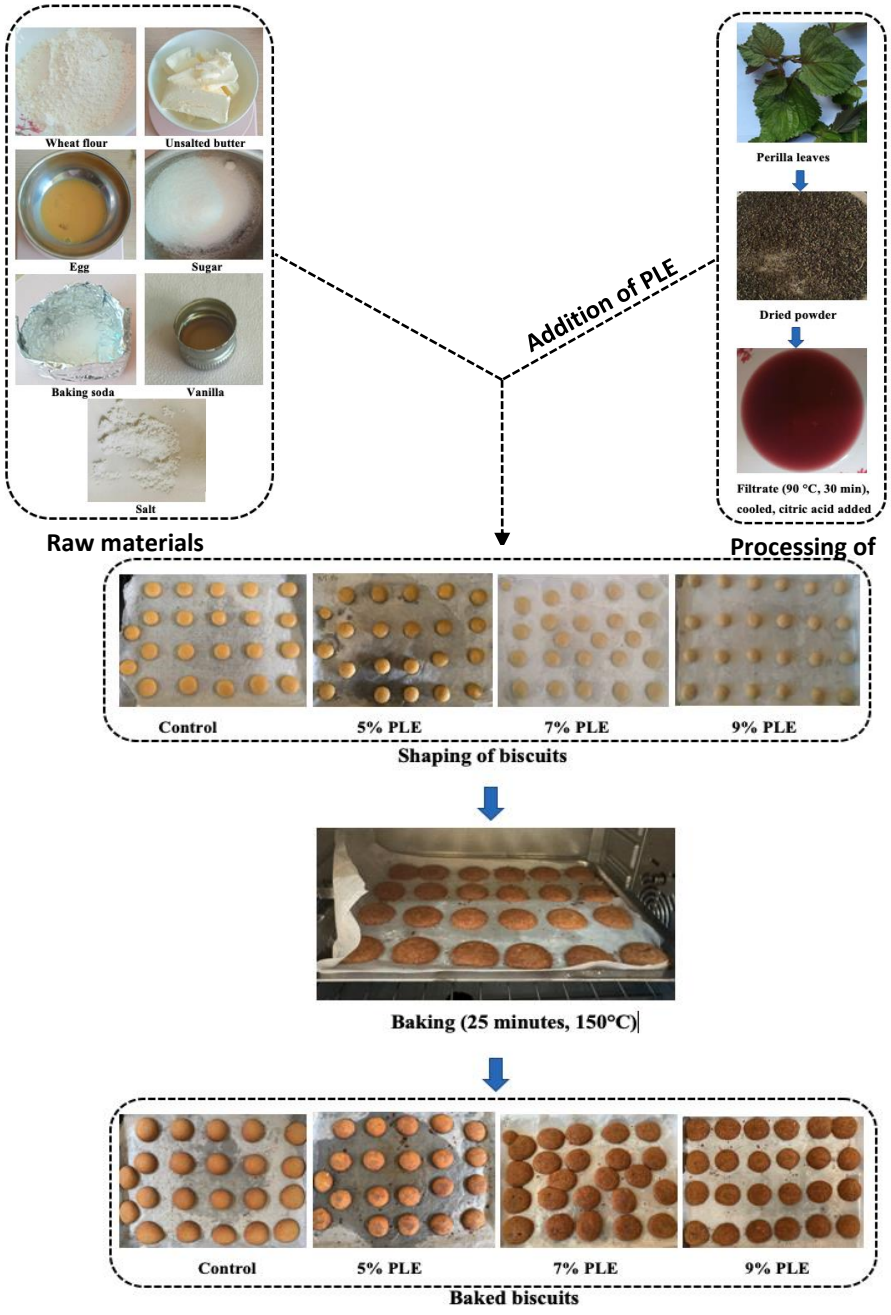

Fig. 2. Processing steps of PLE biscuits

Sensory Evaluation

The evaluation of final product with added PLE was conducted using QDA (Quantitative Descriptive Analysis) based on a quality scale of 1-5 for texture, color, and flavor (Quyen, 2024). The evaluation team (10 panelists) were lecturers and students from the Biotechnology and Food Technology Department of the Institute of Green and Sustainable Technology, Thu Dau Mot University, Vietnam.

Statistical Analyses

Statistical analyses were conducted by Minitab 16 software. One-way ANOVA was used to test for differences among treatments, and Tukey's post-hoc test was used to identify significant pairwise differences at a 5%

significance level ($p < 0.05$). The mean ± SD, with three replications, is displayed in all experimental data.

Results and Discussion

Phytochemical Screening for Flavonoids and Polyphenols in Perilla Leaf Extract

Polyphenols are phytochemicals, the primary source of antioxidants in the human diet. They are classified into four most essential subgroups: flavonoids, phenolic acids, stilbenes, and lignans (Ciupei, Colişar, Leopold, Stănilă, & Diaconeasa, 2024). In particular, anthocyanins are polyphenolic compounds with potent antioxidant and anti-inflammatory properties, which can help prevent various chronic diseases, including cardiovascular disease, neurodegeneration, and diabetes (Zhang & Zhu, 2023). To improve the efficiency of anthocyanin extraction, a preliminary investigation was conducted to determine the presence and content of flavonoids and polyphenols in perilla leaf extract.

After extraction, the mixture was filtered (tube 1). Then, reagents were added, yielding a yellow precipitate (tube 2) and a bluish-green appearance (tube 3) (Fig. 3), indicating the presence of flavonoids and polyphenols in perilla leaf extract (Table 2).

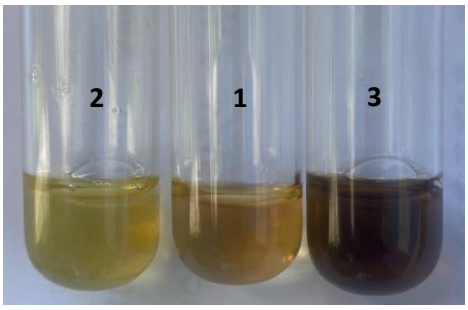

Fig. 3. Qualitative analysis of perilla leaf. (1) Sample before reaction, (2) qualitative analysis of flavonoids, and (3) qualitative analysis of polyphenols

Many studies reported that ferilla contained many polyphenols and flavonoids (Skowyra, Falguera, Azman, Segovia, & Almajano, 2014; Nguyen, Truong, & Nguyen, 2024; Lia & Baron, 2025). Perilla leaves contain various active constituents, including carotenoids, polyphenols, α-tocopherol, phytosterols, and anthocyanins. According to Zhang *et al*. (2022), anthocyanin was present in perilla at a concentration of 8.37 $mg.g^{-1}$.

Table 2- The presence of flavonoids and polyphenols in perilla leaf extract

Bioactive compounds	Test	Perilla leaf extract
Flavonoids	Lead acetate 10%	+
Polyphenols	Ferric (III) chloride 5%	+

(+) presence

Effect of Sample-to-water Ratio on Total Anthocyanin Content in Perilla Leaf

The sample-to-solvent ratio is a crucial factor influencing the efficiency of the extraction process. The amount of water used must be sufficient to ensure that the material is completely submerged, allowing the water to contact the sample and maximize extraction efficiency. In this study, the sample-to-water ratios treatments were 1:10, 1:15, 1:20, and 1:25 (g:mL). After extraction, the TAC was measured for each treatment (ratio) with three replications. The results of these experiments are presented in Table 3.

Table 3- Effect of sample-to-water ratio on TAC in perilla leaf

Sample/water (g:mL)	TAC (mg.g^{-1} DW)
1:10	$0.15^{c} \pm 0.03$
1:15	$0.13^{c} \pm 0.01$
1:20	$0.47^{a} \pm 0.03$
1:25	$0.28^{b} \pm 0.01$

*The means with different letters indicate a significant difference at the 5% level, according to the Tukey's test

The results in Table 3 show that the TAC obtained increased gradually as the amount of water increased from 10 to 20 mL, and the highest TAC (0.47 mg.g^{-1} DW) was obtained in the treatment with a sample-to-water ratio of 1:20 (g:mL). However, the TAC decreased (0.28 mg.g^{-1} DW) when the amount of water increased to 25 mL. When the water volume was only 10 - 15 mL, the solvent was insufficient to fully extract anthocyanins from the plant cells, resulting in lower TAC. However, increasing , the amount of water (25 mL) did not increase the amount of anthocyanin in the extract because the anthocyanin content in the sample was fixed (Pham & Pham, 2025).

The findings of the statistical analysis showed that the sample-to-water ratio significantly affected the TAC content ($p < 0.05$) (Table 3). As a result, 1:20 (g:mL) was the proper sample-to-water ratio for this experiment.

Effect of Extraction Temperature on Total Anthocyanin Content in Perilla Leaf

Anthocyanin is a standard water-soluble pigment in plants, responsible for the characteristic colors of red, orange, purple, and blue. The stability of anthocyanins is influenced by various factors, including pH, temperature, light, atmospheric oxygen, ascorbic acid, and enzymes (Enaru, Drețcanu, Pop, Stănilă, & Diaconeasa, 2021). During the extraction process, temperature is an essential factor because as the temperature increases, the viscosity of the solution decreases, thereby increasing the diffusion rate. This promotes the transport of soluble substances, including anthocyanin, from the raw material into the solvent, allowing the process to proceed more quickly (Nhon *et al.*, 2025). However, excessively high temperatures can cause anthocyanins to degrade or decompose (*Nhut et al.*, 2019; Thuy, Han, Minh, & Tai, 2022). Therefore, determining the optimal extraction temperature is necessary to maximize extraction efficiency and achieve the highest anthocyanin content in the extract.

The results of the temperature effect on anthocyanin content in perilla leaf are presented in Table 4.

Table 4- Effect of extraction temperature on TAC in perilla leaf

Temperature (°C)	TAC (mg.g^{-1} DW)
60	$0.15^{d} \pm 0.03$
70	$0.34^{c} \pm 0.02$
80	$0.55^{b} \pm 0.00$
90	$0.63^{a} \pm 0.05$

*The means with different letters indicate a significant difference at the 5% level, according to the Tukey's test

TAC extracted from perilla leaf powder showed a statistically significant difference ($p < 0.05$) when different extraction temperatures (60°C, 70°C, 80°C, and 90°C) were applied. The results showed that the application of 90°C yielded the highest TAC, reaching 0.63 mg.g^{1} DW. Yu, Shiau, Pan, & Yang, (2024) reported that temperature is an essential factor affecting the extraction efficiency of bioactive compounds. Increasing the extraction temperature not only reduces the viscosity of the solvent but also promotes the diffusion, mass transfer, and osmosis of the solvent into plant tissue. At the same time, high temperature

can break the structural bonds of the cell wall, creating favorable conditions for the solvent to contact and dissolve intracellular compounds, including anthocyanin. According to Thuy *et al*. (2022), TAC in Peristrophe bivalvis L. Merr leaf extract increased with increasing extraction temperature from 80°C to 90°C, but TAC content decreased when extracted at 100°C. Similiarly, Yu *et al.* (2024) also reported that the highest TAC was obtained when butterfly pea flower and grape skin powders were extracted with water at a solid-to-solvent ratio of 2% (w/v). The optimal extraction conditions were 90°C for 30 - 90 minutes for butterfly pea flower and 90°C for 30 minutes for grape skin. Under these conditions, TACs were 1.75 and 2.79 mg.g^{-1} DW, respectively. Conversely, Nhon *et al.* (2025) showed that perilla leaf powder (1 g) extracted with 20 mL of 72% ethanol at 63°C for 90 minutes yielded an optimal anthocyanin content of 3.373 mg.g^{-1} DW. Differences in results may be due to variations in extraction conditions such as: source of raw material, extraction temperature and time, extraction method, sample particle size, solids-to-solvent ratio, stirring conditions, and analytical methods used to analyze TAC (Yu *et al*., 2024).

Based on experimental results, the optimal extraction temperature for anthocyanin recovery from perilla leaf powder was determined to be 90°C.

Effect of Extraction Time on Total Anthocyanin Content in Perilla Leaf

A perilla powder-to-water ratio of 1:20 (g:mL) and a temperature of 90°C were selected for the extraction process. The extraction of anthocyanins also depends on the extraction time. If the extraction time is too short, the solvent may not have sufficient time to dissolve all the anthocyanins present in the raw material. Conversely, if the extraction time is too long, the quality of the extract may be affected due to the dissolution of undesirable compounds. Additionally, prolonged exposure to high temperatures may lead to the degradation of anthocyanins (Thuy *et al*., 2022).

In this study, extraction times of 20, 25, 30, and 35 minutes were applied to determine the optimal duration for obtaining the highest anthocyanin content. The results corresponding to each extraction time are presented in Table 5.

Table 5- Effect of extract time on TAC in perilla leaf

Time (minute)	TAC (mg.g^{-1} DW)
20	$0.55^{c} \pm 0.00$
25	$1.13^{b} \pm 0.09$
30	$1.70^{a} \pm 0.29$
35	$1.16^{b} \pm 0.03$

*The means with different letters indicate a significant difference at the 5% level, according to the Tukey's test

According to the results presented in Table 5, the TAC at 20 minutes of extraction was 0.55 mg.g^{-1} DW. TAC increased to 1.13 mg.g^{-1} DW at 25 minutes. The highest TAC was observed at 30 minutes, reaching 1.70 mg.g^{-1} DW. However, at 35 minutes, the anthocyanin content decreased to 1.16 mg.g^{-1} DW. This indicates that extraction time significantly affects the anthocyanin yield. Extraction times of 20 and 25 minutes seem insufficient for the complete dissolution of anthocyanins into the solvent. At 30 minutes, optimal extraction conditions allow maximal solute diffusion into the solution. Nevertheless, extending extraction time beyond equilibrium does not enhance extraction efficiency. Additionally, anthocyanins are susceptible to oxidation by heat and atmospheric oxygen during prolonged extraction (Thuy *et al*., 2022), which likely causes the decrease observed at 35 minutes.

Similarly, according to Nhut *et al*. (2019), the highest anthocyanin recovery from *Hibiscus sabdariffa* L. (Roselle) flowers was 180.821 mg.L^{-1} at an extraction temperature of 60°C with a 50% ethanol and an extraction period of 30 minutes at a liquid-solid ratio of 8:1.

Thus, in this experiment, 30 minutes was chosen to extract anthocyanin from perilla leaf powder.

Application of Perilla Leaf Extract (PLE) in Coloring Butter Biscuit

The dimensions of the butter biscuit produced by adding different amounts of PLE are shown in Table 6. The diameter of the sample increased progressively, and biscuit yield reduced as the amount of PLE added to the biscuits increased. This may be due to increasing the water content originated from PLE, which made the dough softer, allowing the dough to spread and rise more quickly during the initial stage of baking. The extra water also helped to form more air bubbles, resulting in a lighter texture that reduced the biscuit's weight and led to a slightly larger diameter (Miller, Hoseney, & Morris, 1997; Mandala, Ioannou, & Kostaropoulos, 2006).

Table 6- Different dimensions of the PLE biscuits prepared by different formulations

Sample added PLE	Diameter (cm)	Biscuit yield
Control	$3.99^{b} \pm 0.12$	$85.97^{a} \pm 3.71$
5%	$3.99^{b} \pm 0,10$	$86.24^{a} \pm 1.21$
7%	$4.55^{a} \pm 0.33$	$85.00^{ab} \pm 0.67$
9%	$4.75^{a} \pm 0.23$	$82.62^{b} \pm 0.76$

*The means with different letters indicate a significant difference at the 5% level, according to the Tukey's test

The proportion of PLE added to the dough mixture significantly affected the color parameters L*, a*, b*, and h◦ of the product ($p < 0.05$) (Table 7).

Table 7- Color analysis of the PLE biscuits prepared by different formulations

Sample added PLE	L*	a*	b*	h°
Control	$69.26^{a} \pm 1.47$	$5.35^{b} \pm 1.59$	$32.61^{a} \pm 1.13$	$80.74^{a} \pm 2.40$
5%	$55.30^{b} \pm 0.63$	$10.69^{a} \pm 0.87$	$27.22^{b} \pm 2.13$	$68.57^{c} \pm 0.08$
7%	$49.90^{c} \pm 1.43$	$10.77^{a} \pm 0.47$	$29.44^{ab} \pm 1.32$	$69.88^{bc} \pm 1.36$
9%	$47.31^{c} \pm 2.69$	$12.62^{a} \pm 0.85$	$28.82^{ab} \pm 2.13$	$66.28^{c} \pm 2.19$

*The means with different letters indicate a significant difference at the 5% level, according to the Tukey's test

The L* value of the butter biscuits gradually decreased with increasing PLE content, indicating a reduction in product brightness. At PLE levels of 7% and 9%, the biscuits exhibited the lowest L* values (49.90 and 47.31, respectively) and a deeper red coloration. In addition, the h◦ value also decreased as the PLE concentration increased, indicating a color shift from light yellow to red–brown tones. This trend is consistent with previous studies on biscuits and functional food products incorporating pigment-rich plant ingredients. Choi, Oh, & Lee, (2009) reported that cookies supplemented with 1% and 3% perilla powder showed reduced L* values (54.38 and 43.22, respectively) and improved functionality. Similarly, Najjar *et al.* (2022) observed that cookies containing Khalas date powder exhibited darker coloration, with the 7% formulation being the most preferred (L* = 40.06). More recently, Biswas *et al.* (2025) found that increasing red dragon fruit peel powder from 0 to 9% resulted in decreases in both L* and h◦ values, with the 6% sample being the most preferred (L* = 42.57; h◦ = 59.65).

The results of evaluating the hardness of butter biscuits supplemented with PLE are presented in Table 8. The hardness of the butter biscuits tended to decrease as the PLE content in the dough increased. This suggests that adding high amounts of PLE may increase the formation of air pockets during baking, resulting in a more porous texture compared to the control; therefore, the hardness of the butter biscuits decreased with increasing PLE. The hardness values from 3.31 to 3.94 kg showed no significant difference ($p > 0.05$), which is consistent with the study of Biswas *et al.* (2025), who observed that replacing red dragon fruit peel powder (0 - 9%) did not significantly

affect the hardness of the biscuits (hardness from 3.33 to 3.59 kg).

The results of sensory evaluation of finished butter biscuits supplemented with PLE (0 - 9%) (Fig. 4) on texture, color, and tatse are presented in Table 9.

Table 8- Texture analysis of the PLE biscuits prepared by different formulations

Sample added PLE	Hardness (kg)
Control	3.94[a] ± 0.65
5%	3.65[a] ± 0.30
7%	3.35[a] ± 0.55
9%	3.31[a] ± 0.52

*The means with different letters indicate a significant difference at the 5% level, according to the Tukey's test

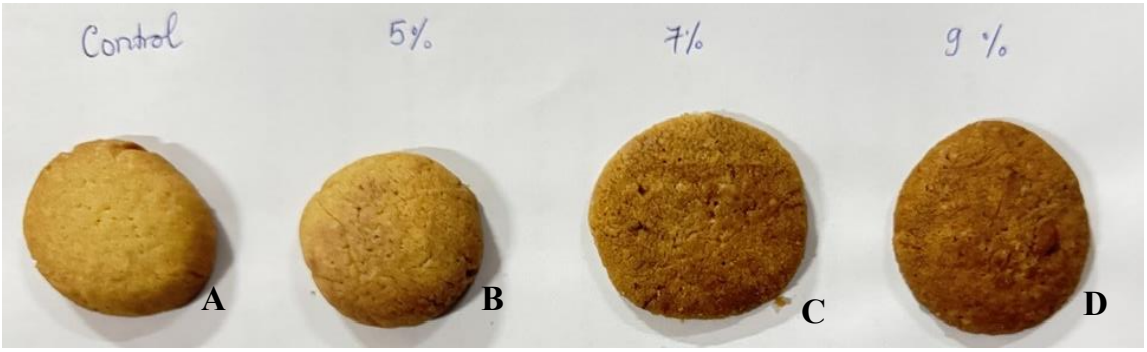

Fig. 4. Butter biscuit with added perilla leaf extract. A. 5% extract; B. 7% extract; C. 9% extract

In terms of texture, the sensory scores were higher in samples with added PLE, particularly in the sample with a 9% addition (4.70 points). This may be due to the porous, crisp texture of the biscuit samples, which have a high extract ratio. According to hardness measurements, biscuits containing PLE had lower hardness compared to the control sample. Hardness is a texture characteristic that plays a vital role in evaluating baked goods. The lower this parameter, the more desirable the product is for biscuits (Najjar *et al*., 2022).

Color is considered a fundamental physical characteristic of food. It significantly impacts the evaluation of a product's visual quality. When evaluating the perceived color of a product, panelists are not only interested in brightly colored products but also in the product's characteristic color. In this experiment, butter biscuits with added PLE, which had a deep red color, were scored higher than the control sample, especially the sample containing 9% PLE (4.4 points). Similarly, Najjar *et al*. (2022) also reported that the cookie sample with a high percentage of added date powder (7.5%) was preferred over the sample with a low percentage of added date powder or the control.

Taste scores were also higher for biscuits containing 9% PLE, with an average score of 4.30 compared to 2.30 for the control sample ($p < 0.05$). The addition of PLE may incorporate to formation a distinctive flavor.

Based on the analyzed sensory criteria, the 9% PLE sample was scored the highest in terms of texture, color, and taste. Therefore, the 9% PLE ratio was chosen as the optimal level to be included in the butter biscuit formulation (Fig. 5). The addition of this natural ingredient not only enhances the sensory value but also has the potential to improve the nutritional and functional value of the product.

Table 9- Sensory evaluation of the PLE biscuits prepared by different formulations

Sample	Sensory score		
	Texture	Color	Flavor
Control	$3.40^{c} \pm 0.70$	$2.00^{c} \pm 0.67$	$2.30^{c} \pm 0.95$
5%	$3.60^{bc} \pm 0.70$	$2.90^{b} \pm 0.74$	$3.20^{bc} \pm 0.92$
7%	$4.30^{ab} \pm 0.95$	$3.70^{ab} \pm 0.67$	$4.00^{ab} \pm 0.47$
9%	$4.70^{a} \pm 0.48$	$4.40^{a} \pm 0.84$	$4.30^{a} \pm 0.67$

*The means with different letters indicate a significant difference at the 5% level, according to the Tukey's test

Fig. 5. Butter biscuits with added 9% PLE and product packaging

Conclusion

The highest anthocyanin content was obtained using a perilla powder-to-water ratio of 1:20 g:mL, extraction at 90°C for 30 minutes (1.70 $mg.g^{-1}$ DW). The study also demonstrated the success of using PLE (9%) to create the characteristic color of Biscuit butter , while simultaneously enhancing their nutritional and functional properties. These results showed that using natural colorants in food improves both the vision and nutritional quality of baked goods, which aligns well with what consumers want nowadays safer, healthier food options. Further work should focus on optimizing extraction, testing compound stability in foods, and evaluating consumer response. This study highlights the potential of PLE for both food and medicinal purposes.

Author Contributions

Pham Thi My Tram designed the experiments. **Nguyen Ngoc Thanh Phuong** has done studies, guided and supervised by Pham Thi My Tram. **Pham Thi My Tram** and **Nguyen Ngoc Thanh Phuong** carried out the calculations. The paper was written by **Pham Thi My Tram**. All authors agreed to the final version of this manuscript.

Funding Sources

This research did not received any specific grant from funding agencies in the public, commercial, or not-for-profit sectors.

Acknowledgments

We would like to thank Thu Dau Mot University for helping with the experiments and technical assistance.

Conflict of Interest

Authors declare no conflict of interest.

References

1. Adam, G., Robu, S., Flutur, M.M., Cioanca, O., Vasilache, I.A., Adam, A.M., Mircea, C., Nechita, A., Harabor, V., Harabor, A., & Hancianu, M. (2023). Applications of *Perilla frutescens* extracts in clinical practice. *Antioxidants, 12*(3), 727. https://doi.org/10.3390/antiox12030727

2. Ahmed, H.M. (2019). Ethnomedicinal, phytochemical and pharmacological investigations of *Perilla frutescens* (L.) Britt. *Molecules*, *24*(1), 102. https://doi.org/10.3390/molecules24010102
3. Alappat, B., & Alappat, J. (2020). Anthocyanin pigments: Beyond aesthetics. *Molecules*, *25*(23), 5500. https://doi.org/10.3390/molecules25235500
4. Apoorva, M., Pooja, S., & Vidyasagar, G.M. (2021). Phytochemical screening for secondary metabolites and nutraceutical value of *Sesbania grandiflora* (L.) Pers leaf extract. *Indo Global Journal of Pharmaceutical Sciences*, *11*(1), 28-32. https://doi.org/10.35652/IGJPS.2021.111004
5. Azuan, A.A., Mohd Zin, Z.Z., Hasmadi, M., Rusli, N.D., & Zainol, M.K. (2020). Physicochemical, antioxidant and sensory characteristics of cookies supplemented with different levels of spent coffee ground extract. *Food Research*, *4*(4), 1181-1190. https://doi.org/10.26656/fr.2017.4(4).058
6. Biswas, M., Alam, M., Akhtaruzzaman, M., Ahmed, S., Uddin, M.S., Talukder, A.H.M.R., Alam, A., & Biswas, B. (2025). Valorization of red dragon fruit peel (*Hylocereus polyrhizus*) as a functional ingredient for fortified biscuits: Physicochemical, nutritional, and sensory implications. *Future Foods*, *12*, 100768. https://doi.org/10.1016/j.fufo.2025.100768
7. Choi, H.Y., Oh, S.Y., & Lee, Y.S. (2009). Antioxidant activity and quality characteristics of Perilla leaves (*Perilla frutescens* var. *japonica* HARA) cookies. *Korean Journal of Food Cookery Science*, *25*(5), 521-530. https://doi.org/10.3746/jkfn.2011.40.2.267
8. Ciupei, D., Colişar, A., Leopold, L., Stănilă, A., & Diaconeasa, Z.M. (2024). Polyphenols: from classification to therapeutic potential and bioavailability. *Foods*, *13*(24), 4131. https://doi.org/10.3390/foods13244131
9. Cuong, V.T., Tung, N.Q., Duc, H.T., & Quynh, P.T.H. (2021). Research to complete the process of distillation of purple essential oil in Vietnam (*Perilla frutescens* var. *crispa*) and applications in food processing. *Journal of Science & Technology*, *57*(6), 124-128. (Vietnamese). https://vjol.info.vn/index.php/dhcnhn/article/view/65189/54963
10. Dam, S.M., & Lam, K.K. (2013). Extraction of anthocyanins from leaves of *Perilla ocymoides* L. var. bicolorlaciniata grown in Vietnam. *Acta Horticulturae*, *989*, 293-297. https://doi.org/10.17660/ActaHortic.2013.989.38
11. Enaru, B., Drețcanu, G., Pop, T.D., Stănilă, A., & Diaconeasa, Z. (2021). Anthocyanins: factors affecting their stability and degradation. *Antioxidants*, *10*(12), 1967. https://doi.org/10.3390/antiox10121967
12. Hoang, T.N.N., Nguyen, T.Q.T., Nguyen, M.P., Tran, T.H.L., & Le, T.H.A. (2024). Optimal extraction and spray-drying anthocyanin from *Perilla frutescens*. *JST: Engineering And Technology For Sustainable Development*, *34*(5), 1-10. https://doi.org/10.51316/jst.178.etsd.2024.34.5.1
13. Hou, T., Netala, V.R., Zhang, H., Xing, Y., Li, H., & Zhang, Z. (2022). *Perilla frutescens*: A rich source of pharmacological active compounds. *Molecules*, *27*(11), 3578. https://doi.org/10.3390/molecules27113578
14. Lee, J. (2005). Determination of total monomeric anthocyanin pigment content of fruit juices, beverages, natural colorants, and wines by the pH differential method: collaborative study. *Journal of AOAC International*, *88*(5), 1269-1278. https://doi.org/10.1093/9780197610145.003.3423
15. Lia, F., & Baron, B. (2025). Analysis of polyphenolic composition, antioxidant power and stress-response effects of fractionated *Perilla* leaf extract on cells in vitro. *Biologics*. *5*(1), 2. https://doi.org/10.3390/biologics5010002
16. Mandala, I.G., Ioannou, C.A., & Kostaropoulos, A.E. (2006). Textural attributes of commercial biscuits: Effect of relative humidity on their quality. *International Journal of Food Science & Technology*, *41*(7), 782-789. https://doi.org/10.1111/j.1365-2621.2005.01092.x

17. Meng, L., Lozano, Y., Bombarda, I., Gaydou, E.M., & Li, B. (2009). Polyphenol extraction from eight *Perilla frutescens* cultivars. *Comptes Rendus. Chimie*, *12*(5), 602-611. https://doi.org/10.1016/j.crci.2008.04.011
18. Miller, R.A., Hoseney, R.C., & Morris, C.F. (1997). Effect of formula water content on the spread of sugar‐snap cookies. *Cereal Chemistry*, *74*(5), 669-671. https://doi.org/10.1094/CCHEM.1997.74.5.669
19. Moczkowska‐Wyrwisz, M., Jastrzębska, D., & Wyrwisz, J. (2022). Application of new sources of bioactive substances (*Perilla frutescens* L. and *Tagetes erecta* L.) in the chosen cookies production. *International Journal of Environmental Research and Public Health*, *19*(18), 11504. https://doi.org/10.3390/ijerph191811504
20. Najjar, Z., Alkaabi, M., Alketbi, K., Stathopoulos, C., & Ranasinghe, M. (2022). Physical chemical and textural characteristics and sensory evaluation of cookies formulated with date seed powder. *Foods*, *11*(3), 305. https://doi.org/10.3390/foods11030305
21. Nguyen, N.T.K., Truong, H.A.V., & Nguyen, H.K.T. (2024). Optimizing conditions to improve polyphenol content and screening antioxidant capacity with DNA protection activity of *Perilla frutescens*. *Hue University Journal of Science: Natural Science*, *133*(1B), 35–48. https://doi.org/10.26459/hueunijns.v133i1B.7087
22. Nhon, H.T.N., Tran, N.T.Q., Phuc, N.M., Linh, T.T.H., & Anh, L.T.H. (2025). Optimal extraction and spray-drying anthocyanin from *Perilla frutescens*. *Journal of Science and Technology: Engineering and Technology for Sustainable Development*, *34*(5), 001-010. https://doi.org/10.51316/jst.178.etsd.2024.34.5.1
23. Nhut, P,.T., Phu, N.T.N., Duc, L.T., Hien, T.T., Chinh, N.D., Vo, D.V.N., Le, X.T., Do, S.T., & Giang, B.L. (2019). *Effects of various solvent concentration, liquid-solid ratio, temperatures and time values on the extraction yield of anthocyanin from Vietnam Hibiscus sabdariffa L.(Roselle).* IOP Conference Series: Materials Science and Engineering, Xiamen, China. https://doi.org/10.1088/1757-899x/542/1/012033
24. Patra, S., Makhal, P., Jaryal, S., More, N., & Kaki, V.R. (2022). Anthocyanins: Plant-based flavonoid pigments with diverse biological activities. *International Journal of Plant Based Pharmaceuticals*, *2*(1), 118-127. https://doi.org/10.62313/ijpbp.2022.22
25. Pham, A.G.Q., & Pham, T.T.M. (2025). Studying the extraction conditions on rosmarinic acid content and antioxidant activity of Basil (*Ocimum basilicum* L.). *Indonesian Journal of Chemistry*, *25*(3), 709-718. https://doi.org/10.22146/ijc.99415
26. Phuc, T.B., Ngoc, V.T.K., & Thu, L.T. (2022). Research and development of cocoa bean shell biscuits. *Journal of Science and Technology – Nguyen Tat Thanh University, Vietnam*, *18*, 74-80 (Vietnamese). https://doi.org/10.55401/sv5yr725
27. Quyen, D.K. (2024). Effects of ingredients on the physical properties and sensory quality of taro biscuits. *Dong Thap University Journal of Science*, *13*(2), 58–64 (Vietnamese). https://dthujs.vn/index.php/dthujs/article/view/840/1318?lang=en_US
28. Singh, T., Pandey, V.K., Dash, K.K., Zanwar, S., & Singh, R. (2023). Natural bio-colorant and pigments: Sources and applications in food processing. *Journal of Agriculture and Food Research*, *12*, 100628. https://doi.org/10.1016/j.jafr.2023.100628
29. Skowyra, M., Falguera, V., Azman, N.A., Segovia, F., & Almajano, M.P. (2014). The effect of *Perilla frutescens* extract on the oxidative stability of model food emulsions. *Antioxidants*, *3*(1), 38-54. https://doi.org/10.3390/antiox3010038
30. Thuy, N.M., Han, D.H.N., Minh, V.Q., & Tai, N.V. (2022). Effect of extraction methods and temperature preservation on total anthocyanins compounds of *Peristrophe bivalvis* L. Merr. leaf.

Journal of Applied Biology & Biotechnology, *2*, 146-153. https://doi.org/10.7324/jabb.2022.100218

31. Vega, E.N., Ciudad-Mulero, M., Fernández-Ruiz, V., Barros, L., & Morales, P. (2023). Natural sources of food colorants as potential substitutes for artificial additives. *Foods*, *12*(22), 4102. https://doi.org/10.3390/foods12224102
32. Yu, Y., Shiau, S., Pan, W., & Yang, Y. (2024). Extraction of bioactive phenolics from various anthocyanin‐rich plant materials and comparison of their heat stability. *Molecules*, *29*(22), 5256. https://doi.org/10.3390/molecules29225256
33. Zhang, P., & Zhu, H. (2023). Anthocyanins in plant food: current status, genetic modification, and future perspectives. *Molecules*, *28*(2), 866. https://doi.org/10.3390/molecules28020866
34. Zhang, X., Zhao, Y., Li, B., Guo, M., Lv, J., & Wei, Y. (2022). Comparison of three extraction methods for anthocyanins from *Perilla frutescens* leaves. *Sustainable Chemistry and Pharmacy*, *29*, 100817. https://doi.org/10.1016/j.scp.2022.100817

نشریه پژوهشهای علوم و صنایع غذایی ایران
https://ifstrj.um.ac.ir

مقاله پژوهشی
جلد ۲۲، شماره ۱، فروردین- اردیبهشت ۱۴۰۵، ص. ۴۹-۳۵

اثر شرایط استخراج بر میزان کل آنتوسیانین *Perilla frutescens* (L.) Britton و کاربرد آن در رنگ‌دهی بیسکویت کره‌ای

فام تای مای ترام[۱*]- نوین نوک سان فونگ[۱]

تاریخ دریافت: ۱۴۰۴/۰۸/۱۹
تاریخ پذیرش: ۱۴۰۴/۱۰/۱۷

چکیده

گرایش مصرف‌کنندگان به سوی غذاهای ایمن و سالم، پژوهش و کاربرد رنگ‌های طبیعی را در محصولات سنتی بیسکویت به‌منظور بهبود کیفیت و ارزش حسی افزایش داده است *Perilla frutescens* (L.) Britton .گیاهی از خانواده Lamiaceae است که به‌طور گسترده در کشورهای شرق آسیا یافت می‌شود و هم به‌عنوان ادویه در آشپزی و هم در طب سنتی مورد استفاده قرار می‌گیرد. این گیاه سرشار از آنتوسیانین‌ها، دسته‌ای از ترکیبات پلی‌فنولی است که به‌عنوان رنگ‌دهنده‌های طبیعی عمل کرده و دارای خواص آنتی‌اکسیدانی قوی هستند. هدف این مطالعه، ارزیابی فرآیند استخراج برگ پریلا برای افزایش میزان کل آنتوسیانین و کاربرد آن در رنگ‌دهی بیسکویت‌های کره‌ای بود. عوامل مورد بررسی شامل نسبت نمونه به آب (۱:۱۰، ۱:۱۵، ۱:۲۰ و ۱:۲۵ گرم:میلی‌لیتر)، دمای استخراج (۶۰، ۷۰، ۸۰ و ۹۰ درجه سانتی‌گراد) و زمان استخراج (۲۰، ۲۵، ۳۰ و ۳۵ دقیقه) بودند. عصاره به‌دست‌آمده از نظر میزان آنتوسیانین با استفاده از روش اختلاف pH مورد تجزیه‌وتحلیل قرار گرفت. نتایج نشان داد که نسبت نمونه به آب ۱:۲۰ گرم:میلی‌لیتر، دمای استخراج ۹۰ درجه سانتی‌گراد و زمان استخراج ۳۰ دقیقه، مناسب‌ترین شرایط برای دستیابی به بیشترین میزان کل آنتوسیانین (۱,۷۰ میلی‌گرم بر گرم وزن خشک) هستند. افزودن عصاره برگ پریلا (PLE) به‌طور معنی‌داری بر ویژگی‌های فیزیکی بیسکویت‌ها (قطر، بازده، روشنایی و سختی) تأثیر گذاشت؛ به‌طوری‌که با افزایش میزانPLE ، بیسکویت‌ها تیره‌تر و تردتر شدند. ارزیابی حسی نشان داد که بیسکویت‌های غنی‌شده با PLE از نظر بافت، رنگ و طعم امتیاز بالاتری نسبت به نمونه شاهد دریافت کردند. نتایج همچنین نشان داد که بیسکویت‌های دارای بیشترین امتیاز در تمامی شاخص‌ها، حاوی ۷,۵٪ PLE بودند. به‌طور کلی، این مطالعه نشان می‌دهد که با افزودن عصاره برگ پریلا می‌توان بیسکویت‌های کره‌ای با رنگی متمایز و ارزش تغذیه‌ای بهبودیافته تولید کرد.

واژه‌های کلیدی: آنتوسیانین، استخراج، بیسکویت کره‌ای، Lamiaceae، *Perilla frutescens*

۱- مؤسسه فناوری سبز و پایدار، دانشگاه تو دائو موت، شهر هوشی مین، ویتنام
(*- نویسنده مسئول: Email: tramptm@tdmu.edu.vn)

https://doi.org/10.22067/ifstrj.2026.96395.1506

Iranian Food Science and Technology Research Journal
Homepage: https://ifstrj.um.ac.ir

Research Article
Vol. 22, No. 1, March- April, 2026, p. 51-72

Development of Active PCL/β-Glucan Films Enriched with Natural Extracts and Gold Nanoparticles for Packaging of Cold Plasma-Treated Fish Paste

A. Asdagh[1], S. Pirsa[1*], M.K. Pirouzifard[1]

1- Department of Food Science and Technology, Faculty of Agriculture, Urmia University, Urmia, Iran
(*- Corresponding Author Email: S.pirsa@urmia.ac.ir)

Received: 11.11.2025
Revised: 01.12.2025
Accepted: 03.12.2025
Available Online: 21.02.2026

How to cite this article:
Asdagh, A., Pirsa, S., & Pirouzifard, M.K. (2026). Development of active PCL/β-Glucan films enriched with natural extracts and gold nanoparticles for packaging of cold plasma-treated fish paste. *Iranian Food Science and Technology Research Journal*, *22*(1), 51-72. https://doi.org/10.22067/ifstrj.2025.96443.1508

Abstract

Growing concerns about conventional plastic packaging due to its non-degradability, risk of transferring toxic compounds to food, and environmental pollution have necessitated the development of environmentally friendly alternatives such as edible and biodegradable films. This study aimed to develop an active packaging system based on a polycaprolactone/beta-glucan (PCL-BG) nanocomposite film modified with oak fruit pair extract (OFPE), apricot kernel extract (AKE), and gold nanoparticles (AuNPs) and study its suitability for packaging fish paste treated with cold plasma. The evaluation of the film's antibacterial properties showed that the active compounds had a strong inhibitory effect, with the largest inhibition zones of 27.78 mm against *Bacillus cereus* and 21.38 mm against *Escherichia coli* observed in the film prepared with the highest extract concentration. Thermal analysis (DSC) showed a significant improvement in thermal stability, with the melting temperature of the final composite film increasing to 81.6 °C. Microbiological and chemical evaluations over 30 days of storage showed that the combined treatment significantly ($p < 0.05$) reduced microbial growth (Total Viable Count), reduced the production of volatile nitrogen compounds (TVB-N), controlled lipid oxidation (TBA), and maintained pH stability and sensory acceptance. Regression models for all quality parameters showed high accuracy and predictive power ($R^2 > 99.27\%$). This study clearly demonstrates the effectiveness of the combined strategy of cold plasma and active packaging in maintaining the quality and increasing the shelf life of fish paste.

Keywords: Active packaging, Antibacterial, Biodegradable film, Cold plasma

Introduction

Conventional plastic packaging has raised significant concerns due to its non-degradability, the transfer process of potentially toxic compounds to food, and its role in environmental pollution. These challenges have driven the development of environmentally friendly alternatives, including edible and biodegradable films (Dadkhah, Pirsa, Javadi, & Mohtarami, 2024; Eslami, Pirsa, Mohtarami, & Bener, 2025; Forouzan, Pirsa, & Alirezalu, 2024; Pirsa, Bener, & Şen, 2024). In this context, polycaprolactone (PCL), a biodegradable aliphatic polyester, has gained attention for its favorable mechanical properties and processability. However, the standalone application of PCL faces limitations, particularly the need to enhance its functional properties. To address these limitations, combining PCL with natural polymers such as beta-glucan (BG) presents a promising solution. BG is a polysaccharide known for its

Authors retain the copyright. This is an open access article distributed under Creative Commons Attribution 4.0 International License (CC BY 4.0).
https://doi.org/10.22067/ifstrj.2025.96443.1508

film-forming ability and high biocompatibility. Furthermore, incorporating natural active ingredients like oak fruit pair extract (OFPE) and apricot kernel extract (AKE) which are rich in phenolic and antioxidant compounds, respectively along with antimicrobial gold nanoparticles (AuNPs), can facilitate the development of advanced composite films with both antioxidant and antimicrobial capabilities. Such nanocomposites are highly valuable for minimizing the growth of spoilage microorganisms during food processing and storage, thereby extending shelf life and improving food safety. Gold, being the least reactive metal, possesses very stable chemical properties. It is non-toxic, exhibits good biocompatibility, and is multivalent, allowing it to bind different types of ligands (Gupta *et al*., 2016).

The extremely large specific surface area of AuNPs provides abundant sites for binding to target bacteria. AuNPs have shown antibacterial activity against both Gram-positive and Gram-negative bacteria (Slavin, Asnis, Häfeli, & Bach, 2017). Compared to conventional antibiotics, AuNPs do not easily induce drug resistance because they target a variety of molecules (DNA and protein). Therefore, it becomes difficult for bacteria to develop a system that can defend against all damages (Zhao *et al*., 2018). The preparation and antibacterial properties of AuNPs have been extensively studied, but no comprehensive summary has been published to date. Recently, non-thermal discharge plasma (Cold plasma) has attracted much attention as a means to kill microorganisms due to its high efficiency and environmental compatibility (Barba, Koubaa, do Prado-Silva, Orlien, & de Souza Sant'Ana, 2017). Furthermore, cold plasma treatment can be conducted at room temperature and atmospheric pressure, making it a safe and energy-efficient method. Various plasma sources are available, including dielectric barrier discharge (DBD), corona discharge, and microwave discharge (Misra *et al*., 2018; Bahmanpour, Asefi, Alizadeh, & Pirsa, 2024). The inactivation of bacteria during plasma discharge is primarily attributed to two main factors: the strong electric field generated within a specific range and the diverse active species produced by the plasma. While plasma technology has been widely utilized in the biomedical field for over a decade, its application has recently expanded into the food industry. For instance, it has been employed for disinfecting food industry wastewater (Patange *et al*., 2018). Specifically, DBD plasma has proven effective in eliminating bacteria and yeast in apple juice (Liao *et al*., 2018).

Fish paste products, commonly known as fish cakes. According to the Korean Food Standards Codex, is characterized as a processed seafood product comprising salt-soluble proteins extracted from fish flesh. Fish muscle is mechanically separated from the bone, thoroughly washed with water, and blended with cryoprotectants to produce a hydrated protein concentrate known as surimi. This Japanese term, which translates to "washed fish mince," refers to the refined fish myofibrillar protein obtained through this process. It is a refined fish myofibrillar protein that is produced through multiple step-by-step processes including heading, gutting, filleting, deboning (mincing), washing, dewatering, mixing with cryoprotectants, freezing, and metal detection for HACCP. Myofibrillar proteins make it an excellent ingredient for the production of food products. It has excellent gelling properties and forms strong, elastic gels when heated. Textural properties such as gel strength are the main determinants of the price and quality of surimi. The quality of surimi and its gelling properties are mainly influenced by both intrinsic factors (effect of fish species, seasonality, sexual maturity and freshness or hardness) and extrinsic factors (harvest, handling, water characteristics, processing time and temperature, solubilization of myofibrillar proteins during processing) (Nishinari & Ooizumi, 2020; Panpipat, Thongkam, Boonmalee, Çavdar, & Chaijan, 2023).

The aim of this study was to develop an antibacterial polycaprolactone/beta-glucan film modified with hydroalcoholic oak fruit pair

extract, apricot kernel extract, and gold nanoparticles for active packaging of cold plasma-treated fish paste.

Materials and Methods

Chemicals

All chemicals used in this study, including polycaprolactone and beta-glucan, were obtained from international and domestic suppliers. The polymer base of the film (polycaprolactone and beta-glucan) was purchased from the official representative of Sigma-Aldrich in Iran. Plant materials, including oak and apricot kernels, were purchased directly from the local market in Urmia and prepared for the extraction process. Also, microbial culture media and other laboratory chemicals were obtained from Merck, Germany and Sigma-Aldrich, USA. The bacterial strains tested (*Bacillus cereus* and *Escherichia coli*) were also obtained from the reputable collection of the Scientific and Industrial Research Organization of Iran.

Preparation of Plant Extracts

Two distinctive extraction methods were selected to optimally address the distinct chemical profiles of each plant material. The Soxhlet method was chosen for oak fruit pair due to its high efficiency in extracting non-polar to semi-polar compounds (e.g., fixed oils, waxes) from its dense and oily tissue. In contrast, the maceration method at room temperature was selected for apricot kernels to gently extract more polar and potentially heat-sensitive target compounds, such as amygdalin, while minimizing their degradation.

Extraction of Oak Fruit Pair Extract (OFPE)

The extraction of oak fruit pair extract was performed using the Soxhlet method with 86% ethanol as the solvent. In this process, 200 g of oak fruit pair powder was mixed with 500 ml of ethanol and kept in the dark for 48 hours with intermittent stirring (20 minutes per day). The resulting solution was then filtered using Whatman filter paper and concentrated using a rotary evaporator at 50 °C under vacuum conditions. The concentrated extract was stored in sterile Petri dishes in an incubator at 40 °C for final evaporation of the residual solvent. The final product was stored in the dark at refrigerator until use (AOAC, 2005; Zhang *et al*., 2020).

Extraction of Apricot Kernel Extract (AKE)

After separating and drying apricot kernels in an oven, the obtained powder was subjected to maceration extraction using 70% ethanol for 72 hours. Specifically, 10 g of the powder was dissolved in 100 ml of ethanol and stirred simultaneously on a magnetic stirrer at medium speed and room temperature. Following the extraction period, the mixture was centrifuged, and the supernatant was filtered through Whatman No. 1 filter paper. The filtered supernatant was then concentrated under vacuum using a rotary evaporator at 45 °C. The final extract was stored in a freezer after complete evaporation of the residual solvent at 45 °C until use (Zhang *et al*., 2020).

Preparation of Composite Film

The nanocomposite film was prepared by first preparing a polymer base solution with equal proportions of polycaprolactone (PCL) and beta-glucan. Specifically, beta-glucan powder (2 g) was dissolved in 50 ml of distilled water and heated on a magnetic stirrer at 80 °C for 2 hours. Simultaneously, a PCL solution was prepared by dissolving 2 g of the polymer in 10 ml of chloroform and stirring for 30 minutes. The PCL solution was then added dropwise to the beta-glucan solution, followed by the addition of Tween 80 as emulsifier (1% w/w of solids). After 30 minutes of stirring, oak fruit pair extract and apricot kernel extract (0.5% w/w each) were incorporated into the formulation, and the mixture was homogenized at high speed for 2 minutes using a homogenizer (model D9I12, Heidolf, Germany). Subsequently, gold nanoparticles (0.03% w/w) were added, and the mixture was magnetically stirred for 10 minutes before being subjected to ultrasonication for 10 minutes. Glycerol (30% w/w of dry matter) was

then introduced as a plasticizer, and stirring continued for 15 minutes at room temperature. Finally, 25 ml of the prepared solution was cast onto 8 cm plates and dried in an oven at 38 °C. The resulting films were carefully peeled off and stored in light-proof bags at room temperature (Pirsa *et al*., 2024).

In addition to the final composite film (PCL/BG/OFPE/AKE/AuNPs), several film formulations with varying concentrations of OFPE, AKE, and AuNPs were prepared based on the experimental design (See Table 1-B and Table 2-A) to investigate their individual and combined effects. These included the base film (PCL/BG) and films containing individual additives (PCL/BG/OFPE, PCL/BG/AKE, PCL/BG/AuNPs) for comparative analysis in DSC and antibacterial tests. The concentration ranges for the additives were selected based on preliminary experiments and literature review. The extract concentrations (0.25-0.75% w/w) were chosen to ensure significant antimicrobial efficacy while maintaining the film's structural integrity and avoiding negative effects on its physical properties. The concentration of AuNPs (0.015-0.045% w/w) was selected due to the fact that low loadings are sufficient to enhance antibacterial activity and thermal stability without causing aggregation or compromising the film matrix.

DSC Examination of Films

In order to determine the DSC (Differential Scanning Calorimetry) of the samples, initially about 0.03 g of each film was placed in an aluminum pan in a package and was carried out at a rate of 10 °C per minute and at the temperature range of 0 to 500 °C for 45 minutes in the presence of helium gas by a differential scanning calorimetry device (10-PT Linsies, Germany).

Antimicrobial Activity of Films and Extracts

The antimicrobial activity of nanocomposite films containing oak fruit pair extract, apricot kernel extract, and gold nanoparticles was evaluated against two bacterial strains - *E. coli* O157:H7 (ATCC 25922) and *B. cereus* (PTCC 1154) - using the disk diffusion method. Film samples were cut into 6-mm diameter discs using a sterile punch and aseptically placed on Mueller-Hinton agar plates. The agar surface had been previously inoculated with 0.1 mL of bacterial inoculum containing 10^5 -10^6 CFU/mL. After incubation at 37 °C for 24 hours, the inhibition zones appearing as clear halos around the film discs were measured in millimeters using a digital caliper.

The antibacterial properties of the extracts were studied using the agar well diffusion method on two strains of bacteria, *E. coli* O157:H7 (ATCC 25922) and *B. cereus* (PTCC 1154). Briefly, the surface of Mueller Hinton agar plates was first inoculated uniformly (by swabbing) with 0.1 ml of inoculum containing 10^6 CFU/ml of the tested bacteria. Then, wells (5 mm in diameter) were created in the inoculated agar using a sterile cork borer. Subsequently, 30 µl of the pure extract was poured into each well. The plates were incubated at 37 °C for 24 hours. Then, the zone of inhibition was measured in millimeters as a clear halo around the wells with a digital caliper (Balouiri, Sadiki, & Ibnsouda, 2016).

Preparation of Cold Plasma Treated Fish Paste

Common carp was freshly obtained from the fish market (Urmia, Iran). It was transferred to the processing laboratory after being stored on ice. The surimi preparation process was carried out manually in the laboratory according to the method of Jeon, Myung, & Min, (2022). After beheading and abdominal emptying, common carp was filleted and washed manually, then deboned. The meat was ground using a meat grinder equipped with a plate with 3 mm diameter holes. After that, the minced meat was washed with cold water at a temperature below 10 °C for three times with a ratio of 4:1 water to fish meat, twice with distilled water and then once with a 0.3% brine solution, each time for 15 minutes. After each washing, the fish meat was poured into a clean cloth to remove excess water. Then, 4% sugar, 4% sorbitol, and 0.3% sodium tripolyphosphate were added to the

prepared surimi and mixed in a meat mixer (Mulinex, 1000w, Made in France). Finally, the prepared fish paste was treated using a Dielectric Barrier Discharge (DBD) plasma device (Diener electronic, Jettingen, Germany). Argon gas (99.997% purity) was used as the feed gas to generate the cold plasma. This gas was chosen due to its inert nature, food-grade safety, efficiency in generating stable plasma, and effectiveness in microbial inactivation while minimizing potential adverse effects on food quality. The prepared fish paste sample was placed on the base inside the device, then argon gas was injected into the device at a constant rate of 6 liters per minute to produce plasma, and the samples were treated under vacuum conditions with a pressure of 600 mTorr and a power of 20-30 watts. The sample was exposed to cold plasma treatment with argon gas for 6 minutes and packaged for subsequent tests (Jeon *et al*., 2022).

Packaging of Fish Paste with Nanocomposite Film

After preparing the cold plasma treated fish paste, the packaging film prepared as mentioned above was used for antimicrobial packaging and preservation. For this purpose, 50 g of cold plasma treated fish paste and 50 g of fish paste treated with conventional heating method were packed in edible film and conventional packaging in the same dimensions and kept at refrigerator for one month (Fig. 2). Sa mples were taken on day 1, 15, 30and the following tests were performed.

Packaged Fish Paste Tests

pH Measurement

One g of fish paste samples was mixed with 9 ml of distilled water (in Falcon tubes) and homogenized with a homogenizer (Ultra Turrax T25, IKA, Germany) at 13,500 rpm for 30 seconds. Then, the pH of the fish paste samples was measured at room temperature using a digital pH meter (Hanna HI9025c, Portugal) (Zhang *et al.*, 2020).

Determination of Total Volatile Nitrogenous Bases (TVB-N)

This test was performed according to the AOAC method (2002) and its amount was calculated in milligrams per hundred grams of fish paste according to the following equation:

$$TVB - N = \frac{M \times 1.4}{N} \times 100$$

where M and N are the amount of sulfuric acid consumed and the weight of the sample, respectively.

Measurement of Thiobarbituric Acid (TBA)

Measurement of Thiobarbituric Acid is based on the spectrophotometric values (HACH, DR/2000, USA) of the pink complex resulting from the reaction of one malonaldehyde molecule obtained from distillation with two thiobarbituric acid molecules added to the distilled solution, and its amount is expressed in milligrams of malonaldehyde per kilogram of sample according to the following equation (Rahman, Al-Amiri, & Al-Riziq, 2021).

$$TBA = \frac{A_s - A_b}{50} \times 200$$

Total Bacterial Count (TVC)

Tryptic soy agar (TSA) medium was used for total bacterial count after preparing serial dilutions, surface culture was performed on the plates and the samples were incubated at 32 °C for 48 hours and then the colonies were counted (AOAC, 2005).

Sensory Evaluation

Sensory evaluation of the samples was carried out according to the 5-point hedonic test by 10 panelists. This study was approved by the Research Ethics Committee of Urmia University. For this purpose, the samples were coded and evaluated in terms of sensory characteristics (overall acceptance). A score of 5 indicated the highest quality of the sensory characteristic and a score of 1 indicated the lowest quality for the sensory characteristic (Lawless & Heymann, 2010).

Statistical Analysis

In this study, response surface methodology and a D-Optimal statistical design were employed for two key objectives:

1. To formulate and screen antibacterial films with different compositions of OFPE, AKE, and AuNPs (as shown in Table 1-B) and modelling their antibacterial responses (Inhibition Zone).
2. To investigate the effect of cold plasma treatment and active packaging on the quality parameters of fish paste during storage (as shown in Table 1-A).

This design was selected due to its high efficiency in providing reliable regression models with the minimum number of required experimental runs, which was particularly advantageous given the practical constraints of the study. For the first objective (film formulation), the factors were the concentrations of OFPE, AKE, and AuNPs.

Table 1-A. List of treatments performed on fish paste based on the D-Optimal design. (CP: Cold Plasma; Active film: PCL-BG-OFPE-AKE-AuNPs)

Run	Factor A: Time (Day)	Factor B: CP*	Factor C: Active film**
1	30	Unused	Used
2	15	Used	Unused
3	1	Unused	Used
4	1	Used	Unused
5	15	Used	Used
6	15	Unused	Unused
7	30	Unused	Unused
8	15	Unused	Used
9	30	Used	Unused
10	1	Unused	Unused
11	30	Used	Used
12	1	Used	Used

*CP: Cld Plasma

**Active film: Polycaprolactone/Beta-Glucan nanocomposite film containing Oak Fruit Pair Extract, Apricot Kernel Extract, and Gold Nanoparticles (PCL-BG-OFPE-AKE-AuNPs)

Table 1-B. List of selected films for testing antibacterial properties. (OFPE: Oak Fruit Pair Extract; AKE: Apricot Kernel Extract; AuNPs: Gold Nanoparticles)

Film Code	OFPE (%)	AKE (%)	AuNPs (%)
F1	0.75	0.25	0.045
F2	0.75	0.75	0.045
F3	0.25	0.25	0.045
F4	0.5	0.5	0.015

For the second objective (fish paste quality), the type of cold plasma treatment (treated and untreated) and the type of packaging (conventional packaging and active packaging) were considered as non-numeric factors, and storage time was included as a covariate. The final design for the application study consisted of 12 experimental runs or treatments (Table 1-A). All analyses were performed independently on each experimental unit. A 95% probability level was used to examine the significance of the means and the models. Design Expert software (version 10) was used for modeling, generating response surface curves, and comparing means.

Results and Discussion

DSC

Fig. 1 presents the DSC curves of the polycaprolactone-beta-glucan composite films. The thermal properties and phase transitions derived from these curves are as follows. The PCL/BG base film exhibited a glass transition (Tg) between 50-60 °C, associated with the amorphous regions of polycaprolactone. A distinct melting temperature (Tm) was observed at approximately 56-58°C, corresponding to the crystalline PCL domains. The measured enthalpy of fusion was 887.5 J/g, indicating a relatively high degree of crystallinity in the base film. Incorporation of apricot kernel extract (PCL/BG/AKE) resulted in a slight reduction in melting temperature to 53-55°C and decreased enthalpy of fusion compared to the base film. This might be due to the interactions between AKE components and the polymer matrix that reduce crystallinity. Similarly, the film containing oak fruit pair extract (PCL/BG/OFPE) showed noticeable alterations in the melting peak and a shift in glass transition toward lower temperatures, likely due to strong interactions between phenolic compounds in the extract and polymer chains. The addition of gold nanoparticles (PCL/BG/Au) significantly enhanced thermal properties, increasing the melting temperature to approximately 64.6 °C and elevating the enthalpy of fusion. These improvements indicate that gold nanoparticles function as nucleating agents, promoting crystallinity and thermal stability. The final composite film (PCL/BG/OFPE/AKE/Au) demonstrated the highest melting temperature at 81.6°C among all samples, forming a complex thermal structure with multiple phase transitions and enhanced thermal stability compared to the base film.

These findings collectively demonstrate that component interactions substantially influence the thermal properties of composite films. While gold nanoparticles enhance thermal stability through nucleation, plant extracts modify crystal structure via polymer chain interactions, ultimately affecting film performance in packaging applications. According to Ma, Shi, Su, & Wang, (2020), pure polycaprolactone of similar molecular weight (Mw ~50,000) exhibits a melting temperature of approximately 63.5°C and fusion enthalpy of about 94.5 J/g. In contrast, our PCL/BG base film showed reduced values for both parameters (Tm: 56-58°C; ΔHm: 887.5 J/g). This reduction primarily stems from the dilution effect and physical interactions with β-glucan, which disrupt PCL crystal ordering. Although molecular weight remained unchanged in our study, the observed decrease in Tm and ΔHm parallels the effects reported by Ma *et al.* for molecular weight reduction. This similarity suggests that the additives inhibit complete polymer chain crystallization, resulting in a crystal structure resembling that of lower molecular weight PCL. Conversely, gold nanoparticles increased both Tm and ΔHm, contrasting with the general trend described in the reference study. This opposing effect clearly indicates that nanoparticles reinforce PCL crystal structure through a distinct mechanism, likely acting as nucleation sites to enhance thermal stability. The comparison demonstrates that while our additives did not chemically degrade the polymer, they significantly influence crystalline microstructure and thermal properties through physical interactions (Ma *et al.*, 2020).

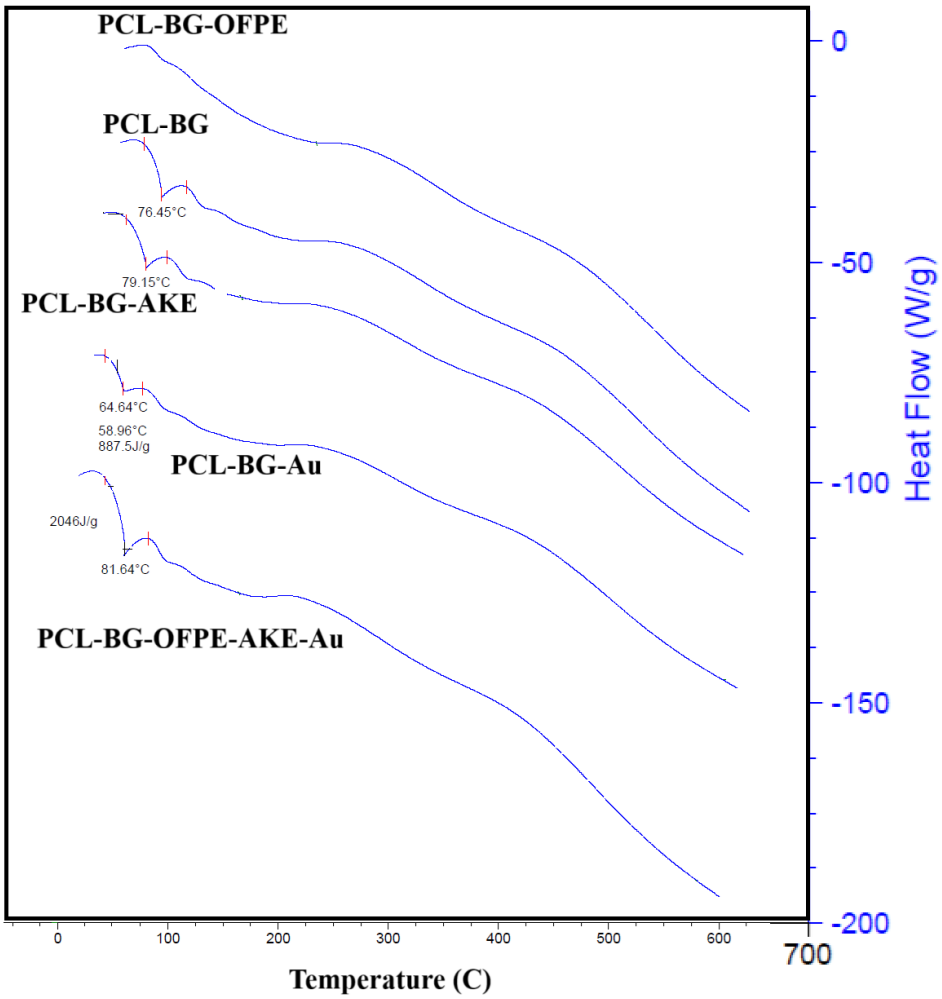

Fig. 1. DSC curves for polycaprolactone-beta-glucan based composite films

Antimicrobial Activity of Composite Films and Extracts

Fig. 2-B and Tables 2-A and 2-B show the antibacterial properties of composite films, incorporated with extracts and gold nanoparticles. Based on the results presented in Tables 2-A and 2-B, the antibacterial activity of composite films and their components against Gram-positive (*Bacillus cereus*) and Gram-negative (*Escherichia coli*) bacteria was investigated. As can be seen in Table 2-A, all composite films containing polycaprolactone/beta-glucan, oak fruit pair extract, apricot kernel extract and gold nanoparticles had inhibitory effects against both bacteria. The film containing the highest concentration of both extracts produced the largest zone of inhibition (27.78 mm for *Bacillus cereus* and 21.38 mm for *Escherichia coli*). This result indicates a strong synergistic effect between the active compounds in the film.

In general, all films produced a larger inhibition zone against *Bacillus cereus* (a Gram-positive bacterium) compared to *Escherichia coli* (a Gram-negative bacterium). This could be due to the complex structure of the cell wall of Gram-negative bacteria, which acts as a physical barrier to the penetration of antibacterial compounds. Comparison of the samples shows that increasing the concentration of gold nanoparticles from 0.015% to 0.045% (holding other factors constant) leads to a significant increase in the diameter of the inhibition zone, indicating the important role of gold nanoparticles in enhancing the antibacterial properties of the

film. Based on the data in Table 2-B, each of the compounds alone also has significant antibacterial activity. Oak fruit pair extract at a concentration of 0.75% produced a larger zone of inhibition (20.41 mm) against *Bacillus cereus* compared to *Escherichia coli* (15.65 mm). This effect is probably due to the presence of phenolic and flavonoid compounds with strong antibacterial properties in this extract. Apricot kernel extract at the same concentration also showed a greater inhibitory effect on *Bacillus cereus* (18.08 mm) than *Escherichia coli* (13.28 mm), which could be related to compounds such as amygdalin and its derivatives. Gold nanoparticles at a concentration of 0.045% showed a more balanced antibacterial effect against both bacteria (19.24 mm for *Bacillus cereus* and 18.31 mm for *Escherichia coli*). The mechanism of action of gold nanoparticles is probably through the production of reactive oxygen species, cell wall destruction, and disruption of intracellular processes in bacteria. The results of this section clearly show that the prepared composite films have a favorable and strong antibacterial effect against both Gram-positive and Gram-negative bacteria. The synergistic effect between the different components present in the film (plant extracts and gold nanoparticles) has led to a significant enhancement of the antibacterial properties. These films have a high potential for use in active packaging of food products, especially sensitive products such as fish paste. The generally larger inhibition zones observed against *Bacillus cereus* (Gram-positive) compared to *Escherichia coli* (Gram-negative) can be attributed to the fundamental structural differences in their cell walls. Gram-positive bacteria possess a thick, porous peptidoglycan layer that is more accessible to the antibacterial compounds (e.g., phenolics from extracts) released from the film. In contrast, Gram-negative bacteria have a complex outer membrane rich in lipopolysaccharides, which acts as a formidable hydrophobic barrier, initially restricting the penetration of these antimicrobial agents. The mechanism of cold plasma, involving reactive species that cause lipid peroxidation, is particularly effective at disrupting this outer membrane in Gram-negative bacteria. The more balanced effect of AuNPs against both types suggest their mode of action, potentially involving physical damage and oxidative stress, is less hindered by the structural differences in the cell envelope.

According to the results of the present study and the study of Holešová *et al.* (2021), the antibacterial performance of polycaprolactone (PCL) films containing nanoparticles is compared as follows. In the present study, the PCL/BG nanocomposite film containing plant extracts and gold nanoparticles produced a growth inhibition zone of 27.78 mm against *Bacillus cereus* and 21.38 mm against *Escherichia coli*, while in the study of Holešová *et al.*, the PCL film containing nano-clays functionalized with silver ions reported a growth inhibition zone of 12.5 mm against *Staphylococcus aureus* and 10.5 mm against *Escherichia coli*. In the present study, the antibacterial mechanism of action was a combination of multiple factors including the release of phenolic and flavonoid compounds from plant extracts, the synergistic effect of gold nanoparticles in the production of reactive oxygen species and disruption of the bacterial cell membrane, while in the reference study, the mechanism of action was mainly based on the release of silver ions from nano-clay and disruption of bacterial cell function. In the present study, the synergistic effect between different compounds led to a significant increase in antibacterial efficacy. The nanocomposite film produced in the present study had higher antibacterial efficacy than the films in Holešová's study. This superiority could be due to the following factors: the simultaneous use of multiple antibacterial mechanisms, the synergistic effect between different compounds and the higher potential of plant compounds and gold nanoparticles in inhibiting bacterial growth. Both studies showed that the modification of PCL films with nanoparticles and active compounds can lead to the development of active packaging with

effective antibacterial properties. However, the use of natural compounds in the present study could have additional advantages in terms of safety and environmental friendliness (Holešová *et al.*, 2021).

Both the present study and the research conducted by Cesur, Köroğlu, & Yalçın, (2018) independently validate that incorporating natural compounds and nanomaterials to enhance the antibacterial properties of polycaprolactone films. In the study by Cesur and colleagues, the inclusion of nano minerals and chitosan into the PCL matrix demonstrated significant antibacterial efficacy against both Gram-positive and Gram-negative bacteria. This result is consistent with our findings, where the combination of plant extracts and gold nanoparticles in the PCL/BG film resulted in strong bacterial inhibition. Both studies demonstrate that modifying the structure of PCL with active natural materials is an effective strategy for the development of antimicrobial packaging. Although the additives used are different, the results of both studies clearly emphasize the scientific principle that the formation of a nanocomposite network in a polymer matrix can significantly enhance the antibacterial efficacy of packaging films, confirming the potential of this strategy for application in the food industry (Cesur *et al.*, 2018).

Table 2-A- Inhibition zone of composite films against *Bacillus cereus* and *Escherichia coli*

Film Type	OFPE Concentration (%)	AKE Concentration (%)	AuNPs Concentration (%)	*B. cereus* (G+) (mm)	*E. coli* (G-) (mm)
PCL-BG-OFPE-AKE-Au	0.75	0.25	0.045	23.92±0.48*	20.25±0.51
PCL-BG-OFPE-AKE-Au	0.75	0.75	0.045	27.78±0.54	21.38±.37
PCL-BG-OFPE-AKE-Au	0.25	0.25	0.045	13.61±0.35	11.18±0.47
PCL-BG-OFPE-AKE-Au	0.5	0.5	0.015	16.40±0.44	12.58±.027

*The data were the average of three replicates.

Table 2-B- Inhibition zone of extracts and nanoparticles against *Bacillus cereus* and *Escherichia coli* bacteria

Compound	Concentration (%)	*B. cereus* (G+) (mm)	*E. coli* (G-) (mm)
OFPE	0.75	20.41±0.28*	15.65±.044
AKE	0.75	18.08±.029	13.28±0.55
AuNPs	0.045	19.24±.037	18.31±0.42

*The data were the average of three replicates.

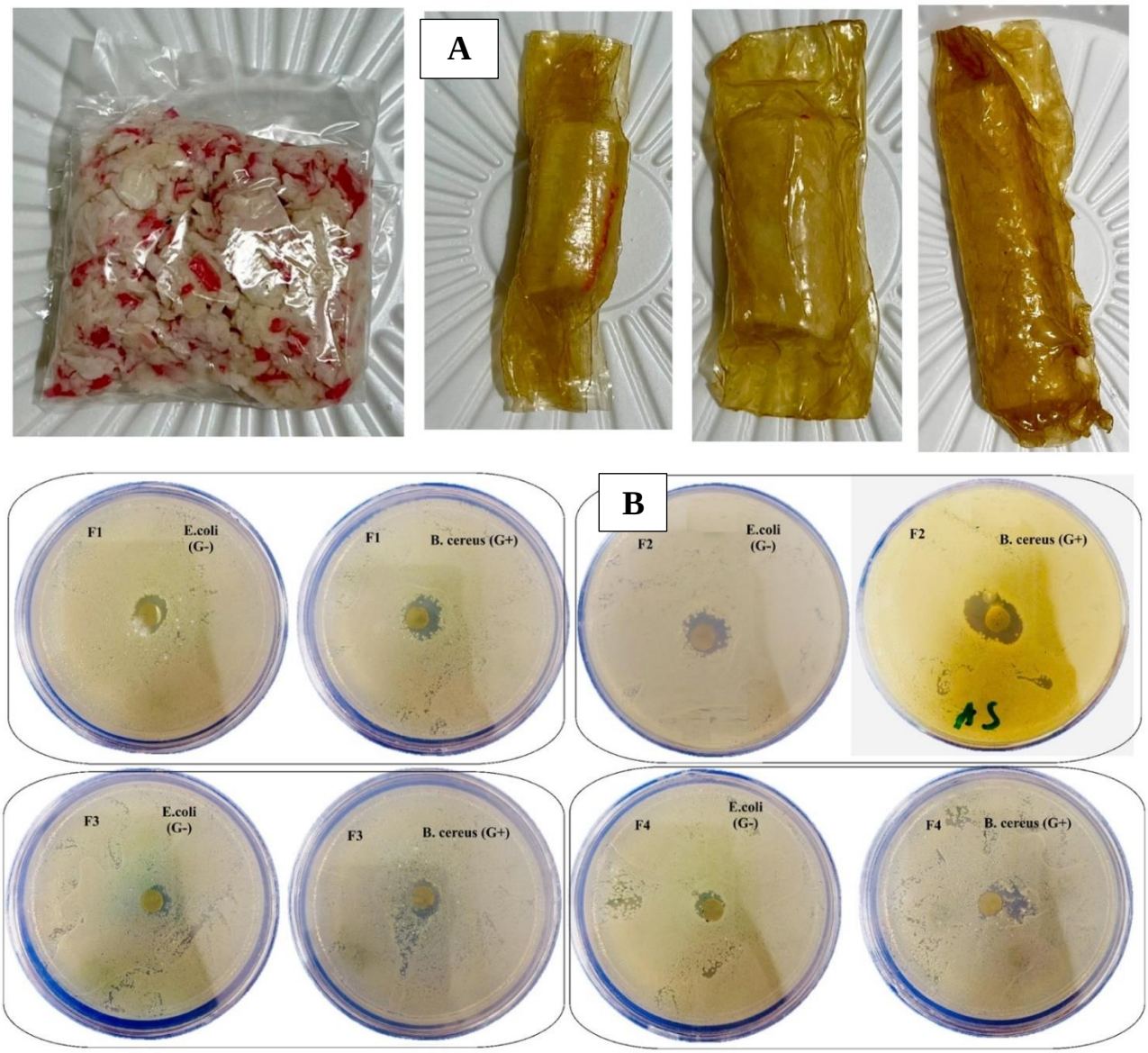

Fig. 2. Packaging of fish paste treated with head plasma with active composite films (A) and antibacterial properties of composite films (B)

pH of Fish Paste

Fig. 3 shows the three-dimensional diagram and interaction curve of the effect of storage time, cold plasma treatment and active film packaging on the pH of fish paste. Changes in the pH of fish paste during the storage period were observed based on the results obtained from the analysis of variance (ANOVA) of the quadratic response surface model. The presented model was statistically significant (p-value < 0.0001) and was able to explain 99.75% of the response changes. The values of R^2 (0.9975), adjusted R^2 (0.9932) and predicted R^2 (0.9692) indicate the favorable fit and high predictive power of the model. Among the studied factors, the storage time (A) was identified as the most effective factor on pH changes (p-value > 0.0001). The effects of cold plasma treatment (B) and active film packaging (C) were also significant at 99.96% and 99.72% confidence levels, respectively. Among the interaction effects, the interaction between time and cold plasma treatment (AB) and time and packaging type (AC) significantly affected pH,

while the interaction between cold plasma treatment and active film (BC) was not significant. The quadratic effect of time (A^2) was also significant, indicating a nonlinear trend in pH changes over time. The final regression equation was obtained as follows:

$pH= 6.57 + 0.33*A + 0.080*B + 0.048*C + 0.066*A*B + 0.059*A*C - 0.00917*B*C + 0.083*A^2$

The response surface and plots clearly showed the relationship between the independent variables and pH. With the increase in storage time, the pH of fish paste increased significantly. However, it was observed that the combined application of cold plasma treatment and active film packaging effectively prevented the sharp increase in pH - which is generally caused by bacterial spoilage and the production of alkaline compounds - and slowed down the spoilage process. Based on these findings, it can be concluded that the designed model has a high efficiency for predicting pH changes and the use of antibacterial active film in combination with cold plasma treatment is an effective strategy to maintain pH stability and shelf life of fish paste during storage.

Both the current investigation and the earlier work by Remya *et al.* (2016) provide independent confirmation of the positive effect of active packaging on maintaining pH stability in fish products. In Remya's study, the use of chitosan-containing film significantly prevented the increase in pH of barracuda fillets during refrigerated storage. This result is fully consistent with the findings of the present study, by which active packaging with polycaprolactone/beta-glucan film containing plant extracts and gold nanoparticles effectively inhibited the increase in pH of fish paste. Both studies indicate that active packaging plays a key role in maintaining pH stability and, consequently, extending the shelf life of fishery products by delaying the accumulation of alkaline compounds caused by microbial spoilage. This consistency of results confirms the effectiveness of active packaging strategy in controlling chemical indicators of spoilage in various fish products (Remya *et al.*, 2016).

TBA and TVB-N

Fig. 4 shows the three-dimensional diagram and interaction curve of the effect of storage time, cold plasma treatment and active film packaging on TBA and TVB-N of fish paste.

Changes in the thiobarbituric acid index of fish paste during the storage period were observed based on the results of the analysis of variance of the quadratic response surface model. The presented model was statistically significant at the 99.99% confidence level (p-value < 0.0001) and was able to explain 99.90% of the response changes. The R^2 values (0.999) and adjusted R^2 (0.997) indicate the optimal fit of the model. Storage time (A) was identified as the most effective factor in increasing the TBA index. This increase is mainly due to the intensification of lipid oxidation over time, which is accompanied by the formation of secondary oxidation products such as malondialdehyde (MDA). Cold plasma treatment (B) significantly reduced the TBA index, which is probably due to: inactivation of oxidative enzymes, reduction of the population of bacteria responsible for oxidation, and structural changes in fish tissue. Packaging with active film (C) showed the highest inhibitory effect in controlling oxidation, which can be attributed to the following: the presence of antioxidant compounds in plant extracts, the synergistic effect of gold nanoparticles, and the creation of a physical barrier against oxygen. The interaction effect of time and cold plasma treatment (AB) showed that the application of cold plasma can reduce the rate of oxidation caused by storage time. The interaction effect of time and active packaging (AC) showed the synergistic effect of these two factors in controlling oxidation in longer storage periods. The quadratic effect of time (A^2) indicates a nonlinear and intensifying pattern of oxidation in the final storage periods. The final regression equation was obtained as follows:

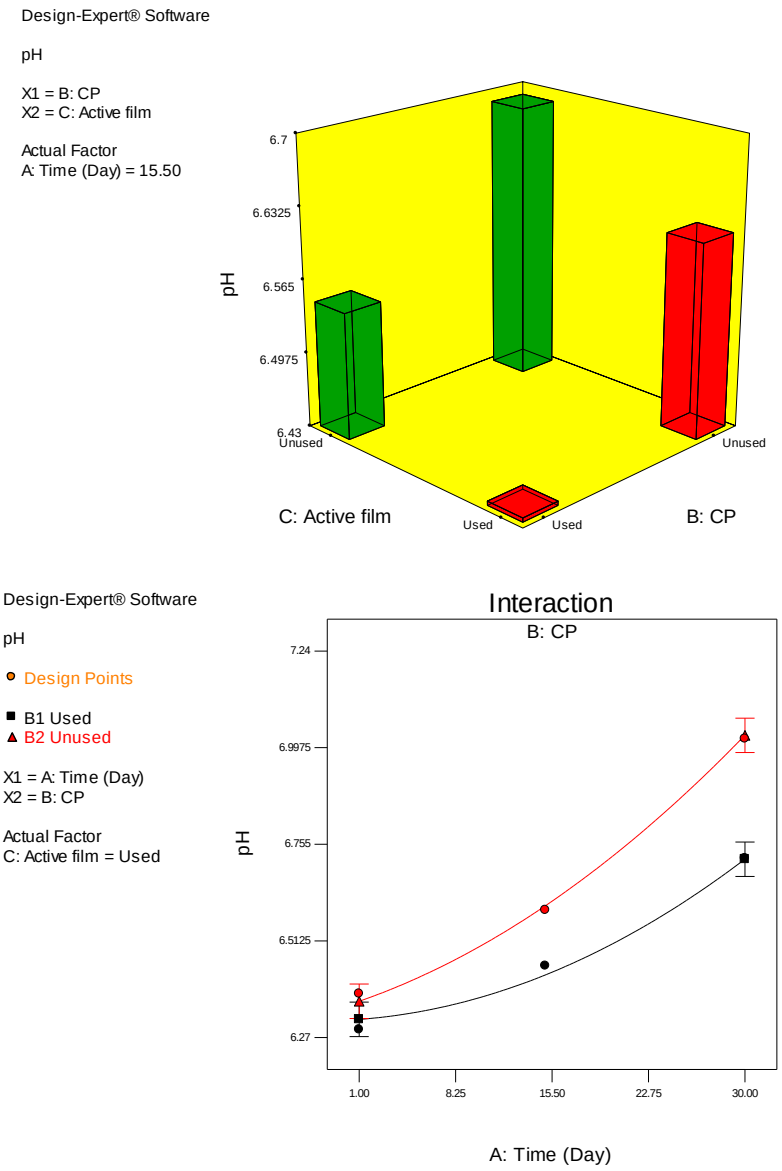

Fig. 3. Three-dimensional diagram and interaction curve of the effect of storage time, cold plasma treatment, and packaging with active film on the pH of fish paste

$$TBA = 0.95 + 0.91*A + 0.078*B + 0.18*C + 0.074*A*B + 0.19*A*C + 0.17*A^2$$

The response surface plots clearly showed that the simultaneous application of cold plasma treatment and active packaging could effectively prevent the increase of TBA index during the storage period.

The changes of the total volatile basic nitrogen index (TVB-N) of fish paste during the storage period were observed based on the results of the analysis of variance of the two-factor interaction (2FI) response surface model. The presented model was statistically significant at the 99.99% confidence level (p-value < 0.0001) and was able to explain 99.38% of the response variations. The values of R^2 (0.993) and adjusted R^2 (0.986) indicate the good fit of the model. Storage time (A) was identified as the most effective factor in increasing the TVB-N index. This increase is mainly due to the activity of endogenous proteolytic enzymes and the activity of spoilage microorganisms, which leads to the production of volatile nitrogen-containing compounds

such as ammonia, amines and trimethylamine. Cold plasma treatment (B) significantly reduced the TVB-N index, which might due to the inactivation of proteolytic enzymes and spoilage microorganisms by plasma active species and the reduction of the rate of protein degradation reactions. Packaging with active film (C) also showed a significant inhibitory effect on the formation of volatile nitrogen-containing compounds, which probably acts through the following mechanisms: antimicrobial activity of plant extracts presents in the film, reduction of oxygen permeability and creation of an unfavorable environment for the growth of TVB-N-producing bacteria, and absorption or neutralization of volatile nitrogen-containing compounds. The interaction effect of time and cold plasma treatment (AB) showed that the application of cold plasma could effectively reduce the rate of TVB-N accumulation during the storage time. The interaction effect of time and active packaging (AC) showed the synergistic effect of these two factors in controlling the production of volatile nitrogen compounds during longer storage periods. The interaction effect of cold plasma treatment and active film (BC) was not statistically significant, which probably related to the independent function of these two technologies in controlling different spoilage pathways. The final regression equation was obtained as follows:

TVB-N = 21.75 + 11.22*A + 2.41*B + 2.03*C + 2.51*A*B + 2.01*A*C - 0.12*B*C

The response surface and counter plots clearly showed that the simultaneous application of cold plasma treatment and active packaging can effectively prevent the increase of TVB-N index during the storage period.

This study demonstrates that the combination of cold plasma treatment and active packaging utilizing a film incorporated with antioxidant compounds represents an effective strategy for controlling lipid oxidation and extending the shelf life of fish paste. The synergistic effect of these two methods can simultaneously target different oxidation mechanisms and maintain the quality of the product during the storage period. Also, the combination of cold plasma treatment and active packaging with a film containing antimicrobial compounds can be an effective strategy to control the production of volatile nitrogen compounds and prevent growth of spoilage bacteriain fish paste. The synergistic effect of these two methods in controlling the TVB-N index indicates the high potential of this combined strategy in maintaining the quality and increasing the shelf life of fishery products.

Both the current investigation and the research conducted by Julyaningsih, Latief, & Dirpan, (2020) independently validate the efficacy of active packaging in regulating chemical indicators of fish spoilage. In Julyaningsih's study, the implementation of smart packaging incorporating chitosan-gelatin nanofibers substantially reduced thiobarbituric acid (TBA) values and total volatile basic nitrogen (TVB-N) levels in tuna fillets throughout the storage period. This finding is fully consistent with the results of the present study, in which active packaging with a polycaprolactone/beta-glucan nanocomposite film containing plant extracts and gold nanoparticles effectively prevented the increase in TBA and TVB-N indices in fish paste. Both studies indicate that active packaging plays a key role in maintaining the quality and increasing the shelf life of fishery products by inhibiting lipid oxidation, reducing TBA, and reducing TVB-N. This concordance of results confirms the effectiveness of active packaging strategy in simultaneously controlling oxidative and microbial spoilage in different fish products (Julyaningsih *et al.*, 2020).

Both the present study and Erkan's (2017) study independently confirm the role of active packaging in controlling chemical spoilage indices of fish. In Erkan's study, the use of active packaging significantly reduced the values of total volatile nitrogen (TVN) and thiobarbituric acid in traditional Turkish salted and dried fish (chiruz) during the storage period. This finding is fully consistent with the results of the present study, in which active

packaging with polycaprolactone/beta-glucan nanocomposite film containing plant extracts and gold nanoparticles effectively prevented the increase of TVB-N and TBA indices in fish paste. Both studies show that active packaging plays a key role in maintaining the quality and increasing the shelf life of fishery products, both dried fish and processed products such as fish paste, by inhibiting lipid oxidation, reducing TBA, and delaying the production of volatile nitrogen compounds. This concordance of results confirms the effectiveness of active packaging strategies in simultaneously controlling oxidative and microbial spoilage in different types of fish products (Erkan, 2017).

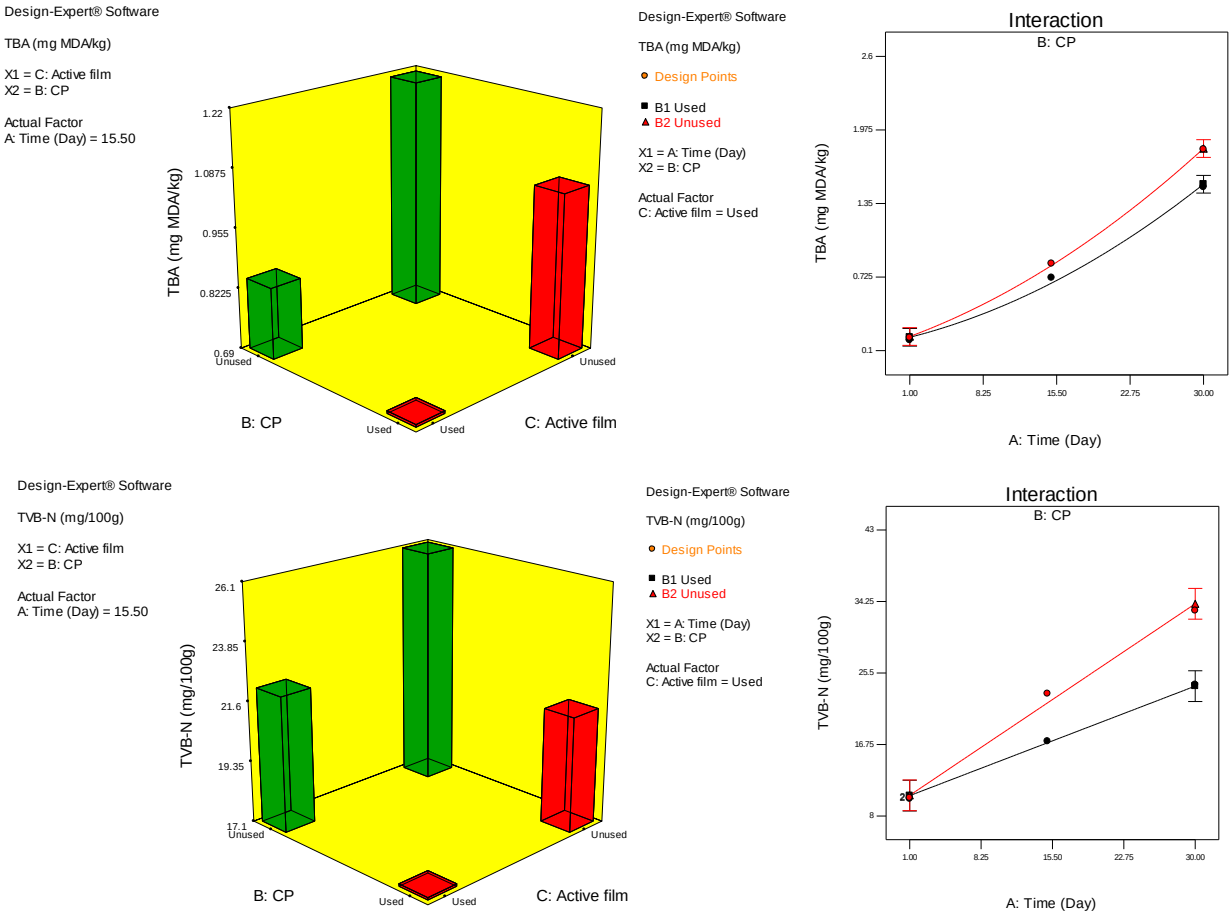

Fig. 4. 3D diagram and interaction curve of the effect of storage time, cold plasma treatment, and packaging with active film on TBA and TVB-N of fish paste

TVC

Fig. 5 shows the three-dimensional diagram and interaction curve of the effect of storage time, cold plasma treatment and active film packaging on the total microbial count of fish paste. The changes in the total microbial count of fish paste during the storage period were observed based on the results of the analysis of variance of the two-factor interactive response surface model (2FI). The presented model was statistically significant at the 99.99% confidence level (p-value < 0.0001) and was able to explain 99.27% of the response variations. The R^2 values (0.992) and adjusted R^2 (0.984) indicate the optimal fit of the model. Storage time (A) was identified as the most effective factor in increasing the microbial count. This natural increase is due to the proliferation and growth of microorganisms inherent to the food under storage conditions.

Cold plasma treatment (B) significantly reduced TVC, which can be attributed to the following mechanisms: direct destruction of the bacterial cell walls by plasma active species, destruction of bacterial DNA and cellular proteins, and oxidative damage to the cell membrane of microorganisms. Active film packaging (C) also showed a significant inhibitory effect on microbial growth, which works through the following: gradual release of antimicrobial compounds from plant extracts, synergistic effect of gold nanoparticles in inhibiting microbial activity, and creation of a physical barrier against secondary contamination. The interaction effect of time and cold plasma treatment (AB) showed that the application of cold plasma can effectively reduce the rate of microbial growth during storage time. The interaction effect of time and active packaging (AC) showed the synergistic effect of these two factors in controlling microbial growth during longer storage periods. The interaction effect of cold plasma treatment and active film (BC) was not statistically significant, which probably indicates different mechanisms of action of the two technologies. The final regression equation was obtained as follows:

TVC = 6.26 + 1.17*A + 0.29*B + 0.24*C + 0.29*A*B + 0.21*A*C + 0.051*B*C

The response surface and contour plots clearly showed that the simultaneous application of cold plasma treatment and active packaging could effectively prevent the increase of microbial counts during the storage period. This study suggests that the combination of cold plasma treatment and active packaging with a film containing antimicrobial compounds could be an effective strategy for controlling microbial growth and enhancing the shelf life of fish paste.

Both the current investigation and the research performed by Chen *et al*. (2020) independently validate the efficacy of active packaging in controlling microbial growth in fishery products. In Chen's study, the use of active film containing chitosan and plant extract significantly reduced the total viable count (TVC) in fried fish fillets during storage. This finding is fully consistent with the results of the present study, by which active packaging with polycaprolactone/beta-glucan nanocomposite film containing plant extracts and gold nanoparticles effectively inhibited microbial growth (TVC) in fish paste. Both studies show that natural active compounds incorporated in packaging films including plant extracts in the present study and Herba lophatheri extract in Chen's study can inhibit bacterial growth and extend the shelf life of various fishery products by gradually releasing antimicrobial compounds. This consistency of results confirms the effectiveness of the strategy of using natural compounds in active packaging to control microbial spoilage in different fish products (Chen *et al*., 2020).

Overall Acceptance

Fig. 6 shows the three-dimensional diagram and interaction curve of the effect of storage time, cold plasma treatment and active film packaging on the overall acceptance of fish paste. The changes in the overall sensory acceptance of fish paste during the storage period were observed based on the results of the analysis of variance of the quadratic response surface model. The presented model was statistically significant at 99.99% confidence level (p-value < 0.0001) and was able to explain 98.7% of the response changes. The R^2 values (0.987) and adjusted R^2 (0.954) indicate the optimal fit of the model. Storage time (A) was identified as the most effective factor in reducing overall acceptance. This reduction was mainly due to undesirable sensory changes caused by lipid oxidation, formation of off-odor compounds resulting from microbial spoilage, leading to textural changes and loss of product freshness characteristics. Both cold plasma treatment (B) and active film packaging (C) significantly maintained sensory quality, which can be attributed to the following: reducing the rate of spoilage by inhibiting microbial activity, reducing the rate of lipid oxidation, and maintaining the desired sensory properties of the product for a longer period of time.

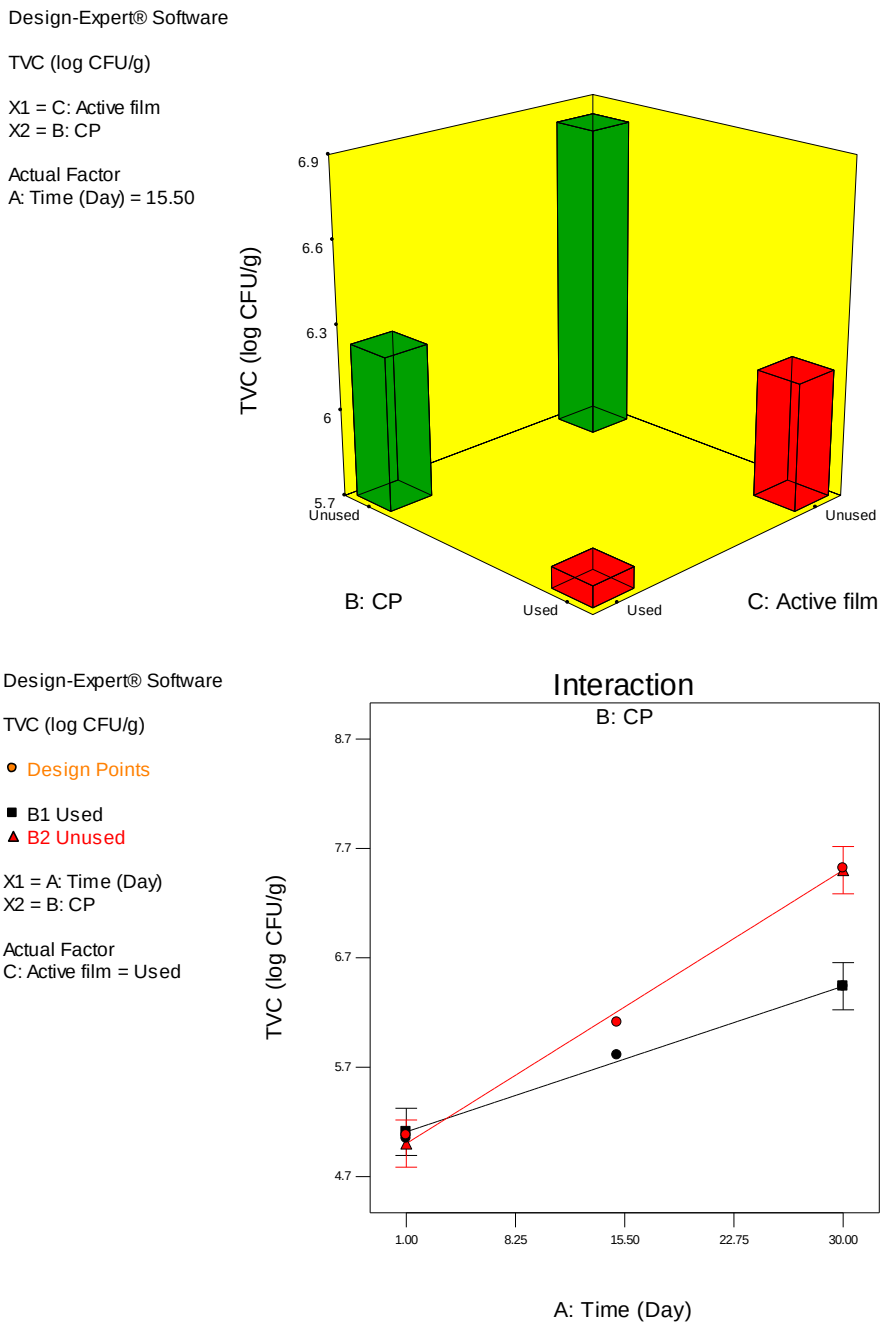

Fig. 5. 3D diagram and interaction curve of the effect of storage time, cold plasma treatment, and active film packaging on the total microbial count of fish paste

The interaction effects of time and cold plasma treatment (AB) and time and active packaging (AC) were all significant, indicating that these treatments can reduce the negative effects of time on sensory quality. The interaction effect of cold plasma treatment and active film (BC) was not statistically significant, possibly indicating that these two technologies affect sensory quality independently. The quadratic effect of time (A^2) was significant, indicating a nonlinear pattern of overall acceptance decline over time. The

final regression equation was obtained as follows:

Total acceptance=+4.47-1.00*A-0.25*B-0.25*C-0.25*A*B-0.25*A*C+0.00*B*C-0.47*A2

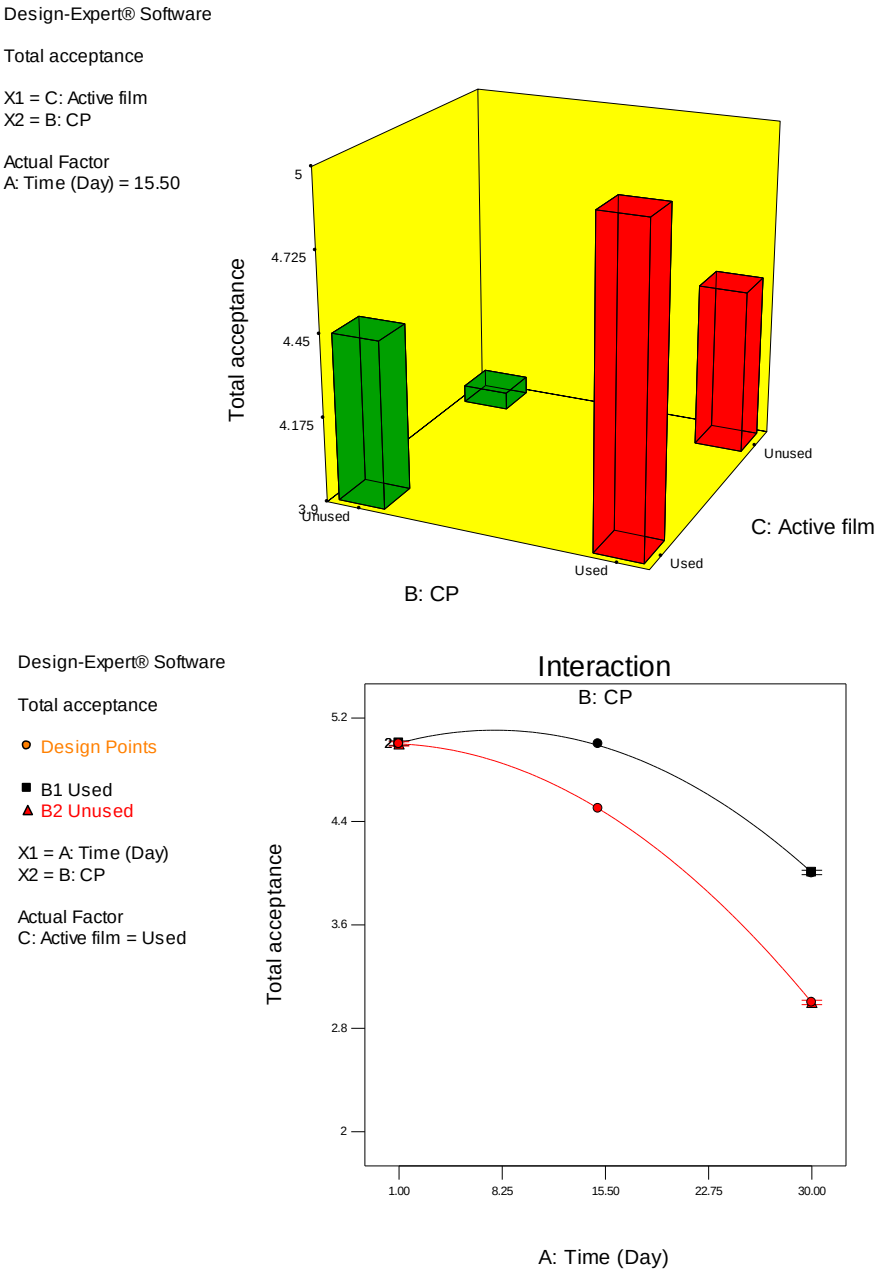

Fig. 6. 3D diagram and interaction curve of the effect of storage time, cold plasma treatment, and active film packaging on the overall acceptance of fish paste

The negative coefficients in the equation indicate the reducing effect of the variables on the overall acceptance. This study shows that the combination of cold plasma treatment and

active packaging can be an effective strategy to maintain the overall sensory acceptance of fish paste during the storage period. Although both treatments individually are able to reduce the sensory quality, their synergistic effect together can significantly increase the overall acceptance during the storage of the product.

Conclusion

The findings of this study clearly show that the prepared nanocomposite film containing plant extracts and gold nanoparticles, along with cold plasma treatment, is a comprehensive and effective solution in maintaining the quality, safety and shelf life of fish paste. This active packaging system, with its strong antibacterial and antioxidant properties, has the ability to simultaneously inhibit the main factors of spoilage, including the growth of microorganisms, lipid oxidation and the production of volatile compounds. The synergistic interaction between the active compounds in the film and the effects of cold plasma has led to the creation of a multiple protective barrier against spoilage. Cold plasma treatment effectively delays the spoilage process through the inactivation of surface enzymes and microorganisms, while the active film concurrently mitigates spoilage progression during storage by gradually releasing antibacterial compounds and establishing a physical barrier against oxygen ingress. The results of thermal analyses also confirmed the stability and appropriate compatibility of the film components. The presence of gold nanoparticles not only improved the thermal properties of the film, but also enhanced the overall performance of the packaging system by enhancing the antibacterial effect. Given its demonstrated efficacy, this integrated approach shows considerable promise for implementation in the food packaging sector, particularly for preserving perishable fishery products, and presents a viable alternative to conventional preservation techniques. It is suggested that further studies focus on optimizing the production scale, economic evaluation of this technology, and also investigating the synergistic effects of other natural active compounds.

Author Contribution

Sajad Pirsa: conceived of the presented idea, verified the analytical methods and wrote the manuscript and revised it. **Amir Afshar Asdagh:** developed the theory and performed the computations. **Mir Khalil Pirouzifard**: discussed the results and contributed to the final manuscript. **Amir Afshar Asdagh**: out the experiment.

Funding Source

No funding was received for this study.

References

1. AOAC. (2002). *Official methods of analysis* (17th ed.). Association of Official Analytical Chemists.
2. AOAC. (2005). *Official methods of analysis* (18th ed.). Association of Official Analytical Chemists.
3. Bahmanpour, H., Asefi, N., Alizadeh, A., & Pirsa, S. (2024). Assessment of the impact of cold plasma technology on physicochemical properties of corn starch flour and the associated modified corn starch incorporated into milk dessert. *Heliyon, 10*(17). https://doi.org/10.1016/j.heliyon.2024.e37399
4. Balouiri, M., Sadiki, M., & Ibnsouda, S.K. (2016). Methods for in vitro evaluating antimicrobial activity: A review. *Journal of Pharmaceutical Analysis, 6*(2), 71–79. https://doi.org/10.1016/j.jpha.2015.11.005
5. Barba, F.J., Koubaa, M., do Prado-Silva, L., Orlien, V., & de Souza Sant'Ana, A. (2017). Mild processing applied to the inactivation of the main foodborne bacterial pathogens: A

review. *Trends in Food Science & Technology, 66*, 20-35. https://doi.org/10.1016/j.tifs.2017.05.011
6. Cesur, S., Köroğlu, C., & Yalçın, H.T. (2018). Antimicrobial and biodegradable food packaging applications of polycaprolactone/organo nanoclay/chitosan polymeric composite films. *Journal of Vinyl and Additive Technology, 24*(4), 376-387. https://doi.org/10.1002/vnl.21607
7. Chen, H., Wang, J., Jiang, G., Guo, H., Liu, X., & Wang, L. (2020). Active packaging films based on chitosan and *Herba lophatheri* extract for the shelf life extension of fried bighead carp fillets. *International Food Research Journal, 27*(4). https://doi.org/10.47836/ifrj.27.4.02
8. Dadkhah, H., Pirsa, S., Javadi, A., & Mohtarami, F. (2024). Biodegradable film based on sodium alginate/flax seed mucilage modified with norbixin and WO3 nanoparticles: Investigation of physicochemical properties and release of active substances. *Biomass Conversion and Biorefinery, 14*(15), 17663-17675. https://doi.org/10.1007/s13399-023-03780-2
9. Erkan, N. (2017). The effect of active and vacuum packaging on the quality of Turkish traditional salted dried fish "çiroz". *Food and Health, 3*(1), 29-35. https://doi.org/10.3153/FH17004
10. Eslami, A., Pirsa, S., Mohtarami, F., & Bener, M. (2025). Photoluminescence film based on gelatin/phycocyanin nanoliposome/zero-valent iron nanoparticle/gold-iridium composite. *Food Chemistry, 482*, 144114. https://doi.org/10.1016/j.foodchem.2024.144114
11. Forouzan, S., Pirsa, S., & Alirezalu, A. (2024). Biodegradable photocatalytic film based on chia seed mucilage (xylose, glucose, and methyl glucuronic acid polysaccharides) containing barberry extract and SnO_2 nanoparticles. *Carbohydrate Polymer Technologies and Applications, 8*, 100592. https://doi.org/10.1016/j.carpta.2024.100592
12. Gupta, A., Moyano, D.F., Parnsubsakul, A., Papadopoulos, A., Wang, L.S., Landis, R.F., Das, R., & Rotello, V.M. (2016). Ultrastable and biofunctionalizable gold nanoparticles. *ACS Applied Materials & Interfaces, 8*(22), 14096-14101. https://doi.org/10.1021/acsami.6b02548
13. Holešová, S., Čech Barabaszová, K., Hundáková, M., Ščuková, M., Hrabovská, K., Joszko, K., Antonowicz, M., & Gzik-Zroska, B. (2021). Development of novel thin polycaprolactone (PCL)/clay nanocomposite films with antimicrobial activity promoted by the study of mechanical, thermal, and surface properties. *Polymers, 13*(18), 3193. https://doi.org/10.3390/polym13183193
14. Jeon, Y.J., Myung, G.E., & Min, S.C. (2022). In-package cold plasma treatment enhances the antimicrobial efficacy of malic acid-incorporated whey protein edible coating against *Salmonella* and *Listeria monocytogenes* in steamed fish paste. *Food Packaging and Shelf Life, 33*, 100905. https://doi.org/10.1016/j.fpsl.2022.100905
15. Julyaningsih, A.H., Latief, R., & Dirpan, A. (2020). The making of smart and active packaging on tuna fillet. *IOP Conference Series: Earth and Environmental Science, 486*(1), 012053. https://doi.org/10.1088/1755-1315/486/1/012053
16. Lawless, H.T., & Heymann, H. (2010). *Sensory evaluation of food: Principles and practices* (2nd ed.). Springer. https://doi.org/10.1007/978-1-4419-6488-5
17. Liao, X., Li, J., Muhammad, A.I., Suo, Y., Chen, S., Ye, X., Liu, D., & Ding, T. (2018). Application of a dielectric barrier discharge atmospheric cold plasma (Dbd-Acp) for *Escherichia coli* inactivation in apple juice. *Journal of Food Science, 83*(2), 401-408. https://doi.org/10.1111/1750-3841.14045
18. Ma, Q., Shi, K., Su, T., & Wang, Z. (2020). Biodegradation of polycaprolactone (PCL) with different molecular weights by *Candida antarctica* lipase. *Journal of Polymers and the Environment, 28*(11), 2947-2955. https://doi.org/10.1007/s10924-020-01826-4
19. Misra, N.N., Martynenko, A., Chemat, F., Paniwnyk, L., Barba, F.J., & Jambrak, A.R. (2018). Thermodynamics, transport phenomena, and electrochemistry of external field-assisted

nonthermal food technologies. *Critical Reviews in Food Science and Nutrition, 58*(11), 1832-1863. https://doi.org/10.1080/10408398.2017.1287660

20. Nishinari, K., & Ooizumi, T. (2020). Textural characteristics of Japanese foods. *Textural Characteristics of World Foods*, 107-123. https://doi.org/10.1002/9781119430902.ch8
21. Panpipat, W., Thongkam, P., Boonmalee, S., Çavdar, H.K., & Chaijan, M. (2023). Surimi production from tropical mackerel: A simple washing strategy for better utilization of dark-fleshed fish resources. *Resources, 12*(10), 126. https://doi.org/10.3390/resources12100126
22. Patange, A., Boehm, D., Giltrap, M., Lu, P., Cullen, P.J., & Bourke, P. (2018). Assessment of the disinfection capacity and eco-toxicological impact of atmospheric cold plasma for treatment of food industry effluents. *Science of the Total Environment, 631*, 298-307. https://doi.org/10.1016/j.scitotenv.2018.02.269
23. Pirsa, S., Bener, M., & Şen, F.B. (2024). Biodegradable film of carboxymethyl cellulose modified with red onion peel powder waste and boron nitride nanoparticles: Investigation of physicochemical properties and release of active substances. *Food Chemistry, 445*, 138721. https://doi.org/10.1016/j.foodchem.2024.138721
24. Rahman, M.S., Al-Amiri, M., & Al-Riziq, M.A. (2021). Measurement of lipid oxidation in seafood. In *Handbook of Food Chemistry* (pp. 1-25). Springer. https://doi.org/10.1007/978-3-030-48770-9_6-1
25. Remya, S., Mohan, C.O., Bindu, J., Sivaraman, G.K., Venkateshwarlu, G., & Ravishankar, C.N. (2016). Effect of chitosan based active packaging film on the keeping quality of chilled stored barracuda fish. *Journal of Food Science and Technology, 53*(1), 685-693. https://doi.org/10.1007/s13197-015-2018-6
26. Slavin, Y.N., Asnis, J., Häfeli, U.O., & Bach, H. (2017). Metal nanoparticles: Understanding the mechanisms behind antibacterial activity. *Journal of Nanobiotechnology, 15*(1), 65. https://doi.org/10.1186/s12951-017-0308-z
27. Zhao, X., Jia, Y., Li, J., Dong, R., Zhang, J., Ma, C., Wang, H., Rui, Y., & Jiang, X. (2018). Indole derivative-capped gold nanoparticles as an effective bactericide in vivo. *ACS Applied Materials & Interfaces, 10*(35), 29398-29406. https://doi.org/10.1021/acsami.8b11980
28. Zhang, Y., Zhou, L., Zhang, C., Show, P.L., Du, A., Fu, J., & Ashokkumar, V. (2020). Preparation and characterization of curdlan/polyvinyl alcohol/thyme essential oil blending film and its application to chilled meat preservation. *Carbohydrate Polymers, 247*, 116670. https://doi.org/10.1016/j.carbpol.2020.116670

نشریه پژوهشهای علوم و صنایع غذایی ایران
https://ifstrj.um.ac.ir

مقاله پژوهشی
جلد ۲۲، شماره ۱، فروردین- اردیبهشت ۱۴۰۵، ص. ۷۲-۵۱

توسعه فیلم‌های فعال-PCL/β گلوکان غنی‌شده با عصاره‌های طبیعی و نانوذرات طلا برای بسته‌بندی خمیر ماهی تیمار شده با پلاسمای سرد

امیر افشار اصدق[۱]- سجاد پیرسا[۱*]- میر خلیل پیروزی فرد[۱]

تاریخ دریافت: ۱۴۰۴/۰۸/۲۰
تاریخ پذیرش: ۱۴۰۴/۰۹/۱۲

چکیده

نگرانی‌های فزاینده در مورد بسته‌بندی‌های پلاستیکی مرسوم به‌دلیل عدم تجزیه‌پذیری، خطر انتقال ترکیبات سمی به مواد غذایی و آلودگی محیط زیست، توسعه جایگزین‌های سازگار با محیط‌زیست مانند فیلم‌های خوراکی و زیست‌تخریب‌پذیر را ضروری کرده است. این مطالعه با هدف توسعه یک سیستم بسته‌بندی فعال بر اساس فیلم نانوکامپوزیتی پلی‌کاپرولاکتون/بتا-گلوکان (PCL-BG) اصلاح‌شده با عصاره جفت میوه بلوط (OFPE)، عصاره هسته زردآلو (AKE) و نانوذرات طلا (AuNPs) و استفاده از آن برای بسته‌بندی خمیر ماهی که قبلاً با پلاسمای سرد تیمار شده بود، انجام شد. ارزیابی خواص ضد باکتریایی فیلم نشان داد که ترکیبات فعال اثر مهاری قوی دارند، به‌طوری‌که بزرگترین هاله‌های مهاری ۲۷٫۷۸ میلی‌متر در برابر باسیلوس سرئوس و ۲۱٫۳۸ میلی‌متر در برابر اشریشیا کلی در فیلمی با بالاترین غلظت عصاره مشاهده شد. تجزیه و تحلیل حرارتی (DSC) بهبود قابل توجهی در پایداری حرارتی نشان داد، به‌طوری‌که دمای ذوب فیلم کامپوزیت نهایی به ۸۱٫۶ درجه سانتی‌گراد افزایش یافت. ارزیابی‌های میکروبیولوژیکی و شیمیایی طی ۳۰ روز نگهداری نشان داد که تیمار ترکیبی به‌طور قابل توجهی ($p < 0.05$) رشد میکروبی (شمارش کل میکروبی زنده) را کاهش داد، تولید ترکیبات نیتروژن فرار (TVB-N) را کاهش داد، اکسیداسیون لیپید (TBA) را کنترل کرد و پایداری pH و پذیرش حسی را حفظ کرد. مدل‌های رگرسیون برای همه پارامترهای کیفی، دقت و قدرت پیش‌بینی بالایی را نشان دادند ($R^2 > 99.27\%$). این مطالعه به وضوح اثربخشی استراتژی ترکیبی پلاسمای سرد و بسته‌بندی فعال را در حفظ کیفیت و افزایش ماندگاری خمیر ماهی نشان می‌دهد.

واژه‌های کلیدی: آنتی‌باکتریال، بسته‌بندی فعال، پلاسمای سرد، فیلم زیست‌تخریب‌پذیر

۱- گروه علوم و صنایع غذایی، دانشکده کشاورزی، دانشگاه ارومیه، ایران
(*- نویسنده مسئول: Email: S.pirsa@urmia.ac.ir)

https://doi.org/10.22067/ifstrj.2025.96443.1508

Iranian Food Science and Technology Research Journal
Homepage: https://ifstrj.um.ac.ir

Research Article
Vol. 22, No. 1, March- April, 2026, p. 73-94

Physicochemical and Functional Comparison of Gelatin Extracted from Rainbow Trout (*Oncorhynchus mykiss*) and Silver Carp (*Hypophthalmichthys molitrix*) Byproducts

A. Amirafzali[1], M. Rezaei[1*], Sh. Naghdi[1]

1- Seafood Processing Department, Marine Sciences Faculty, Tarbiat Modares University, Noor, Iran
(*- Corresponding Author Email: rezai_ma@modares.ac.ir)

Received: 09.12.2025
Revised: 22.02.2026
Accepted: 08.03.2026
Available Online: 02.05.2026

How to cite this article:
Amirafzali, A., Rezaei, M., & Naghdi, Sh. (2026). Physicochemical and functional comparison of gelatin extracted from rainbow trout (*Oncorhynchus mykiss*) and silver carp (*Hypophthalmichthys molitrix*) byproducts. *Iranian Food Science and Technology Research Journal*, *22*(1), 73-94. https://doi.org/10.22067/ifstrj.2026.96879.1528

Abstract

In this research, gelatin was extracted from various by-products of silver carp (*Hypophthalmichthys molitrix*) (SC) and rainbow trout (*Oncorhynchus mykiss*) (RT), including skin, soft tissue, head, and vertebrae. The extracted gelatins were evaluated for proximate composition, molecular weight, functional properties, and structural characteristics. The findings revealed that the protein content of the gelatin samples ranged from 69.25% to 85.75%, with fat levels below 1.5%. The highest moisture content was observed in RT-skin gelatin (16.8%), while the lowest was found in RT-vertebral bone gelatin (2.97%). SDS-PAGE analysis showed clear 1α (~114–121 kDa) and 2α (~100–112 kDa) chains in skin and cranial soft tissue gelatins, whereas bone-derived samples lacked distinct bands, indicating extensive collagen degradation due to harsh acid treatment. In terms of viscosity, the highest value (11 cP) was recorded for SC-cranial soft tissue gelatin, and the lowest (2.6 cP) for RT-head gelatin. Gel strength ranged from 573.5 g (SC-skin) to 19.6 g (RT-head). The melting point of SC-gelatins was significantly higher than that of RT, with some samples approaching values similar to bovine skin gelatin. SC-vertebral bone gelatin exhibited the greatest foaming capacity (120 ± 2%), while SC-head gelatin demonstrated the highest foam stability (48.03 ± 2.12%). These results suggest that non-commercial by-products from these two fish species, especially SC-skin and cranial soft tissue, represent valuable potential sources for producing high-quality gelatin for food applications.

Keywords: Fish gelatin, Functional properties, *Hypophthalmichthys molitrix*, *Oncorhynchus mykiss*, SDS-PAGE analysis

Introduction

In the past decade, the aquaculture and fishing industries have experienced significant growth, with aquatic production increasing from 128 million tons in 2012 to 223 million tons in 2024 (FAO, 2024). This substantial increase in aquatic animal production aims to meet the growing demand for animal protein and serves various industries including food, healthcare, pharmaceuticals, and more (Naghdi *et al*., 2024). Additionally, rising awareness of the high nutritional value of aquatic products has shifted consumer preference toward seafood. Consequently, the fish processing industry has developed significantly to meet this demand, enabling the efficient processing of whole fish and separation of their various parts.

During fish processing, approximately 20 to 60 percent of the initial weight is considered

Authors retain the copyright. This is an open access article distributed under Creative Commons Attribution 4.0 International License (CC BY 4.0).
https://doi.org/10.22067/ifstrj.2026.96879.1528

non-edible waste, resulting in the generation of large volumes of fish byproducts (Guan *et al*., 2022; Naghdi *et al*., 2024). This not only raises environmental concerns but also reduces the economic profitability of the aquaculture sector. However, these byproducts are rich in fats, proteins, and other valuable compounds (Yuan, Ye, Hou, & Chen, 2024). The protein-rich waste includes meat scraps, spinal bones, heads, skin, ovaries, viscera, and blood. These protein fractions are easily digestible and can be utilized to produce hydrolyzed products, surimi, heat-resistant protein dispersions, various peptides and amino acids, gelatin, collagen, and protamine (Olaniran *et al*., 2024). Among these, gelatin has attracted considerable attention from both industry and researchers due to its diverse applications in food, pharmaceuticals, healthcare, and more (Ruan *et al*., 2023; Wang *et al*., 2024).

Gelatin is a fibrous protein obtained through the partial thermal hydrolysis of collagen. It is a biopolymer with important functional properties and has wide-ranging applications in the food, pharmaceutical, photographic, and other industries (Ruan *et al*., 2023; Wang *et al*., 2024). Currently, most commercial gelatin is derived from mammalian sources, particularly pig and bovine skins (Nurilmala, Suryamarevita, Hizbullah, Jacoeb, & Ochiai, 2022; Usman *et al*., 2022). However, for cultural reasons, such as its non-halal status in Islamic countries, and concerns over zoonotic disease transmission, alternative sources are increasingly in demand (Nurilmala *et al.,* 2022; Usman *et al.*, 2022). As a result, researchers are continuously exploring alternative gelatin sources. Over the past two decades, interest in gelatin derived from fish and poultry has grown (Duasa, Husin, Asmy Mohd Thas Thaker, & Rahman, 2022). Nonetheless, commercial gelatin production from poultry skin and bones has been limited due to low yields. Fish gelatin, in particular, is considered a superior alternative to mammalian gelatin from ethical and religious perspectives (Duasa *et al.*, 2022; Nurilmala *et al*., 2022).

Rainbow trout (*Oncorhynchus mykiss*) and silver carp (*Hypophthalmichthys molitrix*), a phytophagous species, are two of the most widely farmed species globally and in Iran (Iranian Fisheries Organization Statistical Yearbook, 2024). According to the Food and Agriculture Organization (FAO), global production of rainbow trout and silver carp in 2022 was approximately 848,000 tons and 5.1 million tons, respectively (FAO, 2024). Rainbow trout is among the most important farmed migratory species, while silver carp holds the highest production volume among farmed freshwater species worldwide (FAO, 2024).

In Iran, rainbow trout production exceeded 200,000 tons in 2022, while warm-water fish production reached approximately 240,000 tons, the majority of which was silver carp (FAO, 2024). The production of various products, including gutted fish, headed and gutted fish, fillets of these two species, and value-added products based on fish paste, is continuously expanding (Iranian Fisheries Organization Statistical Yearbook, 2024). These diverse processing methods generate a significant volume of waste from both species. For rainbow trout, the head, spinal column, and skin account for approximately 15.52%, 10.78%, and 8.10% of the body weight, respectively, highlighting the substantial amount of waste produced (Abdollahi, Rezaei, & Jafari, 2014). Therefore, the large volume of waste generated from these species, combined with the growing global demand for halal gelatin, underscores the importance of research into gelatin extraction from fish byproducts (Naghdi, Rezaei, Tabarsa, & Abdollahi, 2025). Moreover, differences exist in the quantity and type of collagen cross-links between various byproducts (soft tissues versus bones), which affect collagen solubility and its conversion to gelatin (Silviwanda & Najib Tuisina Naenum, 2024). These differences may lead to variations in the properties of gelatin extracted from different tissues (Silviwanda & Najib Tuisina Naenum, 2024; Yu *et al*., 2023).

Accordingly, the present study aims to investigate and compare the yield and functional properties, and molecular weight analysis of gelatin extracted from various byproducts (skin, spinal column, and head) of rainbow trout and silver carp.

Materials and Methods

Preparation of Fish and Waste Separation

A total of 10 silver carp weighing between 1.5 to 2 kilograms and 20 rainbow trout weighing between 250 to 350 grams were procured from local fish vendors in Noor County. The fish were frozen and transported in polystyrene containers to the central laboratory of the Faculty of Natural Resources and Marine Sciences at Tarbiat Modares University. The skin, bones, and heads of the fish were manually removed gradually until sufficient amounts of skin and other waste were collected. The flesh and additional waste from the skins and bones were separated using a sharp knife before being placed in polyethylene bags, which were then sealed tightly. The bags were stored in a freezer at -20 °C for further experiments (for a maximum of 2 months) (Göçer, 2022).

Proximate Analysis

The proximate analysis of fish byproducts regarding fat, moisture, ash, and protein content was conducted using standard methods numbered 46/950, 08/928, 39/960, and 153/920 (AOAC, 2000). For the proximate analysis of the extracted gelatin samples, the same standards were applied for measuring fat, moisture, and ash content; however, protein content was determined using the Biuret method (Zhou & Regenstein, 2006). In this procedure, 0.1 gram of each gelatin sample extracted from various tissues was dissolved in 10 milliliters of 0.9% NaCl solution at 50 °C. One milliliter of this solution was mixed with 4 milliliters of Biuret reagent and allowed to react for 30 minutes at room temperature. The absorbance of the samples was then measured using a spectrophotometer at 540 nm, and the protein concentration was calculated from a standard curve ($y = 0.0419 x + 0.0008$, $R^2 = 0.9999$). The standard curve was created by diluting a stock solution of bovine serum albumin (BSA) with a concentration of 10 mg/ml.

Extraction of Gelatin

This section presents the methods used for gelatin extraction from various fish processing wastes, categorized by the type of raw material from each fish species.

Gelatin Extraction from Silver Carp (*H. molitrix*) Byproducts

From Silver Carp (SC) Skin

The optimized method of Boran & Regenstein (2009) was applied. Frozen skins were thawed overnight at 4 °C, cut into 0.5 × 0.5 cm pieces, and washed with cold distilled water. The skins were treated sequentially at room temperature with 0.55 N NaOH for 67.5 minutes and 0.1 N HCl for 45 minutes (1:5 v/w). After each treatment, the skins were rinsed with cold water, and excess water was removed by pressing them with cheesecloth. Final extraction was performed at 50 ± 2 °C in a water bath with a 4:1 (w/v) water-to-skin ratio for 3 hours. The gelatin solution was then filtered through cheesecloth, freeze-dried, and stored for analysis.

From SC-Vertebral Bones

Frozen bones were thawed for 30 minutes, cut into 0.5–1 cm piece, and defatted by immersion in warm water (35–40 °C) for 20–30 minutes. Non-collagenous proteins were removed by treatment with 0.1 N NaOH (1:4 w/v) for 24 hours at 4 °C, with solution replacement after 12 hours. The bones were washed until a neutral pH was reached, then demineralized with 3% HCl (3:1 w/v) at room temperature. The acid was replaced every 3 days over approximately 9 days until no hard nuclei remained. The resulting ossein was washed, and gelatin was extracted at 50 ± 2 °C for 16 hours (3:1 w/v). Filtration utilized a Buchner funnel and filter paper due to higher impurities. The gelatin was freeze-dried and

stored (Koli, Basu, Venkteshwarlu, Choukasy, & Nayak, 2013).

From SC-Head

Heads were separated into soft tissue and bones after treatment with 0.1 N NaOH (3:1 w/v) for 3 hours, with hourly solution changes to remove non-collagenous proteins. Soft tissues were acid-treated with 0.15 N HCl (4:1 w/v) for 3 hours, washed, and then extracted at 50 ± 2 °C for 16 hours (3:1 w/v). The bones were dried, crushed, defatted in warm water, demineralized with 3% HCl (3:1 w/v) over approximately 9 days, washed, and extracted similarly. Filtration and freeze-drying followed as described (Elavarasan *et al*., 2017).

Gelatin Extraction from Rainbow Trout (*O. mykiss*) Byproducts

From Rainbow Trout (RT) Skin

Frozen skins were thawed overnight at 4 °C, cut into small pieces, and washed. The skins were treated with 0.19 N NaOH (3:1 w/v) for 3 hours at 7 °C, washed until a neutral/slightly alkaline pH was achieved, and excess water was removed. They were then treated with 0.121 N acetic acid (3:1 w/v) for 3 hours at 7 °C, washed again, and finally extracted at 50 ± 2 °C for 16 hours (3:1 w/v). Subsequent steps matched those for SC-skin (Tabarestani, Maghsoudlou, Motamedzadegan, Sadeghi Mahoonak, & Mahoonak, 2010).

From RT-Vertebral Bones

The extraction procedure was the same as for SC-bones, except the acid treatment lasted about 6 days instead of 9.

From RT-Head

Due to incomplete ossification of the heads (250–350 g), the collected head were ground (3 mm mesh) without separating soft and hard tissues. The ground heads were treated with 0.1 N NaOH (5:1 w/v) for 1.5 hours, washed to a neutral/slightly alkaline pH, pressed to remove excess water, and then treated with 0.018 N HCl (2:1 w/v) for 30 minutes. After washing, final extraction was performed at 55 ± 2 °C for 16 hours (2:1 w/v). The gelatin solution was filtered and freeze-dried as previously described (Tabarestani *et al*., 2010).

Extraction Yield Determination

The extraction yield was calculated based on the dry weight and wet weight of the raw material using the following formulas:

Equation 1: Yield Based on Dry Weight = Weight of dry gelatin / Weight of dry raw material ×100

Equation 2: Yield Based on Wet Weight = Weight of dry gelatin / Weight of wet raw material ×100

Equation 3: Yield Based on Protein Content = Weight of dry gelatin / Protein content of raw material ×100

Measurement of Gel Strength

The gel was prepared according to the method of Kittiphattanabawon, Benjakul, Visessanguan, & Shahidi, (2010). For this purpose, gelatin was dissolved in distilled water at 60 °C to achieve a concentration of 6.67% (w/v). The solution was stirred until the gelatin was completely dissolved and then transferred to a plastic container with a height of 3 cm and a diameter of 2.5 cm. The gelatin solution was allowed to set for 18 hours at 4 ± 2°C to undergo gel maturation before testing its gel strength. After the specified time, the gel strength was measured immediately upon removal from the refrigerator (within 30 seconds), while still in the plastic container. This measurement was conducted using a texture analyzer under the following conditions: a cylindrical piston made of cast iron with a diameter of 12.7 mm, a penetration speed of 1 mm/s, and a penetration depth of 4 mm. The maximum force (in grams) required for the piston to penetrate 4 mm into the gel was recorded and reported as the gel strength.

Measurement of Viscosity

The viscosity of gelatin samples was measured according to the method of Yazid *et al*. (2024). For this purpose, 20 mL of gelatin solutions at a concentration of 6.67% (w/v)

were prepared and maintained at 60 °C for 30 minutes to ensure complete dissolution of gelatin before measurement. Viscosity measurements were conducted at 60 °C using a Brookfield viscometer equipped with spindle S31, operating at a rotational speed of 100 rpm. The viscosity values obtained under these conditions were recorded for analysis.

Determination of Foaming Properties

The foaming ability (FA) and foaming stability (FS) of gelatin were determined according to the method described by Du, Khiari, Pietrasik, & Betti, (2013). A 1% (w/v) gelatin solution was prepared and held at 60 °C for 30 minutes. The solution was then transferred to a beaker. To generate foam, the gelatin solution was homogenized at 10,000 rpm for 5 minutes using a homogenizer. Immediately after homogenization, the solution was quickly transferred to a 250 mL graduated cylinder.

Foaming Ability (FA) was calculated as the ratio of the foam volume to the initial volume of the liquid:

FA=Foam volume / Initial liquid volume ×100

Foaming Stability (FS) was determined by measuring the volume of foam remaining after 30 minutes relative to the initial foam volume:

FS=Foam volume after 30 min / Initial foam volume ×100

Determination of Molecular Weight Distribution

The protein profiles of various gelatin samples were analyzed using the method of Laemmli (1970) with minor modifications. In this procedure, samples were dissolved at a concentration of 2 mg/mL in 5% SDS solution. The resulting mixtures were heated at 85 °C for 1 hour to denature the proteins, followed by centrifugation at 8500 × g for 5 minutes at room temperature to ensure complete dissolution. The dissolved samples were then mixed with sample buffer in a 1:1 (v/v) ratio. After mixing, the samples were heated again at 100 °C for 5 minutes. Finally, 15 µL of the prepared samples and 5 µL of molecular weight marker (standard) were loaded onto a polyacrylamide gel consisting of a 7.5% separating gel and a 4.5% stacking gel. After loading, the gel apparatus cables were connected to the electrodes and electrophoresis was initiated. The initial voltage was set at 50 mV, and once the samples entered the resolving gel, the voltage was increased to 120 mV and maintained at this level until the dye front reached the bottom of the gel. Upon completion of electrophoresis, the gel was carefully removed from the glass plates and stained for 30 minutes in a staining solution. Destaining was performed by immersing the gel in a destaining solution for 15 minutes to remove excess dye and enhance band visibility.

Measurement of Melting Point

The melting point of gelatin was determined according to the BS755 method (BSI, 1975). Gelatin solutions at a concentration of 6.67% (w/v) were prepared using distilled water and poured into test tubes. To remove oxygen bubbles trapped in the samples, the test tubes were placed in a vacuum desiccator for 5 minutes. Subsequently, the test tubes were sealed and heated in a water bath at 60 °C for 15 minutes. Next, the samples were refrigerated at 4 ± 1 °C for 18 hours to allow gel maturation. After the maturation period, 2 to 3 drops of 0.5% (w/v) methyl red-chloroform solution were added to each sample, which were then placed back into the water bath. Starting at an initial water temperature of approximately 4 °C, the temperature was gradually increased. The temperature at which the chloroform droplet began to fall through the gelatin gel was recorded as the melting point of the gelatin.

Statistical Analysis

Data analysis was conducted using SPSS software version 22.0. To assess significant differences among the variables, one-way analysis of variance (ANOVA) was applied, followed by Duncan's multiple range test for pairwise comparisons. Statistical significance was defined at a threshold of $p < 0.05$. All results are presented as the mean ± standard

deviation (SD) based on three independent replicates (n = 3).

Results and Discussion

Extraction Yield of Gelatin

To provide a comprehensive evaluation of extraction efficiency, gelatin yield was calculated based on wet weight, dry weight, and protein recovery percentage, with results presented in Table 1. The extraction yield varied considerably depending on fish species and by-product type (Table 1). In SC, the highest wet weight yield was obtained from skin (15.78%), followed by head bone (11.24%), head soft tissue (3.08%), and vertebral bones (2.85%). Notably, the wet-weight extraction yield of gelatin from SC-skin in the present study (15.78%) was higher than values reported for some other tropical fish species. For example, Barman *et al*. (2021) reported a yield of 10.85% for gelatin extracted from pangas catfish (*Pangasius pangasius*) skin, approximately 5 percentage points lower than the value obtained here. This higher yield may be attributed to the optimized acid–alkali pretreatment, which, compared to conventional extraction methods applied to catfish by-products, more effectively enhances collagen accessibility and consequently improves gelatin recovery. On a dry weight basis, skin again showed the highest yield (43.38%), followed by head bone (18.13%), head soft tissue (13.18%), and vertebral bones (6.34%). Protein recovery was highest in head bone-derived gelatin (38.25%), followed by head soft tissue (13.26%), skin (10.58%), and vertebral bones (6.57%). In RT, skin exhibited the highest wet weight yield (9.58%), followed by head (6.37%) and vertebral bones (1.52%). However, on a dry weight basis, head showed the highest value (31.99%), followed by skin (26.94%) and vertebral bones (3.36%). Protein recovery ranged from 2.15% in vertebral bones to 18.7% in head-derived gelatin, with skin at 3.38%. Overall, skin and head tissues generally produced higher wet weight yields than bony tissues, attributable to greater collagen accessibility and lower mineral content. Bone-derived samples showed lower efficiency, particularly SC vertebral bones, likely due to extended demineralization. The elevated dry weight and protein recovery in SC head bone and RT head may reflect species-specific collagen distribution and extraction optimization. These findings underscore the influence of species and tissue type on gelatin yield, guiding sustainable by-product utilization. The yields obtained in this study align well with literature values reported for fish gelatin extraction. Notably, the silver carp skin yield (15.78% wet weight) substantially exceeds values from the same species reported by Tavakolipour (2011) [7.5% wet weight], likely attributable to optimized alkaline pretreatment conditions. Similarly, the results for rainbow trout in the present study closely match those reported by Duman (2025), with observed differences in reported values probably stemming from variations in initial tissue protein content, extraction solvent composition, or analytical quantification methods (total protein versus gelatin-specific recovery) (Anandito, Purwanto, Praseptiangga, & Zaman, 2024). In a comprehensive study investigating gelatin and oil extraction from mixed by-products of striped catfish (*Pangasius hypophthalmus*), catfish (*Clarias gariepinus*), and tilapia (*Oreochromis mossambicus*) using a hydrothermal process, gelatin yields of 6.4–11.8% were reported. In comparison, our results for SC-skin (15.78%) and SC-head bone (11.24%) demonstrate considerably higher recovery efficiency. This difference suggests that targeting gelatin extraction from specific fish by-product fractions can play a key role in both yield and the quality of the extracted collagen (Adnan, Kresnowati, Marlina, & Bindar, 2024). The significant variations in yield across different tissues and species provide a strategic roadmap for industrial application. The superior yield of SC-skin positions it as the primary raw material for large-scale production, ensuring higher process efficiency and economic viability. Conversely, the lower yields from bone tissues, while less productive, are essential for a

comprehensive biorefinery approach, where every by-product is valorized to minimize environmental impact and maximize total biomass utilization.

Table 1- Extraction yield of gelatin from silver carp (SC) and rainbow trout (RT) by-products

Species	By-product	Yield (Wet weight, %)	Yield (Dry weight, %)	Protein recovery (%)
SC	Skin	15.78	43.38	10.58
SC	Vertebral bones	2.85	6.34	6.57
SC	Head bone	11.24	18.13	38.25
SC	Head soft tissue	3.08	13.18	13.26
RT	Skin	9.58	26.94	3.38
RT	Vertebral bones	1.52	3.36	2.15
RT	Head	6.37	31.99	18.7

Values are expressed as percentages. Wet weight yield was calculated based on the initial fresh weight of raw material. Dry weight yield was calculated based on the dry matter of raw material. Protein recovery (%) represents the ratio of extracted gelatin protein to the initial protein content of the raw material.

Proximate Analysis of Extracted Gelatins from SC-and RT-Byproducts

The proximate analysis of raw materials and extracted gelatins in this study revealed significant insights into the biochemical composition of gelatin derived from SC-and RT-byproducts (Table 2 and Table 3). All extracted gelatins exhibited high protein content. In SC, no significant difference was observed in protein content between gelatin extracted from skin and soft head tissue ($P > 0.05$). Similarly, gelatins obtained from vertebral bones and head bones showed comparable protein levels ($P > 0.05$). However, in rainbow trout, significant difference ($P < 0.05$) was found in protein content among gelatins extracted from different byproducts. Overall, in both species, soft tissue-derived gelatins contained significantly higher protein content than those from bony tissues ($P < 0.05$). These findings align with previous reports by Koli *et al.* (2012), who documented protein contents of 72.63% and 69.49% for skin and bone gelatins of Nile perch, respectively. These results are consistent with the general range of 70-90% protein content in fish gelatins, as reviewed by Karim & Bhat (2009), confirming the suitability of these fish byproducts as valuable gelatin sources. The moisture content analysis revealed significant variation among the extracted gelatins. RT-skin gelatin showed the highest moisture level (16.8%), while the lowest was recorded in bone-derived gelatin (2.97%) from the same species. Similarly, SC-head soft tissue gelatin exhibited elevated moisture content. Notably, all samples except RT-skin gelatin and SC-head soft tissue gelatin complied with the established moisture standard (<15%) for edible gelatin (GME, 2011). The slightly higher moisture content in RT-skin gelatin (exceeding the 15% threshold) may be attributed to variations in drying efficiency or extraction parameters. These findings are consistent with previous studies: Gomez-Guillen, Gimenez, Lopez-Caballero, & Montero, (2011) reported moisture levels of 5-12% in gelatins from various fish species, while He, Zhang, Xu, Ma, & Guo, (2022) documented a moisture content of 8.82% for food-grade pigskin gelatin compared to a range of 4–5% for collagens derived from fish scales. Although all gelatin samples were subjected to identical freeze-drying conditions, noticeable differences in residual moisture content were observed among treatments. These variations are likely attributable to intrinsic differences in tissue origin, molecular weight distribution, and structural characteristics of the extracted gelatins. SDS-PAGE results indicated varying degrees of collagen degradation, particularly in bone-derived samples, which may influence network density, porosity, and water-binding capacity during freeze drying. Additionally, residual mineral components in bone-derived gelatins and differences in initial solid content could affect sublimation efficiency and moisture retention. Therefore, the observed moisture variability is more plausibly related to

structural and compositional differences among tissue-derived gelatins rather than incomplete drying under standardized processing conditions. All gelatin samples demonstrated low lipid content, consistently measuring below 2%, which is characteristic of the predominantly proteinaceous nature of gelatin. These results are in agreement with prior research findings reporting typical fat contents below 1.5% in fish-derived gelatins (He *et al*., 2022; Siburian, Rochima, Andriani, & Praseptiangga, 2020). The extracted gelatins exhibited ash contents ranging from 0.51% to 3.32%, with the highest value observed in SC-head bone gelatin and the lowest in RT-skin gelatin. The elevated ash content in bone-derived samples reflects the inherent mineral richness of the source tissues, particularly the calcium phosphate composition of skeletal structures. It should be noted that the demineralization process for silver carp and rainbow trout bones differed in duration (approximately 9 and 6 days, respectively). This variation was not arbitrarily imposed but was determined by the completion of full demineralization, continuing until no hard bone cores remained, confirming complete mineral removal. Nevertheless, this difference in acid exposure duration may have influenced collagen degradation extent, potentially affecting certain physicochemical and functional properties of the extracted gelatins.

Table 2- Proximate analysis of raw materials used for gelatin extraction

Source	Material	Moisture (%)	Protein (%)	Fat (%)	Ash (%)
SC	Skin	66.63 ± 0.76^{c}	29.8 ± 0.69^{a}	1.73 ± 0.15^{e}	2.42 ± 0.79^{e}
	Bone	54.98 ± 0.04^{d}	19.93 ± 0.34^{e}	5.3 ± 0.28^{b}	21.77 ± 0.16^{b}
	Head Bone	40.42 ± 1.26^{e}	22.3 ± 0.58^{c}	2.8 ± 0.12^{d}	39.24 ± 0.56^{a}
	Soft Tissue (Head)	76.61 ± 0.94^{a}	18.67 ± 0.43^{h}	5.9 ± 0.45^{a}	1.7 ± 0.08^{f}
RT	Skin	71.43 ± 1.2^{b}	24.53 ± 0.96^{g}	1.3 ± 0.11^{f}	1.69 ± 0.06^{f}
	Bone	65.58 ± 1.56^{c}	20.83 ± 0.92^{f}	1.85 ± 0.35^{e}	14.42 ± 0.68^{c}
	Head	69.65 ± 1.33^{b}	23.96 ± 0.16^{b}	3.36 ± 0.09^{c}	3.65 ± 0.37^{d}

Mean ± SD of three replicates. Different letters within each column indicate statistically significant differences ($P < 0.05$). Identical letters indicate no significant difference.

Table 3- Proximate analysis of extracted gelatins from SC-and RT-byproducts

Source	Byproduct	Moisture (%)	Protein (%)	Fat (%)	Ash (%)
SC	Skin	6.04 ± 0.03^{f}	84.64 ± 0.59^{b}	0.63 ± 0.02^{b}	1.11 ± 0.08^{f}
	Bone	9.6 ± 0.08^{e}	68.68 ± 0.46^{d}	0.46 ± 0.12^{c}	3.02 ± 0.14^{c}
	Head Bone	13.54 ± 0.15^{c}	69.25 ± 0.21^{d}	0.27 ± 0.04^{e}	3.20 ± 0.09^{b}
	Soft tissue (head)	15.92 ± 0.12^{b}	84.81 ± 0.35^{b}	1.20 ± 0.28^{a}	2.15 ± 0.31^{d}
RT	Skin	16.8 ± 0.23^{a}	83.66 ± 0.08^{c}	0.15 ± 0.05^{e}	0.51 ± 0.11^{g}
	Bone	2.97 ± 0.05^{g}	79.23 ± 0.18^{e}	0.31 ± 0.34^{d}	1.89 ± 0.14^{a}
	Head	10.56 ± 0.09^{d}	85.75 ± 0.43^{a}	0.36 ± 0.06^{e}	1.32 ± 0.21^{e}

Mean ± SD of three replicates. Different letters within each column indicate statistically significant differences ($P < 0.05$). Identical letters indicate no significant difference.

Molecular Weight Distribution and Electrophoretic Patterns of the Gelatin Samples

Fig. 1 illustrates the molecular weight distribution of proteins in various gelatin samples. As shown, no bands appeared in the electrophoretic patterns of gelatin extracted from the bones of SC-heads and vertebrae. According to Feng *et al*. (2024), acid pretreatment parameters, particularly acid concentration and exposure time, are critical factors influencing the extent of collagen degradation. This effect is evident in SDS-PAGE profiles through reduced intensity or complete absence of high-molecular-weight bands, as observed in gelatin extracted from SC bone samples. This is likely attributable to extensive collagen hydrolysis into low-molecular-weight peptides (<5 kDa) during prolonged acid exposure, though method sensitivity limitations or poor Coomassie staining of small fragments cannot be ruled out.

In contrast, since the acid treatment of RT-vertebral bones was shorter, less hydrolysis occurred, resulting in a faint 2α band at approximately 104 kDa in its pattern. The molecular weights of the 1α (114 kDa) and 2α (105 kDa) components in SC-skin gelatin were slightly higher than those of the corresponding 1α (107 kDa) and 2α (100 kDa) components in RT-skin gelatin. The β components, observed only in the skin gelatin samples of SC-and RT-(approximately 200 kDa and 204 kDa, respectively), indicate less collagen hydrolysis during the pretreatment steps in these samples. In the electrophoretic profiles of gelatin derived from the soft tissues of SC-and RT-heads, two bands corresponding to 1α and 2α chains with nearly similar molecular weights (1α at ~121 kDa and 2α at ~112 kDa) were detected. However, the bands in the SC-soft head tissue gelatin appeared with greater clarity. Valcarcel, Hermida-Merino, Piñeiro, Hermida-Merino, & Vázquez, (2021) reported that gelatin derived from fish skin typically retains higher molecular weight α and β chains, indicating less collagen degradation. This observation aligns with the present findings, where clearer α and β bands were detected in the skin gelatin samples of SC and RT. The presence of β chains, representing collagen dimers, further supports the notion of milder hydrolysis and better preservation of collagen structure in skin-derived gelatin. Furthermore, Alves *et al.* (2022) noted that interspecies and inter-tissue variations in molecular weight profiles can be attributed to differences in collagen cross-linking and extraction conditions. This explains the slight molecular weight differences observed in the α chains between the two species, as well as the greater band clarity in gelatin extracted from the soft head tissue of SC compared to that of RT. Overall, the electrophoretic patterns provide valuable insights into the structural integrity and functional quality of gelatin extracted from different fish byproducts. These results underscore the importance of optimizing pretreatment conditions to achieve a balance between maximizing extraction yield and preserving molecular structure, which directly influences functional properties such as gel strength and viscosity.

Gel Strength

In terms of gel strength (Fig. 2), all extracted gelatins showed significant differences from each other ($P < 0.05$), except for the gelatins derived from RT-skin and the soft tissue of SC-head, which did not differ significantly. In this study, the highest gel strength was recorded for SC-skin gelatin (573.5 g), while the lowest was observed for RT-head gelatin (19.6 g). The gel strength of SC- skin extracted gelatin (573.5 g) was markedly higher than the value reported by Adnan, Kresnowati, Marlina, & Bindar, (2025) for gelatin obtained from striped catfish (*Pangasianodon hypophthalmus*) skin.

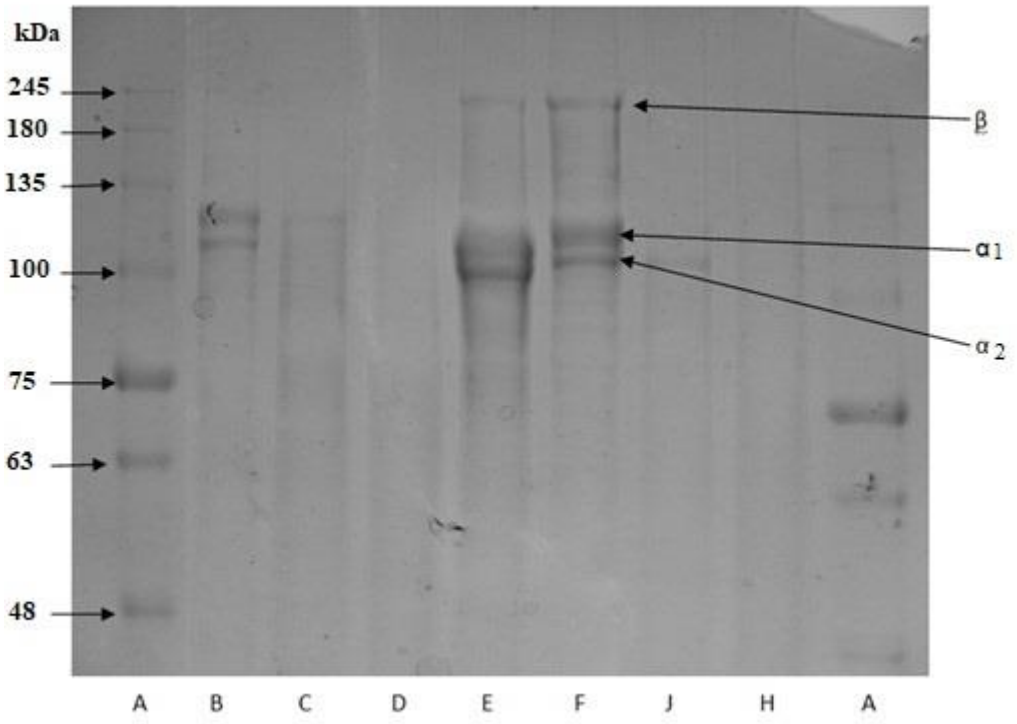

Fig. 1. SDS-PAGE electrophoretic profiles of gelatin extracted from by-products of silver carp (SC) and rainbow trout (RT). Lane A: molecular weight marker (protein ladder); Lane B: SC head soft tissue gelatin; Lane C: RT head gelatin; Lane D: SC head bone gelatin; Lane E: RT skin gelatin; Lane F: SC skin gelatin; Lane G: RT vertebral bone gelatin; Lane H: SC vertebral bone gelatin. Major α- and β-chain bands are indicated where visible

This substantial difference may indicate that SC skin is a superior raw material for producing high-strength gelatin, potentially due to a more stable collagen cross-linking architecture and a higher density of intermolecular hydrogen bonding within the resulting gelatin network. Moreover, the gel strength of gelatin extracted from the soft tissue of SC-head (453 g) was substantially higher than that reported for gelatin from cod fish head soft tissue (123.2 g) (Arnesen & Gildberg, 2006) and even exceeded the gel strength of three types of tilapia scale gelatins (hot water-pretreated gelatin, acetic acid-pretreated gelatin, and pepsin enzyme-pretreated gelatin) reported by Peng *et al.* (2022). Another notable finding was that the gel strength of gelatin extracted from the bones of both species was significantly lower than that of gelatin from their skin and the soft tissue of SC-head ($P < 0.05$). This difference can be attributed to the more intensive hydrolysis of bone collagen due to the use of a stronger acid treatment compared to skin and soft tissue, aimed at further reducing mineral content and extracting more collagen from the mineralized bone matrix to improve extraction yield (Koli *et al.*, 2013). As shown in the protein electrophoretic patterns (Fig. 1), except for the RT-bone gelatin, which exhibited a very faint 2α band, none of the bone samples showed distinct protein bands. This likely results from severe collagen hydrolysis during pretreatment, explaining the lower gel strength of bone gelatin compared to skin gelatin of both species and gelatin from SC-head soft tissue. The lack of distinct protein bands in SC-bone gelatins (Fig. 1) confirms that the harsh demineralization process led to significant cleavage of peptide bonds. This structural disintegration is the primary reason for the

lower gel strength in these samples compared to skin and soft tissue gelatins, where α and β chains were well-preserved. Despite this relatively severe hydrolysis, the gel strength of SC-head bone gelatin (329.3 g) was higher than values reported for channel catfish head bone gelatin (209 g) by Liu, Han, & Guo, (2009), and even exceeded gel strength values reported for skin gelatin of some species such as skipjack tuna (206 g) (Shyni *et al*., 2014), Amur sturgeon (141 g) (Nikoo *et al*., 2014). As mentioned, the lowest gel strength was observed in gelatin extracted from RT-head. Sinthusamran, Benjakul, & Kishimura, (2015) compared the properties of gelatin extracted from sea bass skin of different sizes, reporting that fish size affects gelatin yield and gel characteristics. Larger fish produced gelatin with higher yield and better gel properties. They also noted that gelatin cross-linking plays a fundamental role in gel formation and gel strength. Also, in a study published by Adnan *et al.* (2024), gelatin extracted from the skin of striped catfish exhibited a gel strength of 66.01 ± 0.83 g, which is significantly lower than the values obtained for gelatin in the present study. Furthermore, the study by Wang *et al.* (2024) reported that gelatin extracted from cold-water fish skin had a gel strength of 340 g, which was lower than some samples in the current study, such as gelatin derived from the skin of RT-and SC, as well as the soft tissue of SC-head, but higher than other extracted gelatins. Based on previous studies, it has been established that the gel properties of fish gelatin are influenced by various factors. For instance, processing methods, fish species, and additives affect the protein structure and chemical interactions, thereby impacting gelation (Xie, Tang, & Dong, 2024). Additionally, preparation conditions such as solid-to-liquid ratio, pH, temperature, and time significantly affect gelatin yield and gel strength (Sha *et al*., 2013). Moreover, the unique amino acid composition of fish gelatin results in a lower melting point compared to mammalian gelatin, while its higher molecular weight fractions contribute to increased dynamic viscosity (Bekesheva & Yakubova, 2018). Although gel strength was measured following the general principles of the Bloom test (6.67% gelatin, 18 h maturation at 4 °C, 12.7 mm probe, 4 mm penetration depth), the gel was prepared in a smaller cylindrical container (3 cm height × 2.5 cm diameter) rather than a standard Bloom jar (>100 mL). Therefore, the absolute gel strength values obtained in this study may not be directly comparable to standardized Bloom values reported in the literature. However, since all samples were prepared and analyzed under identical experimental conditions, the results remain valid for relative comparison among treatments within this study. Future studies should consider using standard Bloom jars or appropriately scaled probe–sample dimensions to ensure full methodological standardization. To fully understanding the functional variations between gelatin types, characterizing their total amino acid composition and rheological gelling points is crucial. While not addressed in this paper, evaluating these factors in subsequent studies will provide deeper insights into how the tissue source influences the structure–performance dynamics of the resulting gelatin. If we consider the use of extracted gelatins for applications in the food industry, it can be noted that the high gel strength of SC-skin gelatin (573.5 g) demonstrates its potential for use in the confectionery and pharmaceutical industries. This is because high gel strength is particularly important in products such as pastille candies, where structural integrity and chewability are of great importance (Yin *et al.,* 2025).

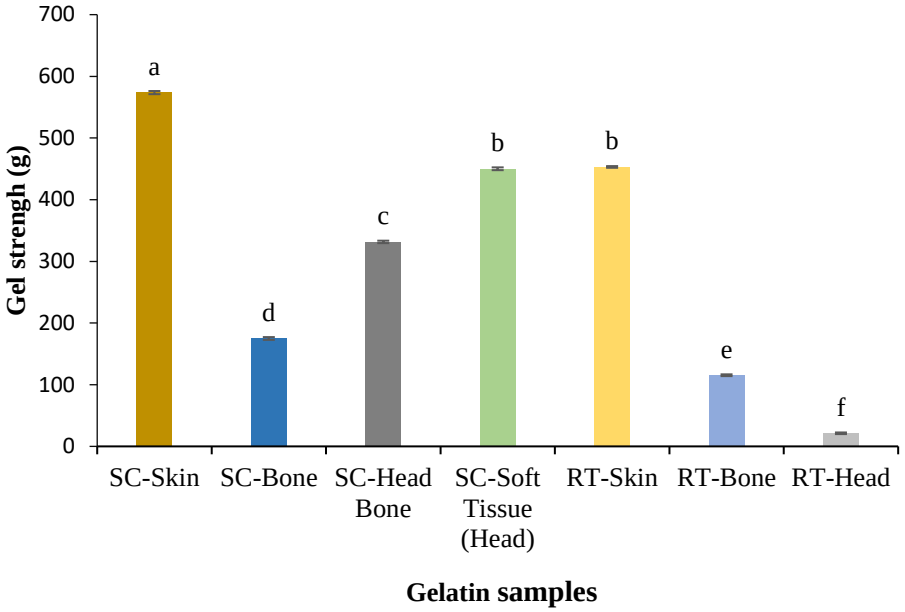

Fig. 2. Gel strength (g) of gelatins extracted from different by-products of silver carp (SC) and rainbow trout (RT). Values are expressed as mean ± SD (n = 3)
Different letters above bars indicate statistically significant differences (P < 0.05).

Viscosity of Gelatin Samples

Viscosity is considered the second most important commercial property of gelatin (Bekesheva & Yakubova, 2018). Fig. 3 illustrates the viscosity values of the extracted gelatins. The viscosity of the samples ranged from 2.6 to 11 cP. The highest viscosity was observed in gelatin extracted from the soft tissue of the SC-head (11 cP), whereas the lowest was recorded for head-derived gelatin from RT (2.6 cP). There was no statistically significant difference (P > 0.05) among the gelatins extracted from the head bone of SC, vertebral bone, and head bone of RT. However, these samples showed significantly lower viscosities compared to gelatin extracted from the skin and bone of SC, the skin of RT, and the soft tissue and head bone of SC (P < 0.05). Interestingly, the relatively high viscosity of SC-head bone gelatin, despite its degraded protein profile, suggests that residual mineral-protein complexes or non-collagenous impurities might contribute to flow resistance, a phenomenon that warrants further purification studies. Also, the viscosity of SC-skin gelatin (over 5 cP) was higher than the 4.62 cP reported for pangas catfish skin gelatin by Barman *et al.* (2021). This difference is notable, as skin-derived gelatins generally retain higher viscosity due to their broader molecular weight distribution. The elevated viscosity observed in SC-skin indicates better preservation of the triple-helix structure and greater retention of β and γ chains during our extraction process compared to the catfish skin gelatin studied by Barman *et al.* (2021). The primary factor influencing gelatin viscosity is the molecular weight distribution and size of its components (Bekesheva & Yakubova, 2018; Kwak *et al.*, 2017). According to Karim & Bhat (2009), the β and γ chains of gelatin play a critical role in enhancing viscosity. As shown in the electrophoretic protein patterns (Fig. 1), gelatins extracted from the skin of both species contained a greater proportion of high-molecular-weight compounds than other samples. The higher viscosity of SC-skin gelatin compared to that of RT may be attributed to its higher content of high-

molecular-weight components (He *et al.*, 2022). However, despite this, the gelatin extracted from the soft tissue of the SC-head exhibited even higher viscosity than skin-derived gelatins, possibly due to the inefficiency of the alkaline treatment in removing non-collagenous proteins, which could have remained in the gelatin solution during thermal extraction. Interestingly, the gelatin obtained from the head bones of SC, despite showing no visible protein bands in its electrophoretic pattern, exhibited higher viscosity than gelatins derived from the vertebral bones of both fish species, and even higher than that of RT-skin. This could be due to the presence of impurities in the gelatin solution, which might be reduced through successive filtration (He *et al.*, 2022; Yu *et al.*, 2023). In addition to the aforementioned points, it has been established that pH is a key parameter influencing gelatin viscosity and its functional properties, typically ranging from 4.5–6.5 for commercial type A/B gelatins (Goudie, McCreath, Parkinson, Davidson, & Liggat, 2023). Furthermore, at the isoelectric point, the net electrical charge of proteins is minimized, leading to chain entanglement (coil entanglement) along with hydrophobic interactions, which in turn increases solution viscosity (Hu *et al.*, 2024). It is worth noting that the high viscosity of the gelatin samples from SC-soft tissue (11 cP) and SC-skin makes them a good candidate for use as a thickening and stabilizing agent in products such as sauces, gravies, and low-fat spreads (Karim & Bhat, 2009).

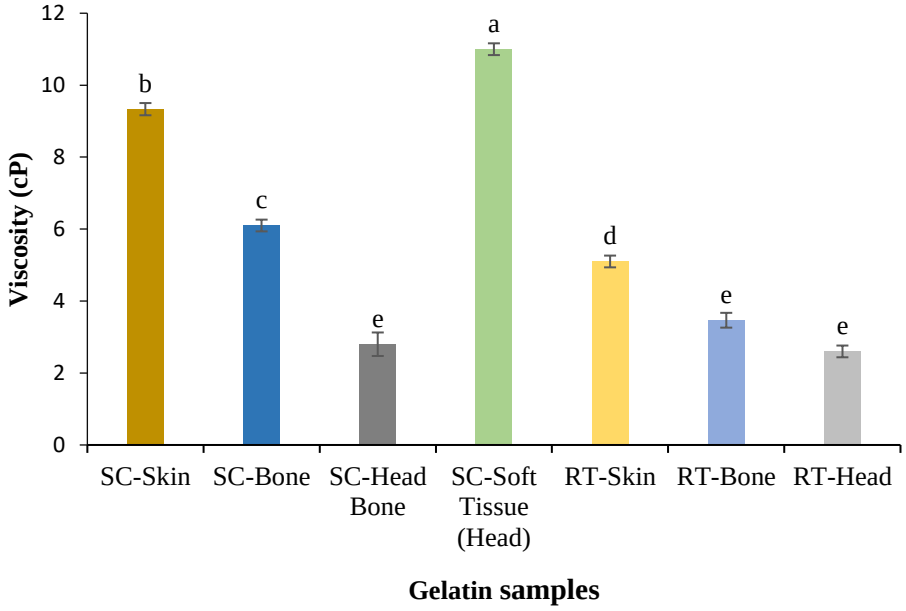

Fig. 3. Viscosity (cP) of gelatins extracted from various by-products of silver carp (SC) and rainbow trout (RT). Values are expressed as mean ± SD (n = 3)
Different letters above bars indicate statistically significant differences (P < 0.05).

Melting Temperature of Gelatin Samples

Melting points of gelatins extracted from various by-products of SC and RT are presented in Fig. 4. Gelatins derived from the skin and bones of RT did not exhibit a statistically significant difference in melting temperature (P > 0.05). However, the melting point of gelatin extracted from the RT-head was significantly different from that of the skin- and bone-derived gelatins (P < 0.05). A slight, statistically insignificant difference (P > 0.05) was observed between the melting points of

gelatin from the skin and soft head tissue of SC. Overall, however, the gelatins extracted from SC by-products exhibited significantly higher melting points compared to those extracted from RT by-products ($P < 0.05$). Among the samples in this study, the melting points of gelatins extracted from SC-skin and soft head tissue were found to be closer to that of bovine skin gelatin. In contrast, the melting points of gelatin extracted from SC-vertebral bones and head bones were lower than the values reported for red snapper (26 °C) and grouper (25 °C), but higher than that reported for mammalian bone gelatin (21 °C) (Shakila, Jeevithan, Varatharajakumar, Jeyasekaran, & Sukumar, 2012). Although fish gelatin has gained attention as a potential substitute for mammalian gelatin, its practical applications remain limited due to its lower melting point and low gel strength. Commercial fish gelatin typically melts at around 7 °C, whereas mammalian gelatin melts at significantly higher temperatures, ranging from 22 °C to 34 °C (Bekesheva & Yakubova, 2018; Derkach, Voron'ko, Kuchina, & Kolotova, 2020; Silviwanda & Naenum, 2024). The relatively lower melting point of fish gelatin compared to mammalian gelatin facilitates better flavor and aroma release during oral processing, making it highly advantageous for applications in texture and aroma-controlled food products (Choi & Regenstein, 2000; Koli *et al.*, 2012; Uddin, Hossain, Sagadevan, Al Amin, & Johan, 2021). According to Karim & Bhat (2009), the melting point of gelatin is closely related to gel maturation time and the concentration of specific amino acids such as proline and hydroxyproline. Also, they reported that the α/β chain ratio also plays a role in determining the melting behavior of gelatin (Huang *et al.*, 2019).

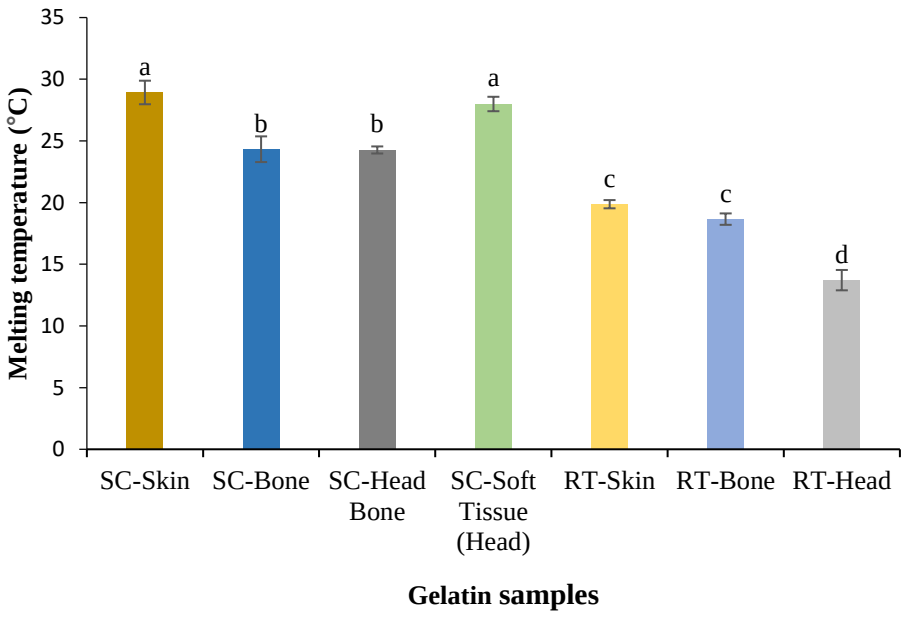

Fig. 4. Melting temperature (°C) of gelatins extracted from different by-products of silver carp (SC) and rainbow trout (RT). Values are expressed as mean ± SD (n = 3)
Different letters above bars indicate statistically significant differences ($P < 0.05$).

Foaming Capacity and Stability

Foaming capacity and foam stability are considered as critical functional properties of gelatin in food applications, particularly in products like marshmallows (Uddin *et al.*, 2021). The foaming capacity and stability of the

extracted gelatins are presented in Table 4. Among all samples, the highest foaming capacity was observed in gelatin extracted from SC-vertebral bones (120 ± 2%), while the greatest foam stability was recorded for gelatin derived from the fish's head bones (48.03 ± 2.12%). The inverse relationship between molecular weight and foaming capacity was evident; SC-vertebral bone gelatin, which underwent the most extensive hydrolysis, exhibited the highest foaming capacity (120%). This confirms that smaller peptide fragments, resulting from prolonged acid treatment, possess higher interfacial mobility than intact collagen chains. Gelatin obtained from the soft tissue of the SC-head also showed relatively good foaming properties (foaming capacity: 99.66 ± 2.08%, foam stability: 44.98 ± 0.10%). In RT samples, the gelatin extracted from the skin and vertebral bones showed no significant difference in foaming capacity ($P > 0.05$); however, both differed significantly from the head-derived gelatin in this regard ($P < 0.05$). Furthermore, foam stability of the gelatin from RT-vertebral bones was significantly higher than that of the skin-derived gelatin ($P < 0.05$). Interestingly, RT-skin gelatin demonstrated significantly higher foaming capacity and stability than that from SC-skin ($P < 0.05$), whereas in the case of other tissues (head, bones), SC gelatins outperformed those from RT. The lowest foam stability was observed in gelatin extracted from the head of RT. According to Nagarajan, Benjakul, Prodpran, Songtipya, & Kishimura, (2012), proteins with shorter chains can migrate more quickly to the interface, resulting in superior foaming behavior. In the present study, gelatin samples derived from the head and vertebral bones of SC, which showed no visible protein bands on SDS-PAGE (Fig. 1), indicating the presence of very low molecular weight compounds, exhibited the best foaming capacity and stability. Conversely, gelatin from RT-vertebral bones, which contained larger protein fragments including a prominent 2α-chain band, demonstrated weaker foaming performance than those from SC. Foam stability depends on multiple factors, including the rate at which surface tension equilibrates, overall solution viscosity, surface viscosity, structural stability of the foam layer, and electrostatic repulsion across the foam interface (Barman *et al*., 2020; He *et al*., 2022). It has been reported that the foaming properties of gelatin are significantly influenced by the pH of the environment, primarily through its effect on the net electrostatic charge of the protein molecules. Near the isoelectric point (pI), where the net charge approaches zero, gelatin molecules exhibit a higher propensity to migrate toward the air-water interface (Goudie *et al*., 2023; Nurul & Sarbon, 2015). This migration reduces surface tension and potentially enhances initial foam formation. Conversely, at pH values distant from the pI, the increased electrostatic repulsion between protein chains prevents molecular aggregation, which can lead to enhanced foam stability (Nurul & Sarbon, 2015).

Table 4- Foam properties of extracted fish gelatins

Source	Byproduct	Foam capacity (%)	Foam stability (%)
SC	Skin	48.33 ± 0.57 ^{e}	20.68 ± 0.24 ^{e}
	Bone	120.00 ± 2.00 ^{a}	44.57 ± 0.32 ^{b}
	Head Bone	68.00 ± 1.00 ^{c}	48.03 ± 2.12 ^{a}
	Soft tissue (head)	99.66 ± 2.08 ^{b}	44.98 ± 0.10 ^{b}
RT	Skin	59.00 ± 2.00 ^{d}	23.52 ± 0.18 ^{d}
	Bone	57.33 ± 1.15 ^{d}	37.68 ± 0.22 ^{c}
	Head	94.33 ± 1.52 ^{f}	non

Mean ± SD of three replicates. Different letters within each column indicate statistically significant differences ($P < 0.05$). Identical letters indicate no significant difference.

Bone-derived gelatins exhibited remarkable performance despite their lower molecular weight distribution. Their high foaming capacity (up to 120%) makes them particularly suitable for aerated food systems. In products such as marshmallows, mousses, and whipped toppings, rapid migration of peptides to the air–water interface is more critical than the development of a strong gel network. Therefore, these bone-derived by-products may have strong potential for targeted application in the confectionery industry as efficient foaming agents.

Conclusion

In conclusion, this study demonstrates that the functional properties of fish gelatin are highly tissue-specific, determining their eventual industrial suitability. Specifically, the gelatin derived from silver carp (SC) head soft tissue, characterized by its remarkably high viscosity, is ideally suited for use as a thickening and stabilizing agent in liquid or semi-solid food systems like sauces and gravies. In contrast, bone-derived gelatins, despite their lower gel strength, exhibit superior foaming properties, making them excellent candidates for aerated confectionery products such as marshmallows and mousses. Furthermore, it should be noted that the moisture content of RT-skin gelatin (16.8%) exceeded the standard limit (15%), which represents a limitation of the current laboratory-scale drying process. Future industrial applications would require optimized dehydration techniques to ensure long-term microbial stability and compliance with commercial quality standards.

Author Contribution

A. Amirafzali: Data curation, Formal analysis, Investigation, Methodology, Writing–original draft. **M. Rezaei:** Conceptualization, Data curation, Formal analysis, Investigation, Methodology, Project administration, Supervision, Resources, Software, Validation, Visualization, Writing – review and editing. **Sh. Naghdi:** Data curation, Formal analysis, Validation, Visualization, Writing– original draft, Writing – review and editing.

Funding Source

This research conducted by Tarbiat Modares University and the Iran National Science Foundation (INSF, Grant No. 4033185) financial support.

Conflict of Interest

The authors certify that they have no conflict of interest.

Acknowledgments

The authors would like to thank Tarbiat Modares University for their support.

References

1. Abdollahi, M., Rezaei, M., & Jafari, E. (2014). Evaluation of production efficiency, by-products, and their nutritional value during the processing of rainbow trout. *JFST*, *2*(4), 23–34.
2. Adnan, S., Kresnowati, M.T.A.P., Marlina, & Bindar, Y. (2024). Sustainable valorisation of freshwater fish by-products to gelatin and fish oil by hydrothermal extraction. *International Journal of Food Science and Technology*, 8224–8235. https://doi.org/10.1111/ijfs.17512
3. Adnan, S., Kresnowati, M.T.A.P., Marlina, & Bindar, Y. (2025). Effect of operational variables on gel strength of fish gelatin striped catfish (*Pangasianodon hypophthalmus*). *AIP Conference Proceedings*, *3295*(1), 70007. https://doi.org/10.1063/5.0269817
4. Alves, A.L., Fraguas, F.J., Carvalho, A.C., Valcárcel, J., Pérez-Martín, R.I., Reis, R.L., Vázquez, J.A., & Silva, T.H. (2022). Characterization of codfish gelatin: A comparative study of fresh and salted skins and different extraction methods. *Food Hydrocolloids*, *124*(December 2020). https://doi.org/10.1016/j.foodhyd.2021.107238

5. Anandito, R.B.K., Purwanto, E., Praseptiangga, D., & Zaman, M.Z. (2024). Optimization of cobia fish (*Rachycentron canadum*) gelatin extraction with response surface methodology. *Food Research*, *8*, 139–147. https://doi.org/10.26656/fr.2017.8(S2).98
6. Arnesen, J.A., & Gildberg, A. (2006). Extraction of muscle proteins and gelatine from cod head. *Process Biochemistry*, *41*(3), 697–700. https://doi.org/10.1016/j.procbio.2005.09.001
7. Association of Official Analytical Chemists. Official Methods of Analysis of AOAC International; AOAC International: Gaithersburg, MD, USA, 2000. https://doi.org/10.1093/9780197610145.003.1380
8. Barman, L.C., Sikder, M.B.H., Ahmad, I., Shourove, J.H., Rashid, S.S., & Ramli, A.N.M. (2020). Gelatin extraction from the Bangladeshi Pangas catfish (*Pangasius pangasius*) waste and comparative study of their physicochemical properties with a commercial gelatin. *International Journal of Engineering Technology and Sciences*, *7*(2), 13–23. https://doi.org/10.15282/10.15282/ijets.7.2.2020.1002
9. Barman, L.C., Sikder, M.B.H., Ahmad, I., Shourove, J.H., Samiur Rashid, S., & Ramli, A.N.M. (2021). Gelatin extraction from the Bangladeshi Pangas Catfish (*Pangasius pangasius*) waste and comparative study of their physicochemical properties with a commercial gelatin. *International Journal of Engineering Technology and Sciences*, *7*(2), 13–23. https://doi.org/10.15282/10.15282/ijets.7.2.2020.1002
10. Bekesheva, A.A., & Yakubova, O.S. (2018). Scientific substantiation of physical properties of fish gelatin. *Vestnik of Astrakhan State Technical University. Series: Fishing Industry*, 132–140. https://doi.org/10.24143/2073-5529-2017-3-132-140
11. Boran, G., & Regenstein, J.M. (2009). Optimization of gelatin extraction from silver carp skin. *Journal of Food Science*, *74*(8), E432–E441. https://doi.org/10.1111/j.1750-3841.2009.01328.x
12. British Standards Institution – BSI. (1975). Methods for sampling and testing gelatin (Physical and Chemical Methods). London: BSI.
13. Choi, S.S., & Regenstein, J.M. (2000). Physicochemical and sensory characteristics of fish gelatin. *Journal of Food Science*, *65*(2), 194–199. https://doi.org/10.1111/j.1365-2621.2000.tb15978.x
14. Derkach, S.R., Voron'ko, N.G., Kuchina, Y.A., & Kolotova, D.S. (2020). Modified fish gelatin as an alternative to mammalian gelatin in modern food technologies. *Polymers*, *12*(12), 1–10. https://doi.org/10.3390/polym12123051
15. Du, L., Khiari, Z., Pietrasik, Z., & Betti, M. (2013). Physicochemical and functional properties of gelatins extracted from turkey and chicken heads. *Poultry Science*, *92*(9), 2463–2474. https://doi.org/10.3382/ps.2013-03161
16. Duasa, J., Husin, A.M., Asmy Mohd Thas Thaker, M., & Rahman, M.P. (2022). An alternative source of collagen for Muslim consumers: halal and environmental concerns. *Journal of Islamic Marketing*, *13*(11), 2232–2253. https://doi.org/10.1108/jima-09-2020-0268
17. Duman, M. (2025). Collagen extraction from rainbow (*Oncorhynchus mykiss*) trout heads and skins. *Revista Cientifica de La Facultad de Veterinaria*, *35*(2), 1–7. https://doi.org/10.52973/rcfcv-e35646
18. Elavarasan, K., Kumar, A., Uchoi, D., Tejpal, C.S., Ninan, G., & Zynudheen, A.A. (2017). Extraction and characterization of gelatin from the head waste of tiger tooth croaker (*Otolithes ruber*). *Waste and Biomass Valorization*, *8*(3), 851–858. https://doi.org/10.1007/s12649-016-9639-5
19. FAO. (2024). *World Fisheries and Aquaculture, FAO:Rome,2022* (pp. 1–11).
20. Feng, Y., Shi, Q., Xie, H., Ouyang, K., Xiong, H., & Zhao, Q. (2024). Combined effects of gelatin extraction methods and hydrolysis protease types on the functional properties of tilapia scale

gelatin hydrolysates. *International Journal of Food Science and Technology*, *59*(9), 6194–6206. https://doi.org/10.1111/ijfs.17354
21. Göçer, M. (2022). Extraction and characterization of collagen from the skin and bone of shabout (*Arabibarbus grypus* Heckel, 1843). *Iranian Journal of Fisheries Sciences*, *21*(3), 671–687. https://doi.org/10.22092/ijfs.2022.126898
22. Gomez-Guillen, M.C., Gimenez, B., Lopez-Caballero, M.E., & Montero, M.P. (2011). Functional and bioactive properties of collagen and gelatin from alternative sources: A review. In *Food Hydrocolloids*, *25*(8), 1813–1827. Elsevier. https://doi.org/10.1016/j.foodhyd.2011.02.007
23. Goudie, K.J., McCreath, S.J., Parkinson, J.A., Davidson, C.M., & Liggat, J.J. (2023). Investigation of the influence of pH on the properties and morphology of gelatin hydrogels. *Journal of Polymer Science*, *61*(19), 2316–2332. https://doi.org/10.1002/pol.20230141
24. GME. (2011). Gelatin Manufacturers of Europe: Raw materials. Retrieved from http://www.gelatine.org/en/about-gelatine/ manufacturing/raw-materials.html
25. Guan, Y., He, J., Chen, J., Li, Y., Zhang, X., Zheng, Y., & Jia, L. (2022). Valorization of fish processing by-products: Microstructural, rheological, functional, and properties of silver carp skin type I collagen. *Foods*, *11*(19). https://doi.org/10.3390/foods11192985
26. He, J., Zhang, J., Xu, Y., Ma, Y., & Guo, X. (2022). The structural and functional differences between three species of fish scale gelatin and pigskin gelatin. *Foods*, *11*(24). https://doi.org/10.3390/foods11243960
27. Hu, B., Cen, S., Sun, W., Zhan, S., Jia, R., Ou, C., & Huang, T. (2024). Effects of different phosphorylation times and pH on fish gelatin: Functional properties, structural and mechanism analysis. *Food Hydrocolloids*, *152*, 109876. https://doi.org/10.1016/j.foodhyd.2024.109876
28. Huang, T., Tu, Z., cai, Shangguan, X., Sha, X., Wang, H., Zhang, L., & Bansal, N. (2019). Fish gelatin modifications: A comprehensive review. *Trends in Food Science and Technology*, *86*(August 2018), 260–269. https://doi.org/10.1016/j.tifs.2019.02.048
29. Iranian Fisheries Organization Statistical Yearbook. (2024). *Iranian Fisheries Organization Statistical Yearbook, 1st ed.; Iranian Fisheries Organization: Tehran, Iran, 2024; p. 30.* 1–30. https://doi.org/10.52547/injvr.1.1.1
30. Karim, A.A., & Bhat, R. (2009). Fish gelatin: properties, challenges, and prospects as an alternative to mammalian gelatins. *Food Hydrocolloids*, *23*(3), 563–576. https://doi.org/10.1016/j.foodhyd.2008.07.002
31. Kittiphattanabawon, P., Benjakul, S., Visessanguan, W., & Shahidi, F. (2010). Comparative study on characteristics of gelatin from the skins of brownbanded bamboo shark and blacktip shark as affected by extraction conditions. *Food Hydrocolloids*, *24*(2–3), 164–171. https://doi.org/10.1016/j.foodhyd.2009.09.001
32. Koli, J.M., Basu, S., Nayak, B.B., Patange, S.B., Pagarkar, A.U., & Gudipati, V. (2012). Functional characteristics of gelatin extracted from skin and bone of Tiger-toothed croaker (*Otolithes ruber*) and Pink perch (*Nemipterus japonicus*). *Food and Bioproducts Processing*, *90*(3), 555–562. https://doi.org/10.1016/j.fbp.2011.08.001
33. Koli, J.M., Basu, S., Venkteshwarlu, G., Choukasy, M.K., & Nayak, B.B. (2013). Optimization of fish gelatin extraction from skins and bones: A comparative study. *Ecology, Environment and Conservation*, *19*(1), 47–56.
34. Kwak, H.W., Shin, M., Lee, J.Y., Yun, H., Song, D.W., Yang, Y., Shin, B.S., Park, Y.H., & Lee, K.H. (2017). Fabrication of an ultrafine fish gelatin nanofibrous web from an aqueous solution by electrospinning. *International Journal of Biological Macromolecules*, *102*, 1092–1103. https://doi.org/10.1016/j.ijbiomac.2017.04.087

35. Laemmli, U.K. (1970). Cleavage of structural proteins during the assembly of the head of bacteriophage T4. Nature, 227, 680–685. https://doi.org/10.1038/227680a0
36. Liu, H.Y., Han, J., & Guo, S.D. (2009). Characteristics of the gelatin extracted from Channel Catfish (*Ictalurus punctatus*) head bones. *LWT-Food Science and Technology*, *42*(2), 540–544. https://doi.org/10.1016/j.lwt.2008.07.013
37. Nagarajan, M., Benjakul, S., Prodpran, T., Songtipya, P., & Kishimura, H. (2012). Characteristics and functional properties of gelatin from splendid squid (*Loligo formosana*) skin as affected by extraction temperatures. *Food Hydrocolloids*, *29*(2), 389–397. https://doi.org/10.1016/j.foodhyd.2012.04.001
38. Naghdi, S., Rezaei, M., Heidari, M.G., Tahergorabi, R., Lorenzo, J.M., & Mirzaei, F. (2024). Insights into fishery by-product application in aquatic feed and food: a review. In *Aquaculture International* (Issue 0123456789). Springer International Publishing. https://doi.org/10.1007/s10499-024-01447-x
39. Naghdi, S., Rezaei, M., Tabarsa, M., & Abdollahi, M. (2025). Structure , functionality and bioactivity of sulfated polysaccharide extracted from rainbow trout byproducts : pH-shift method vs enzymatic hydrolysis. *Food Chemistry*, *479*(March), 143665. https://doi.org/10.1016/j.foodchem.2025.143665
40. Nikoo, M., Benjakul, S., Bashari, M., Alekhorshied, M., Cissouma, A.I., Yang, N., & Xu, X. (2014). Physicochemical properties of skin gelatin from farmed Amur sturgeon (*Acipenser schrenckii*) as influenced by acid pretreatment. *Food Bioscience*, *5*, 19–26. https://doi.org/10.1016/j.fbio.2013.10.004
41. Nurilmala, M., Suryamarevita, H., Hizbullah, H.H., Jacoeb, A.M., & Ochiai, Y. (2022). Fish skin as a biomaterial for halal collagen and gelatin. *Saudi Journal of Biological Sciences*, *29*(2), 1100–1110. https://doi.org/10.1016/j.sjbs.2021.09.056
42. Nurul, A.G., & Sarbon, N.M. (2015). Effects of pH on functional, rheological and structural properties of eel (*Monopterus* sp.) skin gelatin compared to bovine gelatin. *International Food Research Journal*, *22*(2).
43. Olaniran, A.F., Adeoye, O.E., Oyadeyi, O.M., Okonkwo, C.E., Erinle, O.C., Malomo, A.A., Iranloye, Y.M., Olaniran, O.D., & Faloye, O.R. (2024). Utilization and application of bioactive compounds generated from Fish waste and by product as Functional Food Ingredient: A review. *IOP Conference Series: Earth and Environmental Science*, *1342*(1). https://doi.org/10.1088/1755-1315/1342/1/012014
44. Peng, J., Zi, Y., Xu, J., Zheng, Y., Huang, S., Hu, Y., & Liu, B. (2022). Effect of extraction methods on the properties of tilapia scale gelatins. *International Journal of Biological Macromolecules*, *221*(July), 1150–1160. https://doi.org/10.1016/j.ijbiomac.2022.09.094
45. Ruan, Q., Chen, W., Lv, M., Zhang, R., Luo, X., Yu, E., Pan, C., & Ma, H. (2023). Influences of trypsin pretreatment on the structures, composition, andfunctional characteristics of skin gelatin of Tilapia, grass carp, and sea perch. *Marine Drugs*, *21*(8). https://doi.org/10.3390/md21080423
46. Sha, X.M., Tu, Z.C., Wang, H., Shi, Y., Liu, G.X., Man, Z.Z., Huang, T., & Lan, Z. (2013). Preparation and properties on gelatin from fish scale. *Advanced Materials Research*, *647*, 352–356. https://doi.org/10.4028/www.scientific.net/AMR.647.352
47. Shakila, R.J., Jeevithan, E., Varatharajakumar, A., Jeyasekaran, G., & Sukumar, D. (2012). Functional characterization of gelatin extracted from bones of red snapper and grouper in comparison with mammalian gelatin. *LWT-Food Science and Technology*, *48*(1), 30–36. https://doi.org/10.1016/j.lwt.2012.03.007
48. Shyni, K., Hema, G.S., Ninan, G., Mathew, S., Joshy, C.G., & Lakshmanan, P.T. (2014). Isolation and characterization of gelatin from the skins of skipjack tuna (*Katsuwonus pelamis*),

dog shark (*Scoliodon sorrakowah*), and rohu (*Labeo rohita*). *Food Hydrocolloids*, *39*, 68–76. https://doi.org/10.1016/j.foodhyd.2013.12.008
49. Siburian, W.Z., Rochima, E., Andriani, Y., & Praseptiangga, D. (2020). Fish gelatin (definition, manufacture, analysis of quality characteristics, and application): A review. *International Journal of Fisheries and Aquatic Studies*, *8*(4), 90–95.
50. Silviwanda, S., & Najib Tuisina, N. (2024). Physical characteristics of fishbone gelatin (gel strength, viscosity, and pH): Review. *Journal of Tropical Food and Agroindustrial Technology*, *5*(01), 9–18. https://doi.org/10.21070/jtfat.v5i01.1619
51. Sinthusamran, S., Benjakul, S., & Kishimura, H. (2015). Molecular characteristics and properties of gelatin from skin of seabass with different sizes. *International Journal of Biological Macromolecules*, *73*, 146–153. https://doi.org/10.1016/j.ijbiomac.2014.11.024
52. Tabarestani, H.S., Maghsoudlou, Y., Motamedzadegan, A., Sadeghi Mahoonak, A.R., & Mahoonak, A.R.S. (2010). Optimization of physico-chemical properties of gelatin extracted from fish skin of rainbow trout (*Onchorhynchus mykiss*). *Bioresource Technology*, *101*(15), 6207–6214. https://doi.org/10.1016/j.biortech.2010.02.071
53. Tavakolipour, H. (2011). Extraction and evaluation of gelatin from silver carp waste. *World Journal of Fish and Marine Sciences*, *3*(1), 10–15.
54. Uddin, S.M.K., Hossain, M.A.M., Sagadevan, S., Al Amin, M., & Johan, M.R. (2021). Halal and Kosher gelatin: Applications as well as detection approaches with challenges and prospects. *Food Bioscience*, *44*(PA), 101422. https://doi.org/10.1016/j.fbio.2021.101422
55. Usman, M., Sahar, A., Inam-Ur-Raheem, M., Rahman, U., Sameen, A., & Aadil, R.M. (2022). Gelatin extraction from fish waste and potential applications in food sector. *International Journal of Food Science and Technology*, *57*(1), 154–163. https://doi.org/10.1111/ijfs.15286
56. Valcarcel, J., Hermida-Merino, C., Piñeiro, M.M., Hermida-Merino, D., & Vázquez, J.A. (2021). Extraction and characterization of gelatin from skin by-products of seabream, seabass and rainbow trout reared in aquaculture. *International Journal of Molecular Sciences*, *22*(22). https://doi.org/10.3390/ijms222212104
57. Wang, Y., Cui, Q., Wang, X., Wu, C., Xu, X., Dong, X., & Pan, J. (2024). The gelling properties of fish gelatin as improved by ultrasound-assisted phosphorylation. *Food Chemistry*, *449*(December 2023), 139214. https://doi.org/10.1016/j.foodchem.2024.139214
58. Xie, D., Tang, Y., & Dong, G. (2024). Various factors affecting the gel properties of surimi: A review. *Journal of Texture Studies*, *55*(3), e12847. https://doi.org/10.1111/jtxs.12847
59. Yazid, M., Hartina, U., Razali, M., Shaarani, S., Roslan, J., Amirah, R., Noor, M., & Qhairul, N. (2024). Physicochemical and functional properties of buffalo (*Bubalus bubalis*) bone gelatin extracted using acid pre-treatment. *Future Foods*, *10*(August), 100428. https://doi.org/10.1016/j.fufo.2024.100428
60. Yin, Q., Shi, H., Zhao, Y., Yu, G., Wu, H., Xia, G., & Yang, T. (2025). Physiochemical and functional properties of gelatin obtained from frigate mackerel (*Auxis thazard*), skipjack tuna (*Katsuwonus pelamis*), Longtail tuna (*Thunnus tonggol*) and yellowfin tuna (*Thunnus albacares*) skin. *Food Chemistry: X*, *27*, 102360. https://doi.org/10.1016/j.fochx.2025.102360
61. Yu, E., Pan, C., Luo, X., Ruan, Q., Chen, W., Fang, Y., Wang, K., Qin, Y., Lv, M., & Ma, H. (2023). Structural characteristics, component interactions and functional properties of gelatins from three fish skins extracted by five methods. *International Journal of Biological Macromolecules*, *248*(May), 125813. https://doi.org/10.1016/j.ijbiomac.2023.125813
62. Yuan, Z., Ye, X., Hou, Z., & Chen, S. (2024). Sustainable utilization of proteins from fish processing by-products: Extraction, biological activities and applications. *Trends in Food Science & Technology*, *143*, 104276. https://doi.org/10.1016/j.tifs.2023.104276

63. Zhou, P., & Regenstein, J.M. (2006). Determination of total protein content in gelatin solutions with the Lowry or Biuret assay. *Journal of Food Science*, *71*(8), C474–C479. https://doi.org/10.1111/j.1750-3841.2006.00151.x

نشریه پژوهشهای علوم و صنایع غذایی ایران
https://ifstrj.um.ac.ir

مقاله پژوهشی

جلد ۲۲، شماره ۱، فروردین- اردیبهشت ۱۴۰۵، ص. ۹۴-۷۳

مقایسه فیزیکوشیمیایی و عملکردی ژلاتین استخراج شده از ضایعات ماهی قزل‌آلای رنگین‌کمان (*Oncorhynchus mykiss*) و کپور نقره‌ای (*Hypophthalmichthys molitrix*)

علیرضا امیرافضلی[۱]- مسعود رضایی[۱*]- شهاب نقدی[۱]

تاریخ دریافت: ۱۴۰۴/۰۹/۱۸

تاریخ پذیرش: ۱۴۰۴/۱۲/۱۷

چکیده

در این پژوهش، ژلاتین از ضایعات مختلف ماهی‌های کپور نقره‌ای (*Hypophthalmichthys molitrix*) و قزل‌آلای رنگین‌کمان (*Oncorhynchus mykiss*) شامل پوست، بافت نرم جمجمه و ستون فقرات استخراج شد. نمونه‌های ژلاتین استخراج‌شده از نظر ترکیب تقریبی، وزن مولکولی، ویژگی‌های عملکردی و ساختاری مورد ارزیابی قرار گرفتند. نتایج نشان داد که تمامی نمونه‌ها دارای محتوای پروتئینی بالا (بین ۶۹/۲۵ ٪ تا بیش از ۸۵/۷۸ ٪) و چربی بسیار پایین (کمتر از ۱/۵ ٪) بودند. بیشترین میزان رطوبت در ژلاتین پوست قزل‌آلا (۱۶/۸ ٪) و کمترین میزان در ژلاتین استخوان مهره‌ای همان گونه (۲/۹۷ ٪) مشاهده شد. تحلیل SDS-PAGE حضور واضح زنجیره‌های ۱α (۱۱۴~۱۲۱-۱۱۴~ کیلو دالتون) و α۲ (۱۰۰~-۱۱۲ کیلو دالتون) را در ژلاتین‌های پوست و بافت نرم جمجمه نشان داد، در حالی‌که نمونه‌های استخوانی فاقد نوارهای مشخص بودند که نشان‌دهنده تخریب شدید کلاژن در اثر تیمار اسیدی شدید است. از نظر ویسکوزیته، بیشترین مقدار (۱۱ cP) مربوط به ژلاتین بافت نرم جمجمه کپور و کمترین مقدار (۲/۶ cP) مربوط به ژلاتین سر قزل‌آلا بود. قدرت ژل بین ۵۳۷/۵ گرم (پوست کپور) تا ۱۹/۶ گرم (سر قزل‌آلا) متغیر بود. نقطه ذوب ژلاتین‌های کپور به‌طور قابل‌توجهی بالاتر از ژلاتین‌های قزل‌آلا بود و برخی نمونه‌ها به مقادیر مشابه ژلاتین پوست گاوی نزدیک شدند. ژلاتین استخوان مهره‌ای کپور بیشترین ظرفیت کف‌زایی (۱۲۰±۲ ٪) و ژلاتین جمجمه‌ای کپور بیشترین پایداری کف (۲/۱۲ ± ۰۳/ ۴۸ ٪) را نشان دادند. این نتایج بیانگر آن است که ضایعات غیرتجاری این دو گونه ماهی، به‌ویژه پوست و بافت نرم جمجمه کپور نقره‌ای، منابع بالقوه ارزشمندی برای تولید ژلاتین با کیفیت بالا جهت کاربردهای غذایی محسوب می‌شوند.

واژه‌های کلیدی: تحلیل SDS-PAGE، ژلاتین ماهی، ضایعات ماهی، ویژگی‌های عملکردی، *Hypophthalmichthys molitrix*، *Oncorhynchus mykiss*

۱- گروه فرآوری محصولات شیلاتی، دانشکده منابع طبیعی و علوم دریایی، دانشگاه تربیت مدرس، نور، ایران

(*- نویسنده مسئول: Email: rezai_ma@modares.ac.ir)

https://doi.org/10.22067/ifstrj.2026.96879.1528

Iranian Food Science and Technology Research Journal
Homepage: https://ifstrj.um.ac.ir

Short Research Article
Vol. 22, No. 1, March- April, 2026, p. 95-109

Quality Characteristics of Tahitian Chestnut (*Inocarpus fagifer*) and Cowpea (*Vigna unguiculata*) Flour Combinations as Ingredients in Snack Bar

N.A. Mardiana[1*], N.A. Mahmudah[1]

1- Department of Processing of Poultry Product, State Community College of Putra Sang Fajar Blitar, Dr. Sutomo Street No. 29, Blitar, East Java 66133, Indonesia
(*- Corresponding Author Email: nuragustin@akb.ac.id)

Received: 22.09.2025
Revised: 30.12.2025
Accepted: 28.01.2026
Available Online: 02.05.2026

How to cite this article:
Mardiana, N.A., & Mahmudah, N.A. (2026). Quality characteristics of Tahitian chestnut (*Inocarpus fagifer*) and cowpea (*Vigna unguiculata*) flour combinations as ingredients in Snack bar. *Iranian Food Science and Technology Research Journal, 22*(1), 95-109. https://doi.org/10.22067/ifstrj.2026.95576.1477

Abstract

The growing demand for convenient, nutritionally balanced snack products has created opportunities for utilizing underutilized local ingredients in food product development. This study aimed to develop snack bar using Tahitian chestnut (*Inocarpus fagifer*) and cowpea (*Vigna unguiculata*) flours as locally available raw materials and to evaluate their physicochemical, sensory, antioxidant, and microbiological characteristics. Five formulations with varying Tahitian chestnut to cowpea flour ratio [A= 1:1; B= 1:5; C= 2:1; D= 1:2; E= 5:1] were prepared using a completely randomized design. The results showed that the incorporation of Tahitian chestnut and cowpea significantly affected ($p< 0.05$) several physicochemical parameters, including color, texture, moisture, dietary fiber, macronutrient composition, and antioxidant properties, while ash content was not significantly influenced. Sensory attributes and microbiological quality were not significantly affected, with all formulations meeting acceptable hedonic and safety criteria. Based on the Zeleny multi-criteria decision method, formulation E (Tahitian chestnut:cowpea ratio of 5:1) was identified as the most balanced formulation among those evaluated. These findings demonstrate the potential of Tahitian chestnut and cowpea flours for snack bar development and provide baseline information for further utilization of local ingredients in value-added food products.

Keywords: Cowpea, Quality, Snack bar, Tahitian chestnut

Introduction

Indonesia faces significant challenges in addressing nutritional needs while promoting the utilization of local food resources. The shift toward modern lifestyles has increased demand for convenient, ready-to-eat foods that can provide sustained energy and essential nutrients (Ghatge, 2023). This trend has created opportunities for developing snack products that combine convenience with nutritional adequacy, particularly using underutilized local ingredients.

Snack bar have emerged as a popular food category due to their portability, extended shelf life, and ability to deliver concentrated nutrition in a single serving. Globally, snack bar consumption continues to grow, with approximately 37% of the world's population consuming these products in 2024, while the Indonesian market is projected to reach USD 32.94 million (Innova Marketing Sights, 2024; Mordor Intelligence, 2024). This growth reflects consumer demand for convenient

Authors retain the copyright. This is an open access article distributed under Creative Commons Attribution 4.0 International License (CC BY 4.0).

https://doi.org/10.22067/ifstrj.2026.95576.1477

nutrition solutions that fit active lifestyles and varied dietary needs.

Traditional snack bar formulations often rely on imported ingredients or conventional cereals and nuts, creating opportunities for innovation using Indonesia's diverse agricultural resources (Maharani, Pamela, & Kusumasari, 2021). Two particularly promising local ingredients are Tahitian chestnut (*Inocarpus fagifer*) and cowpea (*Vigna unguiculata*), both of which remain underutilized despite their nutritional potential and cultural significance in Indonesian agriculture.

Tahitian chestnut, locally known as *gayam*, was selected in this study due to its potential as an indigenous carbohydrate source with favorable nutritional and functional characteristics. The plant is not cultivated under large-scale plantation systems but grows semi-wild and is traditionally harvested in several regions of Indonesia, including Java and the Maluku Islands (Tetelay & Siahaya, 2018; Veda *et al.*, 2022). Owing to this growth pattern, comprehensive data on cultivated area remain limited. Nevertheless, its consistent availability at the community level and long-standing traditional use indicate its potential as a locally accessible raw material rather than a commodity crop. Previous studies have reported the application of Tahitian chestnut in various food products, such as cookies and crackers (Akhdifa, 2024; Wijanarka *et al.*, 2024). Notably, Tahitian chestnut contains a high dietary fiber content (13.79%) and exhibits a low glycemic index (GI 43), making it suitable for products intended to provide sustained energy (Müller, 2024; Wijanarka, Tifauzah, Khasanah, Nirmala Dewi, & Setyaningsih, 2024). In addition, its flour contributes favorable starch characteristics and textural properties in baked products.

Cowpea (*Vigna unguiculata*) was selected as a complementary ingredient because it is widely cultivated and consumed across Indonesia, including Java, Bali, West Nusa Tenggara, East Nusa Tenggara, Sulawesi, Sumatra, and Kalimantan, with an annual production of approximately 826,351 tons (Fadillah, Purnamawati, & Supijatno, 2020; Tukidi & Erwandi, 2023). Cowpea contributes high-quality plant protein (22.9%) with a relatively low fat content (1.4%) and a rich mineral profile (Anam *et al.*, 2024; Okechukwu-Ezike, Munonye, & Esiegwu, 2020; Olopade *et al.*, 2020). The presence of essential amino acids enhances its value for protein fortification in carbohydrate-based food products. Furthermore, cowpea contributes additional dietary fiber and natural antioxidants derived from its phenolic compounds.

The complementary nutritional characteristics of Tahitian chestnut and cowpea suggest their potential for developing balanced snack bar, in which Tahitian chestnut provides energy-dense carbohydrates and dietary fiber, while cowpea contributes protein and micronutrients. Despite this potential, studies on snack bar formulations based on this specific combination remain limited, particularly regarding the effects of different flour ratios on physicochemical properties, nutritional composition, and sensory acceptance.

Therefore, this study aimed to evaluate the effects of varying proportions of Tahitian chestnut and cowpea flours on the physicochemical characteristics, nutritional composition, sensory attributes, and overall quality of snack bar products, and to identify an optimal formulation that balances nutritional adequacy and product acceptability.

Materials and Methods

Experimental Design

This study used a completely randomized design with one variable, namely the ratio of Tahitian chestnut flour and cowpea flour (1:1; 1:5; 2:1; 1:2; 5:1) in the production of snack bar as presented in Table 1. This study was conducted in triplicate.

Biomaterials and Chemicals

Tahitian chestnut was brought from Yogyakarta, Indonesia, while cowpea was brought from Pasuruan, Indonesia. Other ingredients such as egg whites, skim milk, honey, stevia sugar, salt, and butter were

purchased from Blitar, Indonesia. High-purity analytical grade reagents included distilled water, Kjeldahl tablets, hydrogen sulfide, sodium hydroxide, boric acid, BGC-MR, hydrogen chloride, petroleum benzene, ethanol, DPPH, and colony count agar were procured from commercial suppliers.

Preparation of Sample

Process of Production Tahitian Chestnut Flour

The process of making Tahitian chestnut flour was carried out by modifying the method developed by (Rahayu, Safitri, Sulaeman, & Setiawan, 2024). Tahitian chestnut was sorted to select the quality of Tahitian chestnut, such as those that are not rotten. The Tahitian chestnut washed thoroughly, boiled for 45 minutes at 100 ^{o}C, peeled, sliced thinly, and sun-dried for 7 days. The dried Tahitian chestnut ground into flour and sifted with a 60-mesh sieve.

Process of Production Cowpea Flour

The process of making cowpea flour was carried out by modifying the method developed by (Iswahyudi, Khoirunissa, & Putri, 2022; Prestia, Oktavia, Razak, & Pudjirahaju, 2022). Soaking the beans in clean water for 12 hours with a water to bean ratio of 2:1, changing the water every 6 hours. After soaking, the beans boiled for 5 minutes at 100^{o}C, then drained. Once the beans have cooled, the skins peeling off and dried in the sun for 7 days. The dried cowpea was then ground into flour and sifted using a 60-mesh sieve.

Table 1- Formulation of snack bar

Ingredients	A	B	C	D	E
Tahitian Chestnut Flour (g)	37.5	12.5	50	25	62.5
Cowpea Flour (g)	37.5	62.5	25	50	12.5
Egg White (g)	37.5	37.5	37.5	37.5	37.5
Skim milk	12.5	12.5	12.5	12.5	12.5
Honey (g)	15	15	15	15	25
Water (g)	12.5	12.5	12.5	12.5	12.5
Stevia sugar (g)	3	3	3	3	3
Salt (g)	3	3	3	3	3
Butter (g)	25	25	25	25	25

A: The ratio of Tahitian chestnut flour and cowpea flour (1:1)
B: The ratio of Tahitian chestnut flour and cowpea flour (1:5)
C: The ratio of Tahitian chestnut flour and cowpea flour (2:1)
D: The ratio of Tahitian chestnut flour and cowpea flour (1:2)
E: The ratio of Tahitian chestnut flour and cowpea flour (5:1)

Process of Making Snack Bar

The process of making snack bar was carried out by modifying the method developed by (Day, Cakebread, & Loveday, 2022). First, weigh the ingredients according to the formulation in Table 1. Next, mix the ingredients, shape them, and bake them at 130°C for 20 minutes. The baked products are then cooled and packaged.

Quality assessment

Determination of Physical Properties

The physical parameters evaluated for the snack bar were color and texture. Color measurements were performed using a Konica Minolta CR-410 colorimeter (Minolta Camera Co., Osaka, Japan), calibrated with a standard white plate prior to analysis (Anggraeni, Nurwantoro, Budi, & Abduh, 2017). Measurements were recorded in the CIE L*, a*, and b* color space, representing lightness, redness–greenness, and yellowness–blueness, respectively. Each sample was measured at three different surface points, and the mean value was reported. Texture profile analysis

was conducted using a Lloyd Texture Analyzer type TAI (Ametek Lloyd Instruments, UK). Samples were compressed using a cylindrical probe (diameter 35 mm) at a crosshead speed of 1 mm/s with a compression distance of 50% of sample height (Puspaningtyas *et al*., 2024). Hardness, cohesiveness, and adhesiveness were obtained from the force–time curve.

Determination of Chemical Properties

The chemical composition of the snack bar was evaluated by determining moisture, ash, protein, lipid, carbohydrate, and total dietary fiber contents. Moisture content was determined using the gravimetric method (AOAC 925.10), ash content by dry incineration (AOAC 945.46), protein content by the Kjeldahl method based on total nitrogen determination (AOAC 991.22), total dietary fiber by enzymatic–gravimetric analysis (AOAC 985.29), and lipid content by Soxhlet extraction (AOAC 945.39). Carbohydrate content was calculated by difference from the proximate analysis.

Determination of Sensory Properties

Sensory analysis was conducted by modifying the method developed by (Prayitno, Mardiana, & Rochma, 2021). A total of 31 semi-trained panelists evaluated the snack bar samples on five-point hedonic scale. A rating of 1 reflects a strong dislike, while a rating of 5 reflects a strong liking. Ethical clearance for sensory testing has been granted by the ethics commission of State University of Malang with an approval No.19.06.16/UN32.14.2.8/LT/2026.

Determination of Antioxidant Activity

Antioxidant activity was determined using a modified DPPH radical scavenging method according to (Savira, Wahyuni, & Faradilla, 2020). One gram of each sample was extracted with 25 mL of analytical-grade ethanol by maceration for 6 h. The extract was filtered and diluted to concentrations of 50, 100, 200, 300, 400, and 500 mg/L. A blank solution was prepared by mixing 1 mL of DPPH solution with 4 mL of ethanol, and incubation in the dark for 30 min. Absorbance was measured using a UV–Vis spectrophotometer at 513 nm. Antioxidant activity was expressed as IC_{50}, defined as the concentration of sample required to inhibit 50% of DPPH radicals. Lower IC_{50} values indicate stronger antioxidant activity.

Determination of Microbial Properties

The total count of microorganisms in the product was carried out using the method described by (Mardiana, Kurniawan, Wirawantoro, Purnomo, & Prasetiyo, 2023). Five grams of the snack bar sample were weighed, homogenized, and suspended in 45 mL of sterile distilled water to obtain an initial dilution. Subsequently, 1 mL of the suspension was transferred into 9 mL of sterile distilled water to achieve a 10^{-2} dilution. Serial dilutions were then prepared up to 10^{-4}. One milliliter of the appropriate dilution was pour-plated onto Plate Count Agar (PCA) and incubated at 37 °C for 48 hours. Microbial counts were expressed as colony-forming units per gram (CFU/g).

Determination of the Best Treatment

The best treatment was determined using the Zeleny method (Zeleny, 1998) by considering multiple quality attributes, including physical, chemical, microbiological, sensory, and antioxidant characteristics the procedure involved defining an ideal value for each parameter by specifying the desired maximum or minimum performance, depending on the nature of the attribute. All parameters were normalized to a scale of 0–1 to allow direct comparison among variables with different units. Subsequently, the degree of closeness (dk) and the distance to the ideal solution were calculated using L_1 (Manhattan), L_2 (Euclidean), and $L\infty$ (Chebyshev) distance measures. Equal weighting was applied to all parameters to avoid subjective bias and to ensure that each quality attribute contributed equally to the decision-making process. The best treatment was selected based on the minimum distance values (L_1 , L_2 , and $L\infty$),

indicating the formulation closest to the ideal solution.

Statistical Analysis

All experiments were conducted in triplicate. Data were expressed as mean ± standard deviation. One-way analysis of variance (ANOVA) was performed using Minitab 18 (Minitab LLC, Pennsylvania) to analyze variations among samples. Tukey's multiple-range test was used for pairwise comparisons, with statistical significance set at $p<0.05$.

Results and Discussion

Physical Quality of Snack Bar

The physical quality of snack bar is strongly influenced by formulation composition, as ingredient proportions can affect color development and textural characteristics that shape consumer perception. In this study, variations in the ratio of Tahitian chestnut and cowpea flours resulted in significant differences ($p < 0.05$) in color attributes and hardness, while cohesiveness and adhesiveness were not significantly affected (Table 2).

Table 2- Physical quality of snack bar

Parameters	A	B	C	D	E
L*	49.20 ± 0.53^{b}	51.97 ± 0.55^{a}	47.00 ± 0.44^{c}	48.30 ± 0.15^{b}	45.43 ± 0.15^{d}
a*	3.00 ± 0.10^{a}	1.87 ± 0.06^{c}	2.50 ± 0.10^{b}	2.00 ± 0.10^{c}	2.80 ± 0.10^{a}
b*	19.63 ± 0.21^{a}	18.50 ± 0.10^{b}	16.57 ± 0.25^{d}	17.23 ± 0.15^{c}	16.17 ± 0.15^{d}
Hardness (N)	84.44 ± 2.47^{a}	86.13 ± 1.00^{a}	75.80 ± 1.66^{b}	76.20± 1.04^{b}	60.46 ± 2.54^{c}
Cohesiveness	0.11 ± 0.01^{a}	0.26 ± 0.17^{a}	0.17 ± 0.05^{a}	0.37 ± 0.13^{a}	0.54 ± 0.26^{a}
Adhesiveness (J)	-0.0035± 0.00^{a}	-0.0039 ± 0.00^{a}	-0.0023± 0.01^{a}	-0.0038± 0.0012^{a}	-0.0014 ± 0.00^{a}

Expressed values were mean±SD (n = 3); a same row containing means with the same superscript letters are not significantly different ($p < 0.05$).

A: The ratio of Tahitian chestnut flour and cowpea flour (1:1)
B: The ratio of Tahitian chestnut flour and cowpea flour (1:5)
C: The ratio of Tahitian chestnut flour and cowpea flour (2:1)
D: The ratio of Tahitian chestnut flour and cowpea flour (1:2)
E: The ratio of Tahitian chestnut flour and cowpea flour (5:1)

Increasing the proportion of Tahitian chestnut flour was associated with lower lightness (L*) and yellowness (b*) values, accompanied by higher redness (a*) values, resulting in a darker and slightly more reddish appearance. This trend may be attributed to the darker native color of Tahitian chestnut flour and its susceptibility to enzymatic browning during processing, as previously reported by (Wijanarka, Sudargo, Harmayani, & Marsono, 2017). The increase in a* values is consistent with observations by (Ly, Dyer, Feig, Chien, & Del Bino, 2020), who reported that positive a* values indicate a shift toward red hues in cereal-based products.

Textural analysis showed that snack bar hardness decreased as the proportion of Tahitian chestnut flour increased, indicating a more brittle structure. This behavior is likely related to starch composition, particularly the amylose–amylopectin ratio. Tahitian chestnut starch contains moderate amylose levels (24.09%), which may contribute to reduced structural rigidity compared to starches with higher amylose content (Jariyah, Mulyani, & Setya, 2013). Previous studies have shown that higher amylose levels tend to increase hardness, whereas higher amylopectin proportions result in softer textures (Wulandari, Imam, & Syarifah, 2016). In contrast, cohesiveness and adhesiveness were not significantly influenced by formulation differences. These properties are generally associated with overall starch content rather than starch type alone, as reported by (Iswara, Julianti, & Nurminah, 2019). The low adhesiveness values observed across all formulations indicate that the snack bar was not sticky, which is desirable for

consumer handling and oral processing (Lee, Chung, Lim, Kim, & Ha, 2025).

Chemical Composition of Snack Bar

The protein, fat, water, ash, carbohydrates, and crude fiber of the snack bar were determined, as presented in Table 3.

Table 3- Chemical composition of snack bar

Parameters	A	B	C	D	E
Protein (%wb)	7.35 ± 0.11^{d}	10.62 ± 0.12^{a}	8.10 ± 0.08^{c}	9.77 ± 0.17^{b}	6.93 ± 0.07^{d}
Fat (%wb)	20.18 ± 0.21^{ab}	18.28 ± 0.29^{c}	20.54 ± 0.25^{a}	20.54 ± 0.24^{a}	19.88 ± 0.20^{b}
Moisture content (%wb)	26.75 ± 0.99^{a}	25.25 ± 0.36^{b}	25.43 ± 0.29^{b}	25.22 ± 0.28^{b}	25.26 ± 0.34^{b}
Ash (%wb)	2.24 ± 0.04^{a}	1.94 ± 0.14^{b}	2.07 ± 0.02^{ab}	2.14 ± 0.03^{a}	2.10 ± 0.02^{ab}
Carbohydrate (%wb)	43.14 ± 0.54^{bc}	44.23 ± 0.44^{b}	44.38 ± 0.44^{b}	42.73 ± 0.45^{c}	46.20 ± 0.49^{a}
Dietary fiber (%wb)	7.76 ± 0.08^{c}	7.10 ± 0.08^{d}	8.37 ± 0.14^{b}	7.58 ± 0.10^{cd}	9.75 ± 0.36^{a}

Expressed values were mean±SD (n = 3); a same row containing means with the same superscript letters are not significantly different ($p < 0.05$).

A: The ratio of Tahitian chestnut flour and cowpea flour (1:1)
B: The ratio of Tahitian chestnut flour and cowpea flour (1:5)
C: The ratio of Tahitian chestnut flour and cowpea flour (2:1)
D: The ratio of Tahitian chestnut flour and cowpea flour (1:2)
E: The ratio of Tahitian chestnut flour and cowpea flour (5:1)

The proportion of cowpea flour influenced the protein content of the snack bar, higher levels of cowpea associated with increased protein content. This indicates that cowpea primarily contributes to protein enhancement in the formulation, while Tahitian chestnut functions mainly as a carbohydrate source. The observed effect was statistically significant ($p < 0.05$), confirming that formulation composition affected protein levels. This trend is consistent with previous studies reporting that greater incorporation of cowpea results in higher protein content in processed food products (Wibowo, Swasti, & Pranata, 2023), which can be attributed to the relatively high intrinsic protein content of cowpea, reported to range from 22% to 24% (Shevkani, 2025). When compared with snack bar formulated using other local ingredients, such as Indian almond seeds (9.28%) (Febrianza, Widawati, & Nur'aini, 2024), the protein content obtained in this study (6.93–10.62%) was within a comparable range. These variations are primarily related to differences in the intrinsic protein composition of the raw materials rather than processing conditions.

Differences in fat content among the snack bar formulations can be explained by variations in the proportion of Tahitian chestnut and cowpea flours, although the relationship appears complex and not strictly linear. Formulation B, which contained the highest proportion of cowpea flour (62.5 g) and the lowest proportion of Tahitian chestnut flour (12.5 g), exhibited the lowest fat content (18.28%), consistent with the low intrinsic fat content of cowpea (0.58–2.03%) (Karuwal, Suharsono, Tjahjoleksono, & Hanif, 2021). In contrast, formulations with moderate to high proportions of Tahitian chestnut flour (C: 50 g; D: 25 g) showed the highest fat content (20.54%), whereas formulation E, with the highest Tahitian chestnut proportion (62.5 g), had an intermediate fat level (19.88%) that was statistically lower than C and D. This non-linear pattern suggests that, although Tahitian chestnut contains higher intrinsic fat (2.95–5.38%) compared to cowpea (Rahayu *et al.*, 2024), increases in its proportion do not necessarily correlate positively with final product fat content. Such behavior may be explained by complex interactions within the food matrix, where mixing efficiency, fat

distribution, and thermal processing conditions affect fat retention (Aguilera, 2019). While the fixed addition of butter (25 g, 80% fat) remains the primary contributor to overall lipid content (Pădureț, 2021).

The moisture content of the snack bar varied among formulations and was significantly affected by the proportion of Tahitian chestnut flour and cowpea ($p < 0.05$). An increase in Tahitian chestnut flour generally resulted in higher moisture levels. This trend can be explained by the starch characteristics of Tahitian chestnut, which exhibits a high capacity for water absorption and retention. Starch molecules contain numerous hydroxyl (–OH) groups that readily form hydrogen bonds with water, thereby enhancing water binding within the product matrix (Donmez, Pinho, Patel, Desam, & Campanella, 2021). As a consequence, snack bar with higher moisture content tended to exhibit a softer texture. Tahitian chestnut starch contains a medium amylose content (approximately 24%), which falls within the typical range of 20–25% (Bhardwaj, Salgotra, & Sharma, 2019; Jariyah *et al*., 2013). This amylose level contributes to improved water retention and influences the compactness and softness of the final product.

Ash content did not differ significantly among snack bar formulations ($p > 0.05$), indicating that variations in the ratio of Tahitian chestnut flour and cowpea had little influence on the overall mineral content of the final products. This result is consistent with previous studies reporting comparable ash levels in Tahitian chestnut flour and cowpea, which may explain the similar mineral contribution across formulations (Karuwal *et al*., 2021; Rahayu *et al*., 2024). The use of fixed amounts of other ingredients, such as egg white, skim milk, and butter, may also have contributed to the limited variation in ash content. The ash values obtained in this study are comparable to those reported for snack bar formulated with other local ingredients, including purple sweet potato (Aurelia, Ma'rifah, & Muhlishoh, 2023).

The carbohydrate content of the snack bar differed significantly among formulations ($p < 0.05$) and showed an increasing trend with higher proportions of Tahitian chestnut flour. Formulations dominated by Tahitian chestnut flour exhibited higher carbohydrate levels compared to those with greater amounts of cowpea flour. This pattern reflects the inherent characteristics of the raw materials, as Tahitian chestnut serves as a primary source of complex carbohydrates, whereas cowpea contributes mainly protein (Müller, 2024). Consequently, formulations dominated by Tahitian chestnut flour exhibited higher carbohydrate levels, which may enhance the role of the snack bar as an energy-providing product.

Dietary fiber content also differed significantly among treatments ($p < 0.05$) and demonstrated a clear tendency to increase with increasing proportions of Tahitian chestnut flour. Formulations containing higher levels of Tahitian chestnut flour resulted in greater fiber content, consistent with previous reports indicating that Tahitian chestnut flour contains relatively high levels of dietary fiber, influenced by processing conditions and particle size (Rahayu *et al*., 2024). In contrast, although cowpea seeds are known to be rich in dietary fiber, the fiber content of cowpea flour is generally lower due to dehulling and milling processes (Abebe & Alemayehu, 2022; Swaroopa, Agarkar, & Kshirsagar, 2025). This trend suggests that increasing the proportion of Tahitian chestnut flour plays a key role in enhancing the dietary fiber content of the snack bar, supporting the potential of these local ingredients to produce snack products with competitive fiber levels compared to commercial snack bar (Asriasih, Purbowati, & Anugrah, 2020).

Sensory Evaluation of Snack Bar

Sensory evaluation is an analytical approach that relies on human senses to determine consumer preferences toward food products. This method engages sight, smell, taste, and touch to assess attributes such as texture, appearance, aroma, and flavor (Hussain, 2020). Sensory evaluation of snack bar samples can be seen in Table 4.

Table 4- Sensory of snack bar

Parameters	A	B	C	D	E
Taste	3.55 ± 0.9[a]	3.77 ± 0.84[a]	3.55 ± 0.72[a]	3.74 ± 0.86[a]	3.55 ± 0.68[a]
Texture	3.71 ± 0.64[a]	3.81 ± 0.60[a]	3.71 ± 0.39[a]	3.90 ± 0.60[a]	3.77 ± 0.67[a]
Color	3.52 ± 0.85[a]	3.81 ± 1.14[a]	3.52 ± 0.77[a]	3.61 ± 0.84[a]	3.68 ± 0.83[a]
Aroma	3.32 ± 0.79[a]	3.45 ± 0.89[a]	3.77 ± 0.72[a]	3.29 ± 0.78[a]	3.48 ± 0.85[a]
Overall appearance	3.65 ± 0.75[a]	3.65 ± 0.80[a]	3.87 ± 0.56[a]	3.81 ± 0.75[a]	3.87 ± 0.76[a]

Expressed values were mean±SD (n = 31); a same row containing means with the same superscript letters are not significantly different ($p < 0.05$).

A: The ratio of Tahitian chestnut flour and cowpea flour (1:1)
B: The ratio of Tahitian chestnut flour and cowpea flour (1:5)
C: The ratio of Tahitian chestnut flour and cowpea flour (2:1)
D: The ratio of Tahitian chestnut flour and cowpea flour (1:2)
E: The ratio of Tahitian chestnut flour and cowpea flour (5:1)

The results of the ANOVA test indicated that variations in the proportion of Tahitian chestnut flour and cowpea flour did not produce significant differences ($p>0.05$) in any of the sensory parameters evaluated, which included taste, texture, color, aroma, and overall appearance. The mean hedonic scores given by panelists for taste ranged from 3.55 to 3.77 (liked), texture from 3.71 to 3.90 (liked), color from 3.52 to 3.81 (liked), aroma from 3.32 to 3.77 (liked), and overall appearance from 3.65 to 3.87 (liked). In general, the snack bar samples were well accepted by panelists, despite the absence of significant differences among treatments. Nevertheless, a tendency was observed in which increasing the proportion of cowpea flour led to a decline in panelist preference levels. This phenomenon may be associated with the presence of the characteristic beany flavor of cowpea, which is generally less favored by consumers. Several volatile compounds contributing to the development of this aroma include 3-methyl-1-butanol, 1-pentanol, 1-octen-3-ol, (E,E)-2,4-heptadienal, acetophenone, 1-octen-3-one, and 3-isopropyl-2-methoxypyrazine (Trindler, Annika Kopf-Bolanz, & Denkel, 2022). These findings are consistent with the study of (Ariviani, Sholihin, & Nastiti, 2021), who reported that increasing cowpea proportions in cereal products led to a decrease in sensory characteristics. However, in the present study, the incorporation of butter in the snack bar formulation played a role in masking the distinct aroma of cowpea, thereby enabling the product to be accepted with relatively good hedonic scores by the panelists.

Antioxidant and Microbiology Properties of Snack Bar

The antioxidant activity of the snack bar formulations, expressed as IC_{50} values, ranged from 8,410 to 11,733 µg/ml, with ANOVA results indicating significant differences ($p < 0.05$) among formulations containing different proportions of Tahitian chestnut and cowpea flours. Lower IC_{50} values indicate stronger antioxidant activity, and formulation E exhibited the highest antioxidant activity among the tested samples. This trend may be associated with the higher proportion of Tahitian chestnut flour, as Tahitian chestnut seeds have been reported to contain antioxidant-related compounds such as linoleic acid, ethyl linoleate, ethyl oleate, and homopterocarpine (Sukadana & Santi, 2015). However, despite these differences, the overall antioxidant activity of all snack bar formulations was categorized as very weak, as all IC_{50} values exceeded 200 µg/ml. These results suggest that while Tahitian chestnut proportion influenced antioxidant activity, the formulated snack bar should not be considered a strong source of antioxidants. It should be noted that the antioxidant activity observed in this study was relatively low, which is expected

for a processed snack product rather than a concentrated plant extract. Therefore, antioxidant activity was not considered a primary functional attribute of the developed snack bar.

The total count (TC) of the snack bar samples did not differ significantly among formulations ($p > 0.05$), indicating that variations in the proportion of Tahitian chestnut flour and cowpea flour had no measurable effect on microbial load. This absence of a clear trend suggests that the microbial quality of the snack bar was primarily influenced by processing conditions rather than by differences in raw material composition. The baking process, conducted at 130 °C for 20 min, likely played a major role in reducing microbial populations across all treatments, resulting in comparable TC values (Maghfiroh *et al.*, 2021). Total count is commonly used as an indicator of overall product hygiene and potential shelf stability. The consistently low TC values observed in this study suggest that the developed snack bar possess satisfactory microbiological quality and are suitable for further product development and storage studies. However, additional evaluations, such as shelf-life testing under different storage conditions, would be necessary to fully assess long-term microbiological stability.

Table 5- Antioxidant and TPC of Snack Bar

Parameters	A	B	C	D	E
Antioxidant activity (µg/ml)	$11{,}733 \pm 115^{a}$	$11{,}253 \pm 105^{b}$	$9{,}470 \pm 100^{c}$	$11{,}640 \pm 87^{a}$	8410 ± 170^{d}
TPC (CFU/g)	$4 \times 10^{3\,a}$	2.7×10^{3a}	3.3×10^{3a}	3.3×10^{3a}	3×10^{3a}

Expressed values were mean±SD (n = 3); a same row containing means with the same superscript letters are not significantly different ($p < 0.05$).

A: The ratio of Tahitian chestnut flour and cowpea flour (1:1)
B: The ratio of Tahitian chestnut flour and cowpea flour (1:5)
C: The ratio of Tahitian chestnut flour and cowpea flour (2:1)
D: The ratio of Tahitian chestnut flour and cowpea flour (1:2)
E: The ratio of Tahitian chestnut flour and cowpea flour (5:1)

The Best Treatments by Zeleny's Method

Using the Zeleny multi-criteria decision-making method, the optimal snack bar formulation was identified by integrating physicochemical properties, nutritional composition, sensory acceptance, antioxidant activity, and microbiological quality (Supplementary File 1). Formulation E, with a Tahitian chestnut to cowpea flour ratio of 5:1, was selected as the best treatment because it demonstrated the most balanced overall performance across the evaluated attributes rather than excelling in a single parameter. This formulation achieved a favorable balance between carbohydrate and protein contributions, with moderate textural characteristics appropriate for snack bar consumption. Sensory evaluation further confirmed that formulation E maintained good overall consumer acceptance. Although its antioxidant activity, expressed as IC_{50} values, was relatively weak in absolute terms, formulation E exhibited stronger antioxidant activity compared to the other treatments and also showed the highest dietary fiber content, which may contribute to its functional potential.

Limitation

Economic evaluation was beyond the scope of the present study, which primarily focused on formulation development and product quality assessment. Future studies should incorporate techno-economic and cost–benefit analyses to evaluate the feasibility of large-scale production and commercialization of snack bars formulated with Tahitian chestnut and cowpea flours. Although Tahitian chestnut flour is not yet widely produced at an industrial scale, the processing steps employed in this study (boiling, drying, milling, and sieving) are technically comparable to those used for other tuber and legume-based flours and can be adapted to small and medium-scale production systems. However, further development of raw

material supply chains will be necessary to support sustainable industrial-scale application.

Conclusion

This study demonstrated that Tahitian chestnut and cowpea flours can be incorporated into snack bar formulation as alternative carbohydrate and protein sources, respectively, without compromising product quality. Variations in their proportions influenced nutritional and physicochemical characteristics, particularly protein and dietary fiber contents, while sensory acceptance and microbiological quality remained within acceptable ranges across all formulations. Using a multi-criteria decision approach, formulation E (Tahitian chestnut:cowpea ratio of 5:1) exhibited the most balanced quality profile, characterized by suitable texture for snack bar consumption, good consumer acceptance, relatively higher antioxidant activity among treatments, and the highest dietary fiber content, while maintaining microbiological safety. These findings suggest that Tahitian chestnut–cowpea composite flour has promising potential for the development of functional snack bars, although further studies addressing techno-economic feasibility are required.

Author Contribution

Nur Agustin Mardiana: Conceptualization, funding acquisition, methodology, data processing, and drafting of the manuscript. **Nur Aini Mahmudah**: Data curation, validation, review and editing of the manuscript.

Funding Sources

The authors gratefully acknowledge the financial support provided by the Ministry of Higher Education, Science, and Technology of the Republic of Indonesia through the *Penelitian Dosen Pemula* (PDP) Program in 2025. The funder had no role in the study design, data collection, analysis, interpretation of data, writing of the manuscript, or decision to publish the results.

References

1. Abebe, B.K., & Alemayehu, M.T. (2022). A review of the nutritional use of cowpea (*Vigna unguiculata* L. Walp) for human and animal diets. In *Journal of Agriculture and Food Research* (Vol. 10). Elsevier B.V. https://doi.org/10.1016/j.jafr.2022.100383
2. Aguilera, J.M. (2019). The food matrix: implications in processing, nutrition and health. In *Critical Reviews in Food Science and Nutrition*, *59*(22), 3612–3629. Taylor and Francis Inc. https://doi.org/10.1080/10408398.2018.1502743
3. Akhdifa, S.P. (2024). Analysis of value addition in Gayam (*Inocarpus fagifer*) chips production at Keluarga Sejahtera MSME, Pasuruan Regency. *Journal of Agriculture, Livestock, and Fisheries*, *2*(1), 1–16. https://doi.org/10.3766/hibrida.v1i2.3753
4. Anam, C., Hamidah, E., Kusumawati, D.E., Istiqomah, I., Qibtiyah, M., & Amiroh, A. (2024). Effect of chemical type and concentration on the modification of cowpea protein isolate. *Agrointek: Journal of Agricultural Industrial Technology*, *18*(2), 419–428. https://doi.org/10.21107/agrointek.v18i2.16837
5. Anggraeni, M., Nurwantoro, Budi, S., & Abduh, M. (2017). Physicochemical properties of bread made from wheat flour and different sugar. *Journal of Food Technology Applications*, *6*(1), 52–56. https://doi.org/10.17728/jatp.214
6. Ariviani, S., Sholihin, N.H., & Nastiti, G.P. (2021). Development of cowpea (*Vigna unguiculata*) sprouts flour as a functional cereal high in dietary fiber and antioxidant potential. *Jurnal Teknologi Hasil Pertanian, 14*(2), 84. https://doi.org/10.20961/jthp.v14i2.53422

7. Asriasih, D.N., Purbowati, & Anugrah, R.M. (2020). Nutrition value of mixed flour snack bar (Mocaf & red bean flour) and commercial snack bar. *Jurnal Gizi dan Kesehatan*, *12*(27), 21–28. https://doi.org/https://doi.org/10.35473/jgk.v12i27.57
8. Aurelia, L.C., Ma'rifah, B., & Muhlishoh, A. (2023). High dietary fiber and antioxidant snack bar based on purple sweet potato and black rice as an alternative snack for diabetes mellitus. *Jurnal Gizi Dan Pangan Soedirman*, *7*(2), 196. https://doi.org/10.20884/1.jgipas.2023.7.2.9413
9. Bhardwaj, R., Salgotra, R.K., & Sharma, M. (2019). Studies on correlation of amylose content and grain dimensions in Basmati rice (*Oryza sativa* L.). *Electronic Journal of Plant Breeding*, *10*(2), 364–369. https://doi.org/10.5958/0975-928X.2019.00046.2
10. Day, L., Cakebread, J.A., & Loveday, S.M. (2022). Food proteins from animals and plants: Differences in the nutritional and functional properties. *Trends in Food Science & Technology*, *119*, 428–442. https://doi.org/https://doi.org/10.1016/j.tifs.2021.12.020
11. Donmez, D., Pinho, L., Patel, B., Desam, P., & Campanella, O.H. (2021). Characterization of starch–water interactions and their effects on two key functional properties: starch gelatinization and retrogradation. *Current Opinion in Food Science*, *39*, 103–109. https://doi.org/10.1016/J.COFS.2020.12.018
12. Fadillah, R., Purnamawati, H., & Supijatno. (2020). Production of cowpea (*Vigna unguiculata* [L.] Walp) with low input of fertilizer. *Indonesian Journal of Agronomy*, *48*(1), 44–51. https://doi.org/10.24831/jai.v48i1.27597
13. Febrianza, H., Widawati, L., & Nur'aini, H. (2024). Quality characteristics of high-protein snack bars based on corn flour and tropical almond (*Terminalia catappa*) seeds. *Agriovet*, *6*(2), 106–116. https://doi.org/https://doi.org/10.51158/agriovet.v6i2
14. Ghatge, S.K. (2023). Impact of modern lifestyle on health. *PriMera Scientific Surgical Research and Practice*, *2*(2), 16–19. https://doi.org/10.56831/pssrp-02-048
15. Hussain, S. (2020). The impact of sensory branding (five senses) on consumer: A case study on KFC (Kentucky fried chicken). *ACADEMICIA: An International Multidisciplinary Research Journal*, *10*(6), 47–55. https://doi.org/10.5958/2249-7137.2020.00586.8
16. Innova Marketing Sights. (2024, November 29). *Snacks bars industry trends, global market overview. Snacking*. Innovamarketingsights.Com. https://www.innovamarketinsights.com/trends/global-snacks-bars-industry/
17. Iswahyudi, I., Khoirunissa, Y.S., & Putri, I.E. (2022). Utilization of cowpea flour (*Vigna unguiculata*) and saga tree seeds flour (*Adenanthera pavonina* Linn) in making flakes. *ARGIPA*, *7*(1), 80–92. https://doi.org/10.22236/argipa.v7i1.7768
18. Iswara, J.A., Julianti, E., & Nurminah, M. (2019). Characterization texture of sweet bread from flour, starch, fiber and anthocyanin pigment of purple sweet potatoes. *Jurnal Pangan dan Agroindustri*, *7*(4), 12–21. https://doi.org/https://doi.org/10.21776/ub.jpa.2019.007.04.2
19. Jariyah, Mulyani, T., & Setya, P.P. (2013). Study of nutrition of crackers Gayam. *Journal of Research Results– Rekapangan*, *7*(1), 76–90. https://doi.org/https://doi.org/10.33005/jtp.v7i1.486
20. Karuwal, R.L., Suharsono, Tjahjoleksono, A., & Hanif, N. (2021). Short communication: Characterization and nutrient analysis of seed of local cowpea (*Vigna unguiculata*) varieties from Southwest Maluku, Indonesia. *Biodiversitas*, *22*(1), 85–91. https://doi.org/10.13057/biodiv/d220112
21. Lee, S.Y., Chung, S.J., Lim, J.W., Kim, M.Y., & Ha, C.H. (2025). Texture characterization of semi-solid foods for older adults: Sensory analysis and instrumental approaches. *LWT*, *221*. https://doi.org/10.1016/j.lwt.2025.117582

22. Ly, B.C.K., Dyer, E.B., Feig, J.L., Chien, A.L., & Del Bino, S. (2020). Research techniques made simple: Cutaneous colorimetry: A reliable technique for objective skin color measurement. *Journal of Investigative Dermatology*, *140*(1), 3-12.e1. https://doi.org/10.1016/j.jid.2019.11.003
23. Maghfiroh, L., Soelih Estoepangestie, A.T., Nurhajati, T., Harijani, N., Helmi Effendi, M., & Handijatno, D. (2021). Total plate count of commercial pasteurized milk sold by street vendors in Mulyorejo sub-district Surabaya. *Journal of Halal Product and Research (JHPR)*, *4*(2), 56–61. https://doi.org/10.20473/jhpr.vol.4-issue.2.56-61
24. Maharani, S., Pamela, V., & Kusumasari, S. (2021). The review of snack bar from Chia- mocaf as an antidiabetic food. *Food ScienTech Journal*, *3*, 56. https://doi.org/10.33512/fsj.v3i1.10011
25. Mardiana, N.A., Kurniawan, H., Wirawantoro, A., Purnomo, P., & Prasetiyo, B. (2023). Effect of storage time on quality of Bebek Ungkep in retort pouch. *IOP Conference Series: Earth and Environmental Science*, *1200*(1), 1–5. https://doi.org/10.1088/1755-1315/1200/1/012029
26. Mordor Intelligence. (2024). *Indonesia snack bar market - Size, share & industry analysis*. Mordorintelligence.Com. https://www.mordorintelligence.com/industry-reports/indonesia-snack-bar-market
27. Müller, J.V. (2024). The Tahitian chestnut [*Inocarpus fagifer* (Parkinson ex F.A.Zorn) Fosberg, Fabaceae], a neglected multi-purpose tree from the Asia–Pacific region. *Discover Agriculture*, *2*(1). https://doi.org/10.1007/s44279-024-00020-7
28. Okechukwu-Ezike, N., Munonye, J., & Esiegwu, A. (2020). Comparative evaluation of the proximate cmposition, anti-nutrients and functional properties of some underutilized pulses. *Food Science and Quality Management*, *95*(1), 72–76. https://doi.org/10.7176/fsqm/95-08
29. Olopade, O., Odeniyi, I., Fasanmade, O., Olopade, B., Kayode, O., Anyanwu, A., & Chimah, P. (2020). Glycemic responses of local beans (*Vigna unguiculata* [Linn Walp] varieties) in persons with Type 2 diabetes mellitus and healthy controls - An experimental study. *Journal of Clinical Sciences*, *17*(4), 100. https://doi.org/10.4103/jcls.jcls_61_19
30. Pădureț, S. (2021). The effect of fat content and fatty acids composition on color and textural properties of butter. *Molecules*, *26*(15). https://doi.org/10.3390/molecules26154565
31. Prayitno, S., Mardiana, N., & Rochma, N. (2021). Sensory evaluation of wet noodle products added with *Moringa oleifera* flour with different concentrations. *Kontribusia*, *4*(2), 450–454. https://doi.org/https://doi.org/10.30587/kontribusia.v4i2.2738
32. Prestia, D., Oktavia, I., Razak, M., & Pudjirahaju, A. (2022). The effect of substitution of cowpea flour *Vigna unguiculata* L. and Mungbean flour *Vigna radhiata* on chemical quality, nutritional quality, and organoleptic quality of biscuits as PMT for CED on pregnant women. *Jurnal Pendidikan Kesehatan*, *11*(2), 169–183. https://doi.org/https://doi.org/10.31290/jpk.v11i2.3703
33. Puspaningtyas, D.E., Sari, P.M., Styaningrum, S.D., Sucipto, A., Rahmawati, D.M., & Lestari, G.P. (2024). Color and texture analysis of glucomannan modified growol cookies for diabetic. *Jurnal SAGO Gizi Dan Kesehatan*, *5*(2), 511. https://doi.org/10.30867/gikes.v5i2.1686
34. Rahayu, N.S., Safitri, D.E., Sulaeman, A., & Setiawan, B. (2024). Nutrition content and dietary fiber in Gayam (*Inocarpus fagifer*) flour. *ARGIPA*, *9*(1), 11–19. https://doi.org/10.22236/argipa.v9i1.14541
35. Savira, A.P.I., Wahyuni, S., & Faradilla, RH.F. (2020). Nutritional content analysis, organoleptics and antioxidant activity of snack bars based on organic rice (*Oryza sativa* L.) local varieties (Red Wakawondu, Black Wakombe, and Chocolate Warumbia) as alternative intermediate foods for diabetes mellitus patients. *Journal of Food Science and Technology*, *5*(6), 3436–3452. https://doi.org/https://doi.org/10.33772/jstp.v5i6.15730
36. Shevkani, K. (2025). Structure, technofunctionality and bioactivities of cowpea proteins - a review. *International Journal of Biological Macromolecules*, *333*, 148980. https://doi.org/10.1016/j.ijbiomac.2025.148980

37. Sukadana, I., & Santi, S.R. (2015). Antioxidant compounds of Gayam seed (*Inocarpus fagiferus Fosb*) to prevent atherosclerosis in Wistar rat with high cholesterol diet. *Biomedical and Pharmacology Journal*, *8*(2), 547–555. https://doi.org/10.13005/BPJ/797
38. Swaroopa, G., Agarkar, B.S., & Kshirsagar, R.B. (2025). Comprehensive characterization of soy protein, cowpea, moth bean and wheat gluten as functional ingredients for the development of plant-based extruded meat analogues. *BIO Web of Conferences*, *178*. https://doi.org/10.1051/bioconf/202517803007
39. Tetelay, F.F., & Siahaya, L. (2018). Existance and potential of Gayam as alternative food producing tree in district of west part Seram of Maluku province. *Jurnal Hutan Pulau-Pulau Kecil*, *6*, 310–321. https://doi.org/10.30598/jhppk.2017.1.4.310
40. Trindler, C., Annika Kopf-Bolanz, K., & Denkel, C. (2022). Aroma of peas, its constituents and reduction strategies – Effects from breeding to processing. *Food Chemistry*, *376*. https://doi.org/10.1016/j.foodchem.2021.131892
41. Tukidi, & Erwandi, E. (2023). Growth and years of cocknut (*Vigna unguiculata*) at various plant space. *Mediagro*, *19*(1), 55–64. https://doi.org/https://doi.org/10.31942/mediagro.v19i1.8200
42. Veda, R.C., Wirawan, Y.H., Sakrafilio, G.E., Darmadi, K.K., Kurniawan, D., Pramana, R.C., Putra, T.A.Y.B., Chandra, K.Y., Crisensia, A.Y., Kristyakova, N.S., & Prakasa, F.B.P. (2022). Enhancing the economic potential of Mulyodadi village through the development of Gayam fruit chips. *Atma Inovasia Journal*, *2*(6), 2775–9385. https://doi.org/https://doi.org/10.24002/jai.v2i6.5222
43. Wibowo, K.F., Swasti, Y.R., & Pranata, F.S. (2023). Low fat and high protein meat analogue of cowpea (*Vigna unguiculata*) with stabilizer cocoa pod husk extract (*Theobroma cacao* L.). *Food Research*, *7*(5), 1–11. https://doi.org/10.26656/fr.2017.7(5).789
44. Wijanarka, A., Sudargo, T., Harmayani, E., & Marsono, Y. (2017). Effect of pre-gelatinization on physicochemical and functional properties of Gayam (Inocarfus fagifer Forst.) flour. *American Journal of Food Technology*, *12*(3), 178–185. https://doi.org/10.3923/ajft.2017.178.185
45. Wijanarka, A., Tifauzah, N., Khasanah, F., Nirmala Dewi, A., & Setyaningsih, L. (2024). The glycemic index of Gayam (*Inocarpus fagifer* Forst) cookies as a high dietary fiber food. *Jurnal Info Kesehatan*, *22*(3), 510–520. https://doi.org/10.31965/infokes.Vol22.Iss3.1698
46. Wulandari, N., Imam, R.H., & Syarifah, U. (2016). The effect of corn starch, potato starch and tapioca substitution to the hardness and oily taste of pilus snack. *Jurnal Mutu Pangan*, *3*(2), 87–94.
47. Zeleny, M. (1998). Multiple criteria decision making: eight concepts of optimality. *Human Systems Management*, *17*(2), 97–107. https://doi.org/10.3233/HSM-1998-17203

نشریه پژوهشهای علوم و صنایع غذایی ایران
https://ifstrj.um.ac.ir

مقاله کوتاه پژوهشی
جلد ۲۲، شماره ۱، فروردین- اردیبهشت ۱٤۰۵، ص. ۱۰۹-۹۵

ویژگی‌های کیفی مخلوط آرد شاه بلوط تاهیتی (*Inocarpus fagifer*) و لوبیا چشم بلبلی (*Vigna unguiculata*) به‌عنوان مواد تشکیل‌دهنده در اسنک بار

نور اگوستین ماردیانا[۱*]- نور آیینی محموداه[۱]

تاریخ دریافت: ۱۴۰۴/۰۶/۳۱
تاریخ پذیرش: ۱۴۰۴/۱۱/۰۸

چکیده

تقاضای روزافزون برای محصولات میان وعده‌ای مناسب و متعادل از نظر تغذیه‌ای، فرصت‌هایی را برای استفاده از مواد اولیه محلی کم مصرف در توسعه محصولات غذایی ایجاد کرده است. این مطالعه با هدف توسعه اسنک بار با استفاده از آرد شاه بلوط تاهیتی (Inocarpus fagifer) و لوبیا چشم بلبلی (Vigna unguiculata) به‌عنوان مواد اولیه موجود در محل و ارزیابی ویژگی‌های فیزیکوشیمیایی، حسی، آنتی‌اکسیدانی و میکروبیولوژیکی آنها انجام شد. پنج فرمولاسیون با نسبت آرد شاه بلوط تاهیتی به لوبیا چشم بلبلی متفاوت[A = 1:1 ؛ B = 1:5 ؛ C = 2:1 ؛ D = 1:2 ؛ E = 5:1] با استفاده از یک طرح کاملاً تصادفی تهیه شدند. افزودن شاه بلوط تاهیتی و لوبیا چشم بلبلی به‌طور قابل توجهی ($p < 0.05$) بر چندین پارامتر فیزیکوشیمیایی، از جمله رنگ، بافت، رطوبت، فیبر غذایی، ترکیب درشت مغذی‌ها و خواص آنتی‌اکسیدانی تأثیر گذاشت، در حالی‌که محتوای خاکستر به‌طور قابل توجهی تحت تأثیر قرار نگرفت. ویژگی‌های حسی و کیفیت میکروبیولوژیکی به‌طور قابل توجهی تحت تأثیر قرار نگرفتند و همه فرمولاسیون‌ها معیارهای هدونیک و ایمنی قابل قبولی را برآورده کردند. بر اساس روش تصمیم‌گیری چندمعیاره زلنی، فرمولاسیون E (نسبت شاه بلوط تاهیتی: لوبیا چشم بلبلی ۵:۱) به‌عنوان متعادل‌ترین فرمولاسیون در بین فرمولاسیون‌های ارزیابی شده شناسایی شد. این یافته‌ها پتانسیل آرد شاه بلوط و لوبیا چشم بلبلی تاهیتی را برای توسعه اسنک بار نشان می‌دهد و اطلاعات پایه‌ای را برای استفاده بیشتر از مواد اولیه محلی در محصولات غذایی با ارزش افزوده فراهم می‌کند.

واژه‌های کلیدی: اسنک بار، شاه بلوط تاهیتی، کیفیت، لوبیا چشم بلبلی

۱- گروه پردازش محصولات طیور، کالج دولتی پوترا سانگ فاجار بلیتر، جاوا شرقی، اندونزی
(*- نویسنده مسئول: Email: nuragustin@akb.ac.id)

https://doi.org/10.22067/ifstrj.2026.95576.1477

بسم الله الرحمن الرحیم

مندرجات

مقالات پژوهشی

مقاله کوتاه پژوهشی

نشریه پژوهشهای علوم و صنایع غذایی ایران

با شماره پروانه ۱۲۴/۸۴۷ و درجه علمی–پژوهشی شماره ۳/۱۱/۸۱۰ از وزارت علوم، تحقیقات و فناوری ۸۸/۵/۱۰

"براساس مصوبه وزارت عتف از سال ۱۳۹۸، کلیه نشریات دارای درجه "علمی–پژوهشی" به نشریه "علمی" تغییر نام یافتند. "

جلد ۲۲ **شماره ۱** **فروردین- اردیبهشت ۱۴۰۵**

صاحب امتیاز: دانشگاه فردوسی مشهد

مدیر مسئول: دکتر ناصر شاهنوشی — استاد، اقتصاد کشاورزی، دانشگاه فردوسی مشهد

سردبیر: دکتر مسعود یاورمنش — دانشیار، میکروبیولوژی و بیوتکنولوژی، دانشگاه فردوسی مشهد

اعضای هیئت تحریریه:

دکتر سید علی مرتضوی	میکروبیولوژی و بیوتکنولوژی، دانشگاه فردوسی مشهد
دکتر فخری شهیدی	میکروبیولوژی مواد غذایی، دانشگاه فردوسی مشهد
دکتر محمدباقر حبیبی نجفی	میکروبیولوژی، دانشگاه فردوسی مشهد
دکتر مرتضی خمیری	میکروبیولوژی، دانشگاه علوم کشاورزی و منابع طبیعی گرگان
دکتر سید محمد علی رضوی	مهندسی و خواص بیوفیزیک مواد غذایی، دانشگاه فردوسی مشهد
دکتر رضا فرهوش	شیمی مواد غذایی، دانشگاه فردوسی مشهد
دکتر بی بی صدیقه فضلی بزاز	میکروبیولوژی، دانشکده داروسازی، دانشگاه علوم پزشکی مشهد
دکتر مهدی کاشانی نژاد	مهندسی مواد غذایی، دانشگاه علوم کشاورزی و منابع طبیعی گرگان
دکتر آرش کوچکی	تکنولوژی مواد غذایی، دانشگاه فردوسی مشهد
دکتر محبت محبی	مهندسی مواد غذایی، دانشگاه فردوسی مشهد
دکتر بابک قنبرزاده	مهندسی مواد غذایی، دانشگاه تبریز
دکتر ایران عالمزاده	بیوتکنولوژی مواد غذایی، دانشگاه صنعتی شریف
دکتر قدیر رجب‌زاده اوغاز	نانو فناوری مواد غذایی، مؤسسه پژوهشی علوم و صنایع غذایی، مشهد
دکتر مهیار حیدرپور	زیست مولکولی، بیمارستان زنان و بریگام، ایالت متحده آمریکا
دکتر حمید بهادر قدوسی	میکروبیولوژی غذایی، دانشگاه متروپولیتن لندن
دکتر کیانوش خسروی	بیوتکنولوژی مواد غذایی، دانشگاه علوم پزشکی شهید بهشتی
دکتر مرتضی عباس‌زادگان	مهندسی عمران و محیط زیست، دانشگاه آریزونا
دکتر محمدامین محمدی‌فر	مهندسی تولید مواد غذایی، دانشگاه فنی دانمارک
دکتر منوچهر وثوقی	بیوتکنولوژی مواد غذایی، دانشگاه صنعتی شریف
دکتر هادی الماسی	گروه علوم و صنایع غذایی، دانشکده کشاورزی، دانشگاه ارومیه
دکتر میلاد فتحی	گروه علوم و صنایع غذایی، دانشگاه صنعتی اصفهان
دکتر سلیمان عباسی	گروه علوم و صنایع غذایی، دانشگاه تربیت مدرس.
دکتر نونو بورخس	گروه علوم تغذیه و مواد غذایی، دانشگاه پورتو، پرتغال
دکتر علی عطا معظمی	گروه علوم مولکولی، دانشکده منابع طبیعی و علوم کشاورزی، دانشگاه سوئد
دکتر کلیفورد نکمناسو اوبی	گروه میکروبیولوژی، دانشگاه کشاورزی مایکل اوکپارا، ایالت ابیا، نیجریه
دکتر ساموئل ایوفمی اولالکان آدییه	گروه فناوری غذایی، موسسه تکنولوژی و علم هندوستان، چنای، تامیل نادو، هند

ناشر: دانشگاه فردوسی مشهد

این نشریه درپایگاه‌های زیر نمایه شده است:

AGRIS، Scopus، CABI، DOAJ، EBSCO، Google scholar، Internet Archive، پایگاه استنادی جهان اسلام (ISC)، سامانه نشریات علمی ایران، پایگاه اطلاعات علمی جهاد دانشگاهی (SID)، بانک اطلاعات نشریات کشور (MAGIRAN)، مرجع دانش CIVILICA

پست الکترونیکی: **ifstrj@um.ac.ir**

مقالات این شماره در سایت https://ifstrj.um.ac.ir به‌صورت مقاله کامل نمایه شده است.

این نشریه به تعداد ۶ شماره در سال و به‌صورت آنلاین منتشر می‌شود.

نشریه علمی

پژوهشهای علوم و صنایع غذایی ایران

جلد ۲۲ شماره ۱

سال ۱۴۰۵

شماره پیاپی ۹۷

شاپا: ۴۱۶۱-۱۷۳۵

عنوان مقالات